A comparative proteomics approach to studying skeletal muscle mitochondria from myostatin knockout mice

by

Jonathan Puddick

A thesis submitted in partial fulfillment
of the requirements for the degree

of

Master of Science in Biological Sciences

at the

University of Waikato

2006

Abstract

Myostatin is a negative regulator of muscle growth. When it is not present or non-functional double-muscling occurs, the primary characteristic of this phenotype being an increase in muscle mass. Another characteristic of double-muscling is an increased proportion of type IIB muscle fibres, which rely on glycolysis as their primary energy source, as opposed to type IIA and type I fibres which rely on oxidative phosphorylation. This switch in muscle metabolism directly impacts on the mitochondria, as mitochondria from glycolytic muscle fibres have been shown to have differences in metabolic activity. The increased proportion of glycolytic muscle fibres present in myostatin knockout animals provides a unique model to investigate alterations in muscle fibre type metabolism.

The mouse model of myostatin knockout utilised during this study was generated by genetic deletion of exon three of the myostatin gene. Verification of this knockout was attempted by western blot analysis, but only the latency associated protein (LAP) was detected. Interestingly, the LAP was barely detectable in the knockout muscle suggesting deletion of exon three affects binding of anti-myostatin antibodies to the LAP, as that part of the gene is not deleted.

A comparison of the basal mitochondrial stress levels was made, also by western blot analysis. The knockout mitochondria showed no change in levels of heat shock protein 60 or superoxide dismutase 2, indicating that they are not being subjected to any increased stress due to the myostatin knockout phenotype.

A comparative proteomics approach was used to detect changes in the mitochondrial proteome of myostatin knockout gastrocnemius muscle to gain clues to how mitochondria from glycolytic muscle fibres differ from those present in oxidative fibres. This was undertaken using two-dimensional electrophoresis (2-DE), in-gel tryptic digests and peptide mass fingerprinting by mass spectrometry. A 2-DE gel protein loading of 220μg was shown to give the best protein spot resolution and the most crucial step in the loading process was found to be the laying of the immobilized pH gradient, which had to be performed very carefully to obtain a consistent loading pattern. This study resolved only around 160 protein spots out of the estimated 1,000 to 2,000 proteins present in the mitochondria. Modulation of six proteins was seen at a $p<0.1$ level, but were unable to be identified using the current methodology. More abundant mitochondrial proteins were able to be identified, but showed no significant modulation. Malate dehydrogenase and 3-hydroxyacyl-CoA dehydrogenase, which were identified during this study, have been reported to have decreased activity in mitochondria from glycolytic muscle fibres. This study suggests that the change in activity observed by other researchers is due to inhibition of these enzymes in the glycolytic fibres or activation in the oxidative fibres.

Acknowledgements

I would first and foremostly like to thank my masters supervisor, Dr. Ryan Martinus. Thank you for allowing me the freedom to design my own personal research interests into this study and especially for all the extra effort you have put in this last month, helping me finish this thesis.

Big thanks also go to Dr. Ravi Kambadur and Dr. Mridula Sharma of the Growth and Development Group at AgResearch, Ruakura, Hamilton, for access to the samples used for this study. And to Alex Henebry, who devoted a lot of time to dissecting out the muscles for me.

Thank you to the University of Waikato and the School of Science and Engineering for providing study grants to assist me in this endeavor. Without that extra financial support I don't know whether I could have got through it.

To Kerry Allen, thank you for all your help and for 'baby sitting' me while Julie was away. Lance McLeay for the donation of muscle samples used during the setup phase of this project and for assisting me with my application for ethics approval. And to Wendy Jackson for keeping me company during many hours of database searching.

To everyone in the Molecular Genetics Laboratory at the University, staff and students, thank you for all the advice and assistance, and for letting me occupy the equipment situated in your lab for so much of this year.

To everyone that I've worked with in the Cellular and Molecular Biology Laboratory over the past two years, Julie Goldsbury, Farina Munif, Lisa Hwang, Ajay Waggle Nikki Harcourt and Nikki Wallace, thank you for being there to listen to me go on when things weren't going right, for smiling and nodding when I got way too excited when things did go right, and most of all, for putting up with me occupying all the space in the lab.

And to my friends and family, thank you for understanding why you haven't heard from me for the past three months, and for the support you've given me for the last five years (and hopefully for the next three).

Contents

List of Figures

List of Tables

List of Appendices

Abbreviations Used

The following abbreviations have been using during this thesis:

2-D, two dimensional; 2-DE, two-dimensional electrophoresis; A, amp(s); ACN, acetonitrile; Act RIIB, activin type IIB receptor; Act RI, activin type I receptor; ADP, adenosine-5'-diphosphate; ANT, adenine nucleotide translocase; APS, Arg, arginine; ammonium persulphate; ATP, adenosine-5'-triphosphate; AU, arbitrary unit; β, beta; b, base; BCA, bicinchoninic acid; BG, background; BSA, bovine serum albumin; °C, degrees Celsius; c, centi (10^2); Cdk, cyclin-dependent kinase; CHAPS, 3-[(3-cholamidopropyl) dimethylammonio]-1-propanesulfonate; CO_2, carbon dioxide; CoA, coenzyme A; COX, cytochrome *c* oxidase; Da, Dalton(s); DNA, deoxyribonucleic acid; DTT, dithiothreitol; *E. coli*, *Escherichia coli*; EDL, extensor digitorum longus; EDTA, ethylenediaminetetra-acetic acid; EGTA, ethylene glycol-bis-(beta-aminoethyl ether)- N,N,N',N' tetracetic acid; ETS, electron transport system; $FADH_2$, flavin adenine dinucleotide; g, gram(s); GDF, growth and differentiation factor; GRP, glucose regulated protein; H_2O, water; H_2O_2, hydrogen peroxide; HCCA, alpha-cyano-4-hydroxy-cinnamic acid; HCl, hydrochloric acid; hr, hour(s); hsp, heat shock protein; IAA, iodoacetamide; IEF, isoelectric focusing; IgG, immunoglobulin G; IPG, immobilized pH gradient; k, kilo (10^3); KO, knockout; L, litre(s); LAP, latency associated protein; LC, liquid chromatography; μ, micro (10^{-6}); m, metre and also milli (10^{-3}); M, molar or moles per litre; MALDI-TOF, matrix assisted laser desorption ionization – time of flight; min, minute(s); MRF, muscle regulatory factor; mRNA, messenger ribonucleic acid; MS, mass spectrometry; MS/MS, tandem mass spectrometry; m/z, mass over charge ratio; n, nano (10^{-9}); NADH, nicotinamide adenine dinucleotide; NADPH, nicotinamide adenine dinucleotide phosphate; N-terminal, amino terminal; O_2, oxygen; PAGE, polyacrylamide gel electrophoresis; PBS, phosphate buffered saline; pH, hydrogen ion concentration; pI, isoelectric point; PMF, peptide mass fingerprint(ing); PTM, post-translational modification; PVDF, polyvinylidene fluoride; rcf, relative centrifugal force; rpm, revolutions per minute; Ser, serine; SDS, sodium dodecyl

sulphate; TBP, tributylphosphine; TBS, Tris buffered saline; TBST, Tris buffered saline with Tween; TCA, tricarboxylic acid; TEMED, N,N,N',N'-tetramethylethylenediamine; TFA, trifluoroacetic acid; TGF-β, transforming growth factor beta; Thr, threonine; Tris, 2-amino-2-(hydroxymethyl)-1,3-propanediol; UCP, uncoupling protein; sec, second(s); SOD, superoxide dismutase; V, volt(s); V/hr, volt hour(s); v/v, volume per volume ratio; WT, wild type; w/v, weight per volume ratio.

CHAPTER ONE

Introduction and Literature Review

The following review will cover the biology of myostatin, and the effect its removal has on animals, focusing in on the metabolic consequences of the myostatin knockout phenotype and how comparative proteomics can and has been used to investigate differences in mitochondrial metabolic processes.

1.1 Myostatin

Myostatin, which is also known as growth and differentiation factor (GDF)-8, is a secreted protein which is predominantly expressed in skeletal muscle, and negatively regulates muscle growth by altering transcriptional activity through the activin type II receptor.

1.1.1 *Characteristics of myostatin*

The full length myostatin protein consists of a hydrophobic signal sequence for secretion at the amino terminal (N-terminal), followed by what is called the latency associated protein (LAP) and a small mature region at the carboxyl terminal. The pattern of cysteine residues in the mature region of the protein is highly conserved and forms a cysteine knot when the protein homodimerises (McPherron *et al.*, 1997). These are the common characteristics of the transforming growth factor beta (TGF-β) superfamily, of which myostatin is a member (McPherron *et al.*, 1997).

Myostatin is synthesized as a 52kDa precursor molecule (Thomas *et al.*, 2000) which dimerises with another myostatin molecule by the formation of disulfide bonds in the LAP and the mature region (McPherron *et al.*, 1997). This inactive form of myostatin is secreted into the systemic circulation, where it is proteolytically processed by bone morphogenetic protein-1/tolloid metalloproteinases (Wolfman *et al.*, 2003; Scott *et al.*, 1999) at a highly conserved Arg-Ser-Arg-Arg (R-S-R-R) cleavage site (Thomas *et al.*, 2000). The 40kDa LAP portion of the protein is cleaved from the 12kDa mature region, releasing the 24kDa active myostatin dimmer, which is responsible for inhibition of skeletal muscle growth, see Figure 1.1 *A*.

Myostatin is present in all vertebrates, and shows a high degree of homology between a broad spectrum of animals. McPherron and Lee (1997) compared the amino acid sequence for myostatin from murine, rat, human, baboon, bovine, porcine, ovine, chicken, turkey and zebrafish. All sequences had a punitive secretion signal sequence at the N-terminus, and a proteolytic cleavage site between amino acid 263 and 266. Most of these followed the sequence R-S-R-R except for the zebra fish myostatin. All the animals contained identical spacing of the cysteine residues in the mature region of the protein and six of the ten animals investigated had identical mature regions.

1.1.2 *Myostatin signalling*

Myostatin exerts its effect on muscle cells by binding to the activin type IIB receptor (Act RIIB) on the outside of the cell (Lee and McPherron, 2001). Act RIIB and the type I receptor are trans-membrane serine-threonine (Ser-Thr) receptor kinases with

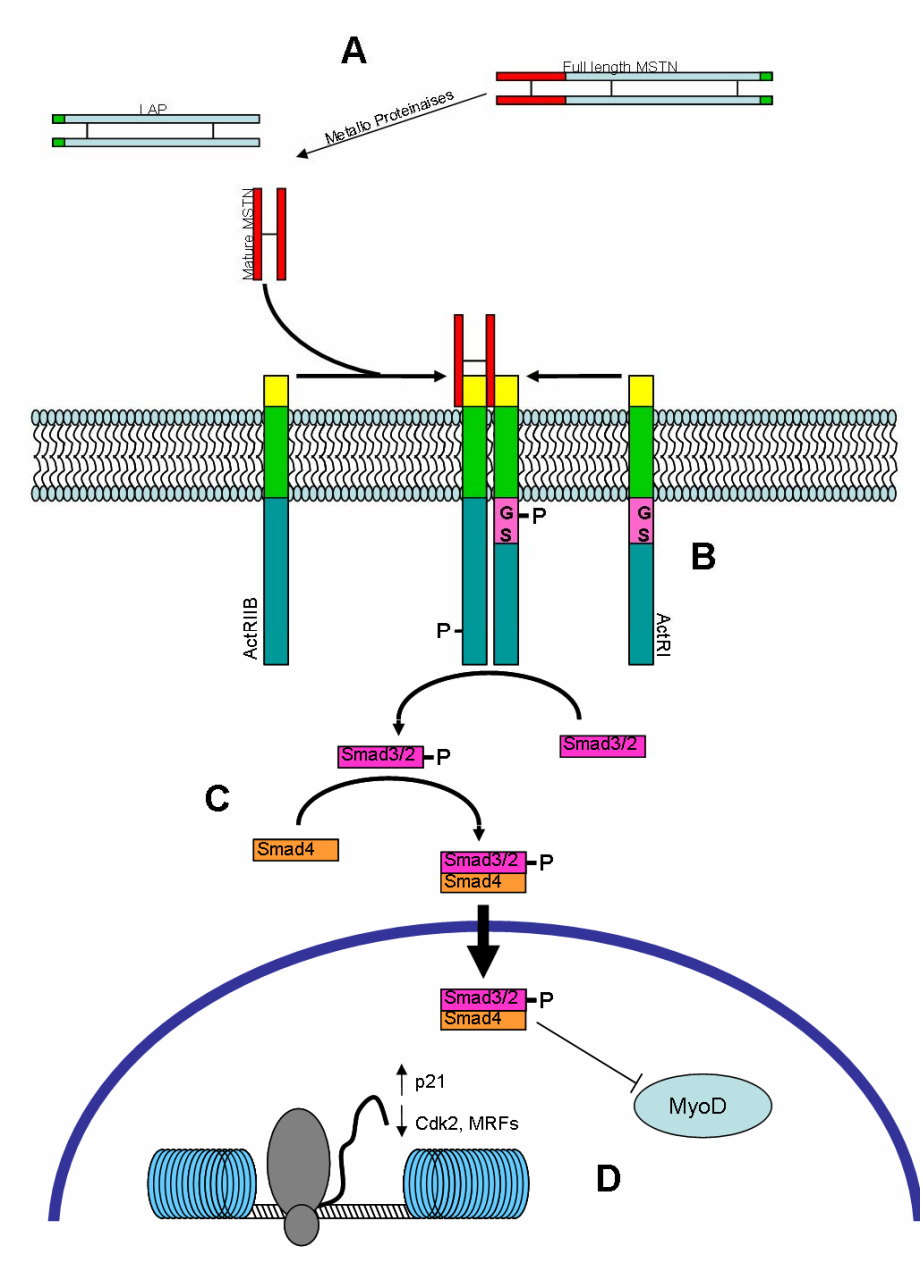

Figure 1.1 *The processing of myostatin and its role as a signaling molecule.* **(A)** Mature myostatin is cleaved from the LAP by metallo proteinaises. **(B)** It can then bind to the activin type IIB receptor, which auto-phosphorylates itself. The activin type I receptor is recruited to the complex and its GS domain is phosphorylated by the type II receptor. **(C)** The type I receptor then phosphorylates Smad2 and Smad3 which form heterodimers with a Smad4. **(D)** This can then translocate the nuclear membrane and alter transcription rates, Smad3 also interacts directly with MyoD to inhibit its action.

cysteine-rich extracellular domains, a membrane spanning domain, and an intracellular Ser-Thr kinase domain. The type I receptor differs from the type II receptor by having a serine-glycine repeat, just before the intracellular Ser-Thr kinase domain, this is termed the GS domain (Shi and Massague, 2003).

The two receptor molecules usually exist as monomers in the cell membrane, but when a ligand binds to the type II receptor, the type I receptor is sequestered to the complex. Upon binding the ligand, the type II receptor phosphorylates itself and the GS domain of the type I receptor, activating its Ser-Thr kinase domain (Shi and Massague, 2003), as shown in Figure 1.1 *B*.

The activated type I receptor goes on to phosphorylate Smad2 and Smad3 in the cytoplasm of the cell (Shi and Massague, 2003). Once phosphorylated, these Smads form heterodimers with Smad 4 and this complex is then able to translocate the nuclear membrane and exert transcriptional control (Shi and Massague, 2003). See Figure 1.1 *C*.

Smad3 and Smad4 have both been shown to interact directly with DNA at Smad binding elements, which consist of a palindromic (GTCTAGAC) sequence, present in the promoter regions of many TGF-β sensitive genes (Dennler *et al.*, 1998; Derynck *et al.*, 1998; Zawel *et al.*, 1998). Binding of the Smad complex to these promoter regions up-regulates and down-regulates an array of genes involved in muscle growth and differentiation, see Figure 1.1 *D*.

1.1.3 *Physiological action of myostatin*

Myostatin inhibits myoblast proliferation by up-regulating the cyclin-dependent kinase (Cdk) inhibitor, p21, and at the same time down-regulating expression of Cdk2. The resulting reduction in Cdk2 activity, from p21 induced inhibition and reduced levels, results in the retinoblastoma protein becoming hypo-phosphorylated. This results in the cell cycle being arrested in G_1 phase (Joulia *et al.*, 2003; McCroskery *et al.*, 2003; Rios *et al.*, 2001).

Myostatin also inhibits myoblast differentiation by down-regulating muscle regulatory factors (MRFs): MyoD, Myf-5 and myogenin. MRF levels are modulated by both over-expression of myostatin (Joulia *et al.*, 2003), and genetic deletion of the protein coding sequence (McCroskery *et al.*, 2003; Langley *et al.*, 2002). Smad 3 also inhibits MyoD directly by interfering with the formation of the active MyoD·E protein complex (Liu *et al.*, 2001).

Myostatin acts as a chalone, a term coined by Bullough in 1962 to describe a secreted molecule which acts upon itself to inhibit various cellular functions. In the case of myostatin, to inhibit growth of the muscle cells it is produced by. When myostatin is not functional, or is not present, there is increased myoblast proliferation and differentiation. The result of this in an increase in muscle mass due to an increase in the number of muscle fibres (hyperplasia), and/or in the size of the individual muscle fibres (hypertrophy) (McCroskery *et al.*, 2003). This phenomenon is called double-muscling, and will be discussed in greater detail in section 1.2.

1.1.4 *Expression of myostatin*

Myostatin is expressed early on during embryogenesis (Amthor *et al.*, 2002; *McPherron et al.*, 1997) and continues to be expressed right into adulthood (Kambadur *et al.*, 1997; McPherron *et al.*, 1997). It is predominantly expressed in skeletal muscle (Potts *et al.*, 2003; Jeanplong *et al.*, 2001; Oldham *et al.*, 2001; Bass *et al.*, 1999; Carlson *et al.*, 1999; Kocamis *et al.*, 1999; Sharma *et al.*, 1999; Ji *et al.*, 1998; Kambadur *et al.*, 1997; McPherron *et al.*, 1997), but has also been detected at much lower levels in other muscles and tissues (Sharma *et al.*, 1999; Ji *et al.*, 1998; McPherron *et al.*, 1997).

Within skeletal muscle, myostatin is further restricted to certain muscle fibre types. Myostatin is expressed in higher amounts in the type II fibres (fast twitch) than it is in type I fibres (slow twitch) (Carlson *et al.*, 1999). The consequence of this unique pattern of expression, when functional myostatin is lost, will be discussed further in section 1.2.1.

1.2 Double-muscling

The double muscling phenomenon was first documented by Culley (1807). It occurs naturally in several cattle breeds, the most well characterised being the Belgian Blue and Piedmontese breeds. Recently, many different methods of inducing double muscling in animals, through myostatin knockout, have been used.

1.2.1 *Characteristics of the double-muscling phenotype*

The primary characteristic of the double-muscling phenotype is an increase in muscle mass and a decrease in fat deposition (McPherron *et al.*, 1997). The double-muscling phenotype is also characterised by reduced connective tissue, a lower proportion of bone, and a reduction in size of organs such as the heart, lungs and liver (Boccard, 1981). Double-muscled cattle are also more susceptible to stress and heat. They have a reduced capacity to dissipate the extra heat generated by their increased muscle mass, due to a reduced respiratory capacity, less body surface per mass unit and poorer circulation. The animals also fatigue faster than normal animals because of increased metabolic acidosis caused by lower aerobic muscle metabolism (Boccard, 1981) and reduced blood circulation (Menissier, 1982) to remove the lactate produced.

Double-muscled animals also have an altered fibre type composition. In the double-muscled tissue there is a larger proportion of type II fibres, and a reduction in the number of type I fibres. There is also an increased amount of type IIB fibres (glycolytic) compared to type IIA fibres (oxidative) (Girgenrath *et al.*, 2005). A transition from type IIA fibres to type IIB fibres naturally occurs as animals age, but

this effect is more exaggerated in animals which lack functional myostatin (Wegner *et al.*, 2000), presumably due to the increased level of type II fibres present in the animals. This has been coined the 'glycolytic switch' and in mice occurs within six weeks of birth (personal communication with Ravi Kambadur).

1.2.2 *Genetic deletion of mature myostatin*

Myostatin was discovered in 1997 by McPherron *et al.*, when they replaced the mature region of myostatin with a neomycin cassette. This resulted in a 10.4kb transcript which lacked the functional region of myostatin (the mature region), instead of the 11.2kb transcript seen in wild type mice. This genetic deletion of myostatin resulted in double-muscling due to both hyperplasia and hypertrophy. Skeletal muscle samples used in this study were obtained from myostatin knockout mice generated from the above genetic deletion.

There are many other methods of inducing double-muscling in animals through myostatin knockout. These are summarised in Table 1.1. It is notable to point out that the mutations which occur in the myostatin gene from Belgian Blue and Piedmontese cattle were naturally occurring mutations which have subsequently been selected for by the meat industry (Bellinge *et al.*, 2005).

Table 1.1 *Methods of myostatin knockout*
Methods of myostatin knockout that have been shown to induce double-muscling in animals and the characteristics that each of these models display.

Method of myostain knockout	Animal used in model	Characteristics of model	Reference
▪ Deletion of nucleotides 821-831	▪ Belgian Blue cattle	▪ Frame shift and premature termination. ▪ Hyperplasia. ▪ Increase in glycolytic fibres.	Grobert *et al.*, 1997; Kambadur *et al.*, 1997; McPherron and Lee, 1997
▪ G to A transition at amino acid 314	▪ Piedmontese cattle ▪ Mice	▪ Cysteine knot cannot form. ▪ Hyperplasia. ▪ Increase in glycolytic fibres.	Berry *et al.*, 2002; Nishi *et al.*, 2002; Grobert *et al.*, 1997; Kambadur *et al.*, 1997; McPherron and Lee, 1997
▪ Deletion of exon 3.	▪ Mice	▪ Hyperplasia and hypertrophy. ▪ Increase in glycolytic fibres.	McPherron *et al.*, 1997
▪ Over-expression of follistatin	▪ Mice	▪ Antagonises myostatin. ▪ Hyperplasia and hypertrophy	Lee and McPherron *et al.*, 2001
▪ Over-expression of the LAP	▪ Mice	▪ Antagonises myostatin. ▪ Hyperplasia and hypertrophy	Lee and McPherron *et al.*, 2001
▪ Postnatal genetic deletion of exon 3 by *cre-loxP*.	▪ Mice	▪ Exon 3 not transcribed when cre-recombinase is expressed. ▪ Hypertrophy and minute hyperplasia.	Grobert *et al.*, 2003
▪ Postnatal administration of anti-myostatin antibodies.	▪ Mice	▪ Antagonises myostatin. ▪ Hypertrophy. ▪ No change in metabolism.	Girgenrath *et al.*, 2005; Whittmore *et al.*, 2003

1.3 How do muscle cells obtain ATP from metabolic processes?

Cellular metabolism is based around three central pathways, which break down substrates to form ATP: glycolysis, the tricarboxylic acid (TCA) cycle and oxidative phosphorylation. The three different processes are localised within the cell, with glycolysis occurring in the cytoplasm, the TCA cycle in the matrix of the mitochondria and oxidative phosphorylation in the mitochondrial inner membrane. The different muscle fibre types discussed thus far, type I, type IIA, and type IIB, are characterised firstly on their twitch speed and then by how they obtain their energy, whether primarily from glycolytic processes or oxidative phosphorylation.

1.3.1 *Glycolysis*

Glycolysis is observed in all organisms. Glucose is broken down in a series of ten reactions to yield two pyruvate molecules, two ATP and two NADH. Different sugars can be fed into glycolysis at various stages and larger sugars and carbohydrates can be broken down to be utilised as a substrate.

The first phase of glycolysis involves priming of the glucose by phosphorylating it twice. The D-fructose-1,6-bisphosphate formed is cleaved into two three carbon sugars, which go on to produce four ATP via substrate-level phosphorylation, two NADH and two molecules of pyruvate in the second phase of glycolysis. For glycolysis to continue functioning, the NADH produced in this reaction must be re-oxidised to NAD^+. In animals, this can occur through the electron transport system in the mitochondria, but not under anaerobic conditions, such as rapidly contracting

muscles. In this situation the pyruvate produced in glycolysis is reduced to lactate, re-oxidising NADH to NAD^+ (Garrett and Grisham, 1999).

1.3.2 *Tricarboxylic acid cycle*

The TCA cycle can feed on more substrates than just pyruvate. Amino acids, glycerol and fatty acids can also be oxidised in the TCA cycle, and the reducing potential produced used to make ATP.

Carbon can enter the TCA cycle at many different locations, but primarily enters as acetyl-CoA which is transferred to oxaloacetate by citrate Synthase. The acetyl-CoA can be produced from pyruvate, being fed into the TCA cycle through the pyruvate dehydrogenase complex, or by β-oxidation of fatty acids. The citrate produced in this reaction goes through a series of eight reactions, removing two CO_2 molecules, and producing one ATP via substrate-level phosphorylation, one $FADH_2$ and three NADH, in addition to the molecule produced by pyruvate dehydrogenase. This series of reactions results in oxaloacetate being formed to act as the carrier in the next cycle (Garrett and Grisham, 1999).

1.3.3 *Oxidative phosphorylation*

Although glycolysis and the TCA cycle produce four ATP by oxidising a single molecule of glucose to carbon dioxide, most of the energy is retained in the reducing potential stored in the molecules of NADH and $FADH_2$ which were produced. This energy is converted into ATP by oxidative phosphorylation, utilising the electron transport system (ETS) and ATP synthase enzyme complex embedded in the

mitochondrial inner membrane. The NADH is used to reduce coenzymes of the respiratory chain and the $FADH_2$ to reduce the flavoproteins. The electron gained from this reduction is passed down from one component of the ETS to the next, due to an increase in the reduction potential of each component. As the electrons move through each of the ETS components, their reduction potential gradually approaches that of O_2/H_2O, until they reach cytochrome *c* oxidase (COX), the terminal electron acceptor. It is here that the electrons are passed onto oxygen and hydrogen, forming water.

The proton from the coenzyme/flavoprotein reduction mentioned before is pushed into the inter-membrane space of the mitochondria, eventually building up a proton gradient. The energy stored in this chemiosmotic gradient is converted into the high energy phosphate bond in ATP by ATP synthase. This protein complex, made up of approximately 24 subunits, acts as a motor and turns as protons flow through its F_0 complex. This drives the conformational changes in the F_1 complex required to synthesise ATP.

Utilising oxidative phosphorylation to fully oxidise the glucose molecule introduced into glycolysis results in approximately 15 times more ATP being produced than with glycolysis. It also provides for the re-oxidation of NADH to NAD^+ in aerobic situations, without lactic acid buildup. But oxidative phosphorylation cannot operate in an anaerobic environment, and is a slower method of energy production than glycolysis (Garrett and Grisham, 1999).

1.3.4 *Muscle fibre type differences in cellular metabolism*

General differences seen between type I and type II fibres are that type I have more mitochondria (Schmidt and Herpin, 1997; Jackman and Willis, 1996) and higher myoglobin content (Donoghue *et al.*, 2005; Kim *et al.*, 2004). This is due to the Type I fibres relying on oxidative phosphorylation for their ATP supply. Type IIB fibres rely primarily on glycolysis for energy production and have increased expression of glycolytic enzymes to support this (Hallauer and Hastings, 2002; Rivero *et al.*, 1998). Even though Type IIA fibres are fast twitch fibres, they rely on oxidative phosphorylation for their energy and have been described as having a more similar mitochondrial profile to type I fibres, than to type IIB fibres (Gueguen *et al.*, 2005A). Because of this, muscle fibres discussed from herein will refer to their method of energy metabolism, oxidative or glycolytic, and not their twitch speed.

Oxidative and glycolytic fibre mitochondria do not show any difference in ATP synthase activity, but oxidative fibre mitochondria do show a greater rate of ATP synthesis (Gueguen *et al.*, 2005B). This was postulated to be due to the increased COX activity seen in mitochondria from oxidative fibres (Gueguen *et al.*, 2005B; Schmidt and Herpin, 1997; Jackman and Willis, 1996). Mitochondrial respiration studies, using mitochondria isolated from oxidative and glycolytic fibres, report high respiratory control ratios, between 4 and 19, indicating well coupled mitochondria (Gueguen *et al.*, 2005B; Mogensen and Sahlin, 2005; Schmidt and Herpin, 1997). Basal respiration (state IV respiration) in mitochondria isolated from oxidative and glycolytic fibres is the same (Gueguen *et al.*, 2005B; Mogensen and Sahlin, 2005), but ADP stimulated respiration (state III respiration) differs. Compared to utilization

of a fatty acid substrate mitochondria from both oxidative and glycolytic fibres respire well of pyruvate. But there is deliberation as to whether glycolytic or oxidative fibres have a higher respiration rate. Both Gueguen *et al.* (2005B) and Jackman and Willis (1996) have reported it higher in oxidative fibres, whilst Mogensen and Sahlin (2005) report conflicting results. But respiration rates of glycolytic fibre mitochondria fed on the fatty acid, palmitoyl-L-carnitine drop dramatically. State III respiration on this substrate was 58% of that seen on pyruvate in the glycolytic fibre mitochondria, whilst oxidative fibre mitochondria maintained 95% of their respiratory activity (Mogensen and Sahlin, 2005). This supports the higher COX activity observed in oxidative fibres (Gueguen *et al.*, 2005B; Schmidt and Herpin, 1997; Jackman and Willis, 1996) and their increased capacity for fatty acid metabolism (reviewed in Cortright *et al.*, 1997).

Mitochondria from oxidative fibres have also been shown to have a lower sensitivity to ADP than those from glycolytic fibres (Gueguen *et al.*, 2005A; Willis and Jackman, 1995). Mogensen and Sahlin (2005) found that glycolytic mitochondria had a higher affinity for ADP when feeding on palmitoyl-L-carnitine. They suggested that this would be advantageous for the animal as it would divert metabolism to the mitochondria and fatty acid metabolism during times of basal respiration, when ATP and oxygen concentrations were high. This would conserve carbohydrate stores for times of exertion when glycolytic metabolism was utilised. However, these studies were performed in the presence of ATP consuming enzymes, Gueguen *et al.* (2005B) later showed the mitochondria's affinity for ADP is inhibited by the presence of ATP. This ATP inhibition was more pronounced in mitochondria from glycolytic fibres

though, supporting the data showing an increased affinity for ADP in glycolytic fibre mitochondria. The mechanism for this ATP mediated inhibition is still to be elucidated, but it is theorised that the ATP could compete with ADP for binding of the adenine nucleotide translocase (ANT) and subsequent transport across the mitochondrial membrane. Interestingly, at basal ATP levels in muscle, 5-8mM, this ATP inhibition could be occurring. This suggests that mitochondrial activity in glycolytic fibres could be more important during the recovery phase after rapid muscle contraction, than during basal respiration.

This shows that there is still deliberation about the function of mitochondria present in the glycolytic muscle fibres. And it still remains to be elucidated, how the changes which have been observed are actually occurring.

1.3.5 *Metabolism in double-muscled animals*

McPherron and Lee (2002) investigated the metabolism of myostatin knockout mice, compared to wild type mice to determine whether the decreased fat accumulation seen in the knockout mice was due to increased oxidative metabolism. They found a decreased metabolic rate compared to the wild type animals, despite similar food intake. This reduced consumption of oxygen (per unit mass) in the knockout animals was supported by a reduced expression of mitochondrial inner membrane uncoupling proteins, UCP2 and UCP3.

Because double-muscled animals have an increased proportion of type IIB fibres (Girgenrath *et al.*, 2005) one could expect the cellular metabolism of the double-

muscled muscle to have an increased capacity for glycolytic metabolism. The role mitochondria play in glycolytic muscle fibres is not well characterised, nor is how they function differently from the mitochondria found in oxidative muscle fibres. But, as described in section 1.3.4, differences in the mitochondria are seen, and would have more impact in double-muscled animals due to the increase in glycolytic muscle fibres.

The muscle would have a reduced capacity for oxidative phosphorylation due to a reduced COX activity (Gueguen *et al.*, 2005B; Schmidt and Herpin, 1997; Jackman and Willis, 1996), and a reduction in the number of mitochondria (Schmidt and Herpin, 1997; Jackman and Willis, 1996). The mitochondria could be utilised to support basal and recovery metabolism, but could not be used during rapid contraction, as the muscles would be operating anaerobically due to the reduced myoglobin content (Donoghue *et al.*, 2005; Kim *et al.*, 2004), which helps sequester oxygen from the blood. The glycolytic fibres are adapted to this however by having increased levels of glycolytic enzymes (Hallauer and Hastings, 2002; Rivero *et al.*, 1998), which provides the quick ATP supply needed to produce the fast contractions seen in the type II fibres. But reliance on glycolysis to generate ATP occurs at the expense of lactate build-up due to pyruvate being converted to lactate to facilitate the re-oxidation of NADH.

1.4 Comparative proteomics

Proteomes are the full compliment of proteins expressed by a given genome in a particular cell or sub-cellular organelle. Proteomes are dynamic in that they can be altered during development and by the changing conditions cells are subjected to. Whilst genetic methods of detecting changes in levels of gene expression goes some way to understanding what is happening in the various tissues, gene expression levels are not always translated into the functional units of the cell, the proteins. Comparative proteomics allows one to see differences in the level of proteins and has the added effect of not having to know what you are looking for. It involves the isolation of individual proteins, quantitating their expression and identifying the proteins which show differences.

1.4.1 *Two-dimensional electrophoresis comparative proteomics*

Two-dimensional electrophoresis (2-DE) is the primary separation tool used for proteomics investigations and will be used during this study. It involves separating a protein mixture first by the protein's net charge by isoelectric focusing (IEF) and then by its molecular weight by sodium dodecyl sulphate - polyacrylamide gel electrophoresis (SDS-PAGE). It allows for the separation of hundreds of proteins on a single gel and can be quantitative (Encarnacion *et al.*, 2005), allowing for differences in protein levels to be deduced. The gel format also allows various analyses to be carried out, protein identification by mass spectrometry (MS) or post translational modification (PTM) detection via western analysis.

Due to the IEF step, solubilising agents for 2-DE are limited to non-ionic detergents and denaturing agents. Generally urea and 3-[(3-cholamidopropyl) dimethylammonio]-1-propanesulfonate (CHAPS) are used, however these agents are limited in their solubilising efficiency of hydrophobic proteins. Stronger non-ionic detergents and denaturants have been used with some success. Molloy *et al.* (1998) used urea, thio-urea, CHAPS and caprylyl sulfobetaine, and was able to detect seven hydrophobic outer membrane proteins in *E. coli*, two of which had not been detected in 2-DE gels before and another two had only been detected as open reading frames. For a hydrophobic protein to be resolved in a 2-DE gel, it not only has to be solubilised from the cell lysate, but also has to remain in solution throughout the focusing step. Many hydrophobic protein losses occur due to absorption to the gel matrix and precipitation as they approach their isoelectric point, resulting in the protein never being transferred to the second dimension (Adessi *et al.*, 1997). Use of the non-ionic reducing agent tributyl phosphine (TBP) has been shown to alleviate this problem as TBP is not charged. This means that it does not migrate as the IEF progresses, so a constant amount is maintained throughout the gel to maintain the protein's reduced state, aiding in its solubility (Herbert *et al.*, 1998).

Even though hydrophobic proteins are still difficult to resolve by 2-DE, many of the other problems it originally faced have been fixed in the last 25 years. When first introduced, carrier ampholyte gels were used for the IEF step. These yielded low resolution separations, had a limited loading capacity and showed low reproducibility. They were replaced with immobilised pH gradients (IPG) in which the chemicals producing the pH gradient were covalently anchored to the polymer

matrix. This allowed for the production of pH gradients which were stable over time, were reproducible, had a high loading capacity and could yield high resolution separations due to narrow pH gradients (less than 0.05pH/cm) (Gorg *et al.*, 1988). IPGs which stretch to a pH of 12 have been developed so that proteins which are highly alkaline can now be resolved (Gorg *et al.*, 2000).

Due to the vast amount of different proteins and protein isoforms present in cells, strategies to increase resolution have had to be developed. The most common strategy to increase resolution is to use a narrower pH gradient, allowing for smaller increments in the pH. A series of overlapping pH gradients can then be used to assess the cell's proteome (Gorg *et al.*, 2004). Another strategy is to look at specific organelles in the cell individually, reducing the number of proteins to be assessed, and enabling them all to be resolved whilst maintaining a lower level of resolution (Ahmed and Rice, 2005). Molloy *et al.* (1998) utilised a differential extraction technique to separate proteins according to their solubility prior to separation by 2-DE, again reducing the amount of protein to be resolved in each gel.

1.4.2 *Protein identification from 2-DE gels*

Proteins in this study were identified by peptide mass fingerprinting (PMF) and matrix assisted laser desorption ionisation – time of flight (MALDI-TOF) MS by performing an in-gel tryptic digest as outlined in Figure 1.2. This involves excising a piece of the gel containing the protein and destaining it, dehydrating the gel piece and drying it. Here the protein can be reduced and alkylated, if this was not performed prior to running the second dimension. It is then incubated in trypsin, which cleaves

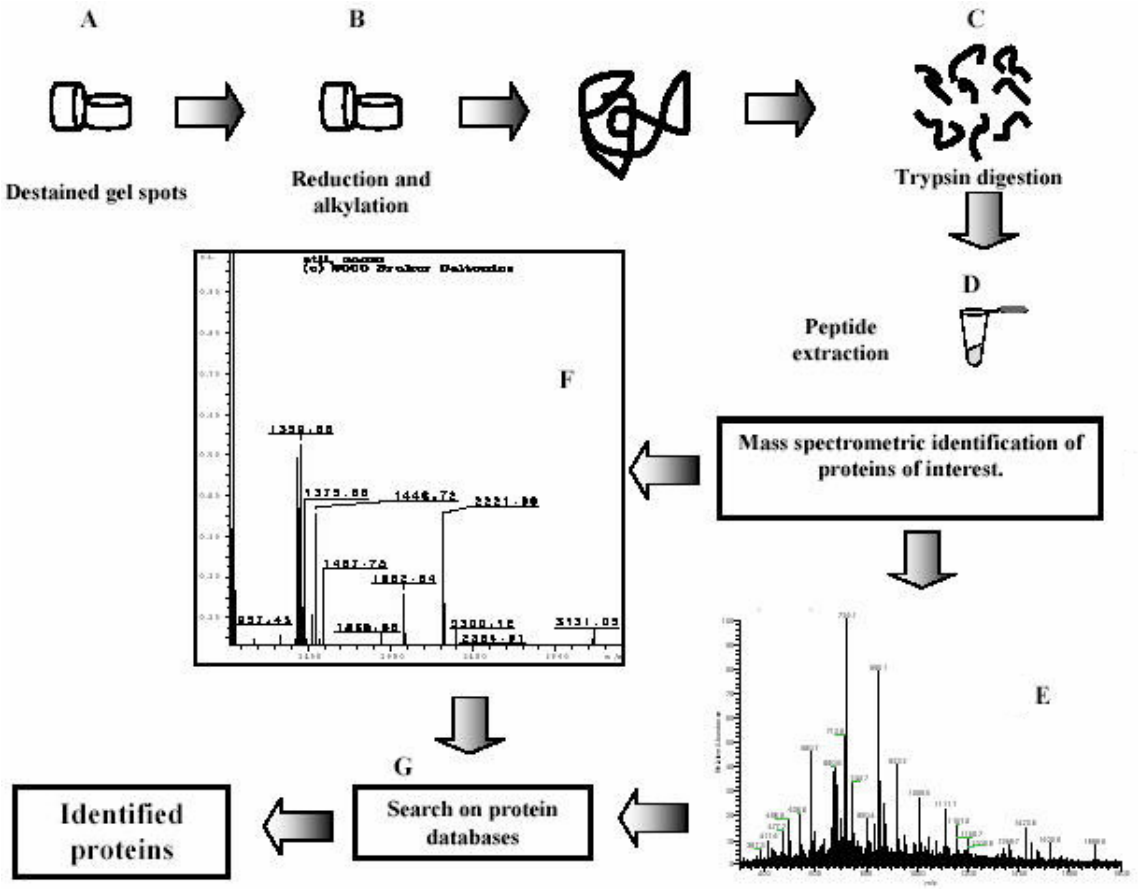

Figure 1.2 *Flow diagram of how proteins are identified from 2-DE gel plugs using in-gel tryptic digests and mass spectrometry.*
(A) Gel plugs are destained depending upon how they were stained. **(B)** After drying, reduction and alkylation of the protein can be performed. **(C)** The protein is cleaved into a series of peptides by trypsin. **(D)** Peptides are extracted from the gel plug into a solution. The peptides can then be analysed by **(E)** PMF using MALDI-TOF MS or **(F)** peptide sequencing by LC-MS/MS. **(G)** The resulting peptide masses or sequences can then be searched against a database to identify the protein. (adapted from Encarnacion *et al.*, 2005)

the protein into a series of peptides which are extracted from the gel into a solution (Encarnacion *et al.*, 2005) and laid on a MALDI-TOF target with a matrix, α-cyano-4-hydroxy-cinnamic acid (HCCA), to facilitate sample ionisation.

Because trypsin cleaves specifically on the carboxylic side of lysine and arginine residues, unless followed by a proline, the peptides resulting from digests are specific for the protein digested. The mass of these peptides are acquired by MS and matched against genetic databases, NCBI or SwissPROT, via a search engine, such as Mascot™. The databases contain protein sequences deduced from genetic sequences submitted to the database, which theoretical tryptic digests have been performed on and the masses of the resulting peptides calculated. Searching the NCBI database, significant matches are achieved by obtaining a protein score from the search, which is higher than that imposed by the database. The score required is altered by defining the organism which the sequence was derived from. If one is more specific with the organism the protein came from, the probability of the observed match being a random event is lowered, and the protein score is lowered. The protein score from the search is equal to $-10 \times log(P)$, where P is the probability that the observed match is a random event. The probability of this function can be altered by decreasing the error allowed for peptide matches, therefore increasing the certainty that the peptides do correspond to the peaks seen in the spectrum.

The other method of identifying proteins by MS is to sequence the peptides, generally by liquid chromatography (LC) coupled with tandem MS (MS/MS). The peptides are separated out by reversed phase LC and then sequence information is acquired by

fragmentation of the peptide in the mass spectrometer. The resulting masses are used to deduce the peptide's sequence, which is then searched against databases to identify the protein. Both of these methods require that the protein's sequence already be present in the database to facilitate identification of the protein. However, if a novel protein was found in a sample, the sequence information acquired via tandem MS acts as a starting point for characterising the protein. By using different proteolytic enzymes, eventually a complete sequence can be built up as the proteinases will cleave at different locations and peptide sequences will overlap.

Other methods of protein identification are avaliable. N-terminal sequencing by Edman degradation can be used much the same as peptide sequencing by LC-MS/MS, matching an acquired sequence with those in protein databases. However this method has a sensitivity in the picamole range, where as MS can detect sample to a fentomole level. Western blotting with antibodies could allow for identification of proteins at a lower level than MS is capable of, but has the inherent disadvantage of having to know which protein you are looking for.

Obtaining an adequate spectrum to identify a protein by MS generally requires a coomassie stained spot (10ng of protein). The use of more sensitive staining techniques, such as fluorescent stains (0.5ng of protein), means that less protein has to be loaded onto the gel to detect a protein, but identification via MS may not be possible due to not enough protein being present. To get around this, preparative gels, overloaded with protein, can be run at the same time as an analytical gel, loaded with less protein, is run. The nicely resolved analytical gel is used for quantitating the

protein expression levels, whilst the preparative gel is used for identifying the proteins which show modulation.

1.4.3 *Mitochondrial proteomics*

Mitochondrial proteomics using the standard 2-DE gel format described in section 1.4.1 has been used to study mitochondria in various situations. From their involvement in neurodegenerative diseases (Zhang *et al.*, 2005; Scheffler *et al.*, 2001) and heart disease (Fountoulakis *et al.*, 2005), to how they are affected by free radicals (Douette *et al.*, 2006; Bailey *et al.*, 2005). Mitochondria have also been shown to differentially express proteins in different tissues (Forner *et al.*, 2006). The number of mitochondrial proteins detected by 2-DE vary depending on the staining and protein loading, one research group reporting detecting up to 1,200 individual proteins (Ruiz-Romero *et al.*, 2006), while others report seeing only 300 proteins (Zhang *et al.*, 2005; Scheffler *et al.*, 2001).

The limitation of using a 2-DE gel format for investigating the mitochondrial proteome is that many of the mitochondrial proteins are highly hydrophobic, and are unable to be resolved by 2-DE so it is restricted to looking at mostly matrix and inter-membrane space proteins. To resolve the membrane bound fraction of the mitochondria, one must undertake extra measures such as sucrose density gradient fractionation (Hanson *et al.*, 2001), affinity techniques to isolate specific complexes (Keeney *et al.*, 2006; Schilling *et al.*, 2005), or blue native electrophoresis (Brookes *et al.*, 2002; Schagger and von Jagow 1991).

1.4.4 *Muscle proteomics*

Only one comparative proteomics investigation has been undertaken comparing double-muscled and normal animals. Bouley *et al.* (2005) used 2-DE to separate skeletal muscle proteins from homozygote, heterozygote Belgian blue cattle and non-double-muscled cattle. The resulting expression pattern showed modulation of different contractile proteins, as well as an increase in phosphoglucomutase and a decrease in fatty acid-binding protein in the double-muscled animal. This fits the increased proportion of glycolytic muscle fibres which they observed, as phosphoglucomutase is involved in glycolytic metabolism and fatty acid-binding is involved in oxidative respiration.

Proteomics investigations have looked at mitochondrial proteins from skeletal muscle, but no studies, to my knowledge have looked specifically at the mitochondria in glycolytic fibres compared to those in the oxidative fibres. But several studies have looked at oxidative muscle tissue compared to glycolytic tissue. They generally found modulation in the levels of contractile proteins, varying between fast twitch isoforms and slow twitch forms, and modulation of some small heat shock proteins. But they also detected an up-regulation, in the oxidative fibres, of myoglobin levels as well as several metabolic proteins, including: Aconitase, ATP synthase, malate dehydrogenase, mitochondrial creatine kinase, NADH dehydrogenase and succinate dehydrogenase. The glycolytic fibres showed an increased level of glycerol-3-phosphate dehydrogenase (Sayd *et al.*, 2006; Donoghue *et al.*, 2005; Okumura *et al.*, 2005).

Studies of this nature could help deduce how the mitochondria are functioning in the glycolytic fibres, as studies discussed in section 1.3.4 have shown that mitochondria isolated from glycolytic fibres show differences to those from oxidative fibres. But much more work needs to be done to deduce the role of the mitochondria in the glycolytic fibre. As yet, no work has been done on the mitochondria in the myostatin knockout model of double-muscling. Due to the increased proportion of glycolytic fibres in myostatin knockout animals, it also provides a model to look at changes associated with differences in muscle fibre type metabolism.

1.5 Outline of this study

Thus far, little work has been done on the metabolism of myostatin knockout animals, and no work has looked at how the mitochondria in the double-muscled animals are affected. This is despite the increased proportion of glycolytic fibres seen in the double-muscled animals, obviously impacting on the mitochondria at some level (Girgenrath *et al.*, 2005). It is not known whether myostatin itself exerts any effect over mitochondria, but is quite possible as almost all of the mitochondrial proteins are translated from nuclear encoded genes (Paschen and Neupert, 2001).

Because of the altered muscle metabolism seen in myostatin knockout mice, they serve as a unique model to further investigate differences seen in mitochondria from glycolytic muscle fibres, due to their increased proportion of type IIB fibres (Girgenrath *et al.*, 2005).

This study aims to: (i) verify the myostatin knockout status of the mice used during this study (ii) investigate whether the mitochondria from myostatin knockout mice show any differences in basal mitochondrial stress levels, and (iii) use a comparative proteomics approach to try and deduce if the mitochondria from knockout skeletal muscle are different from those found in wild type animals.

CHAPTER TWO

Materials and Methods

This chapter reviews the materials and methods which were utilised during this study. It includes all reagents, chemicals and solution compositions, as well as a detailed overview of the methods used.

2.1 Materials

Section 2.1 outlines the commercially available kits and reagents used, the composition of all stock solutions used, and a list of chemical suppliers.

2.1.1 *Commercial kits*

2.1.1.1 *BCA protein estimation assay*

The bicinchoninic acid (BCA) protein assay kit was used to obtain an estimate of the total protein concentration present in samples. It was supplied by Pierce, Rockford, Illinois, USA. A list of its components and their contents are listed in Table 2.1:

Table 2.1 *BCA protein estimation assay*

Reagent Name	Content
BSA Standards	Flame sealed ampules containing 1 mL of 2,000µg/mL BSA in 0.9% saline and 0.05% sodium azide
BCA Reagent A	Sodium carbonate, sodium bicarbonate, bicinchoninic acid, sodium tartrate in 0.1M sodium hydroxide
BCA Reagent B	4% cupric sulfate

2.1.1.2 *Silver stain plus kit*

The silver stain plus kit was used to silver stain 2-DE and SDS-PAGE gels. The kit was supplied by Bio-Rad, Hercules, California, USA. A list of its components and their contents are listed in Table 2.2:

Table 2.2 *Silver stain plus kit*

Reagent Name	Content
Fixative Enhancer Solution	Glycerol
Silver Complex Solution	Silver nitrate, ammonium nitrate
Reduction Moderator Solution	Tungstosilicic acid hydrate
Image Development Solution	Formaldehyde
Development Accelerator Reagent	Sodium carbonate

2.1.2 *Antibodies*

Antibodies used and their sources are listed in Table 2.3:

Table 2.3 *Antibodies*

Antibody	Product #	Lot #	Source
Rabbit polyclonal to GDF8 / Myostatin	Ab996-50	96001	Abcam
Rabbit polyclonal to SOD2	SOD-110	02020602	Stressgen
Rabbit polyclonal to hsp60	SPA-805	007408	Stressgen
Rabbit polyclonal to actin (C-11)-R	sc-1615-R	K1904	Santa Cruz
Goat anti-rabbit IgG (Whole Molecule) - Alkaline Phosphatase conjugate	A3687	123K6037	Sigma

2.1.3 *Enzymes*

Enzymes used and their sources are listed in Table 2.4:

Table 2.4 *Enzymes*

Enzyme	Product #	Lot #	Source
Trypsin Gold, Mass Spectrometry Grade	V5280	203804	Promega

2.1.4 *Common solutions*

Common solutions were routinely made in the lab. Common solutions and their composition are listed in Table 2.5:

Table 2.5 *Common solutions*

Solution	Composition
PBS	8g NaCl (137mM) 0.2g KCl (2.7mM) 1.44g Na_2HPO_4 (4.0mM) 0.24g KH_2PO_4 (1.7mM) Dissolve in 800mL of MilliQ water and adjust to pH 7, make up to 1L, and chill at 4°C
1.5M Tris-HCl pH 8.8	90.83g Tris Dissolve in 400mL with MilliQ water, adjust to pH 8.8 with HCl, then make up to 500mL
0.5M Tris-HCl pH 6.8	15.14g Tris Dissolve in 200mL with MilliQ water, adjust to pH 6.8 with HCl, then make up to 250mL

10% SDS	25g SDS Make up to 250mL with MilliQ water
DTT Solution	250mg DTT in 0.5mL of MilliQ water Store at 4°C
Stock Buffer (Westermeier's)	6.06g Tris (0.5M) 0.4g SDS (0.4%) Dissolve in 80mL of MilliQ water, adjust to pH 6.8 with HCl, and make up to 100mL
Sample Loading Buffer (Westermeier, 1993)	1g SDS (1%) 0.003g EDTA (0.01mM) 0.01g bromophenol blue (0.01%) 1.0mL of DTT solution 2.5mL stock buffer (Westermeier's) 10.0mL glycerol (10%) Make up to 100mL with MilliQ water
5x Electrode Buffer	15g Tris (124mM) 72g Glycine (959mM) 50mL of 10% SDS (0.5%) Make up to 1L with MilliQ water
Fixative	400mL of methanol (40%) 100mL of acetic acid (10%) 500mL of MilliQ water
Coomassie Blue Stain	1g Brillant Blue R-250 (0.1%) Dissolve in 1L of fixative, and filter through #1 filter paper

Towbin Transfer Buffer	7.207g glycine (192mM) 1.514g Tris (25mM) 1.87mL of 10% SDS (1.3mM) 100mL of methanol (20%) Make up to 500mL with MilliQ water, and chill at 4°C
10% Tween 20	25g Tween 20 Make up to 250mL with MilliQ water
10x Tris Buffered Saline (TBS)	12.10g Tris (0.1M) 87.66g NaCl (1.5M) Dissolve in 800mL of MilliQ water, adjust to pH 7.7 with HCl, then adjust to 1L
TBST	100mL of 10x TBS 5mL of 10% Tween 20 (0.05%) Make up to 1L with MilliQ water
Mitochondrial Isolation Buffer	42.78g sucrose (250mM) 1.211g Tris (20mM) 1.491g KCl (40mM) 0.380g EGTA (2mM) 0.5g BSA (1mg/mL) Make up to 500mL with MilliQ water, and chill at 4°C
Mitochondrial Isolation Wash	5mL Percoll (5%) 95mL of Mitochondrial Isolation Buffer Chill at 4°C

TENT Buffer	1.51g Tris (50mM) 10.96g NaCl (150mM) 0.37g EDTA (5mM) 2.5mL of 50% (v/v) Triton X-100 (0.5%) Dissolve in 200mL of MilliQ water, adjust to pH 7.4 with HCl, and make up to 250mL Supplement with 0.4mM phenylmethylsulfonyl fluoride fresh daily
8.5M Urea	51g urea Make up to 100mL with MilliQ water, treat with mixed bed ion exchange resin, vacuum filter, and store at -20°C in 10mL aliquots
IPG Equilibration/Rehydration Solution	9.4mL of 8.5M Urea (8M) 0.2g CHAPS (2%) 100µL of 200mM TBP (2mM) 50µL of 40% (w/v) 3-10 ampholytes (0.2%) Make up to 10mL with MilliQ water
1% Bromophenol Blue	0.1g of bromophenol blue in 10mL of MilliQ water
SDS-PAGE Equilibration Buffer	36g urea (6M) 20mL of 10% SDS (2%) 3.3mL of 1.5M Tris-HCl pH 8.8 (50mM) 40mL of 50% (v/v) glycerol (20%) Make up to 100mL with MilliQ water, and store at -20°C in 12mL aliquots

SDS-PAGE Equilibration Buffer I	240mg DTT (2%) 12mL of SDS-PAGE Equilibration Buffer
SDS-PAGE Equilibration Buffer II	300mg iodoacetamide (2.5%) 12mL of SDS-PAGE Equilibration Buffer
2-DE Agar Overlay	0.5g agarose LE (0.5%) 0.003g bromophenol blue (0.003%) 100mL of 1x electrode buffer Heat in microwave until agar dissolves, store in 100mL schott bottle
50mM Acetic Acid	14.3µL acetic acid Make up to 5mL with MilliQ water
MALDI-TOF Wash Solution	5mL of 1% (v/v) TFA (0.1%) 45mL of 11.11mM $NH_4H_2PO_4$ (10mM) Store at 4°C

2.1.5 *Common laboratory chemicals and reagents*

All common chemicals and reagents used and their sources are listed in table 2.6.

Table 2.6 *Chemicals and reagents*

Chemical or Reagent	**Source**
27% hydrogen peroxide	Andrew Industrial Ltd
Tris; D(+)-sucrose; ethylene glycol-bis-(beta-aminoethyl ether)- N,N,N',N' tetracetic acid (EGTA)	AppliChem
Sodium chloride; sodium dodecyl sulphate; ethylenediaminetetra-acetic acid (EDTA); glycerol; Tween 20; Triton X-100	BDH Ltd
Dithiothreitol; beta-mercaptoethanol; ammonium persulphate; 40% 3-10 ampholytes; electrode wicks; mineral oil; 30% acrylamide, 2.67% bis- acrylamide; N,N,N',N'-tetramethylethylenediamine (TEMED); kaleidoscope pre-stained protein standard; silver stain plus kit; 3-10NL immobilised pH gradients	Bio-Rad
Peptide calibration standard; α-cyano-4-hydroxy-cinnamic acid (HCCA)	Bruker Daltonics
Bovine serum albumin (BSA); 10kDa protein marker	Invitrogen (Gibco BRL)
Glycine	Merck
Bromophenol blue	Park Scientific Ltd

Bicinchoninic acid (BCA) protein assay kit; 1-STEP™ NBT/BCIP	Pierce
Agarose LE	Roche
di-Sodium hydrogen phosphate dodecahydrate; methanol	Scharlau
Brilliant blue R-250; percoll; phenylmethylsulfonyl fluoride; urea; mixed bed ion exchange resin; 3-[(3-cholamidopropyl) dimethylammonio]-1-propanesulfonate (CHAPS); tributylphosphine (TBP); iodoacetamide; trifluoroacetic acid (TFA); sodium sulphite	Sigma-Aldrich
Potassium chloride; potassium dihydrogen orthophosphate; hydrochloric acid (HCl); glacial acetic acid; nitric acid; ammonium dihydrogen orthophosphate	Univar

2.2 Methods

2.2.1 *Sample collection*

Skeletal muscle was dissected from the hind limbs of 14 week old wild type (WT) and myostatin knockout (KO) mice by Alex Henebry of the Growth and Development Group at AgResearch, Ruakura, Hamilton. 14 week old mice were used as they could show any changes in mitochondrial function after the 'glycolytic switch', mentioned in Chapter 1.2.1, which occurs within 39 days of birth (Girgenrath *et al*, 2005).

The mice were asphyxiated with carbon dioxide and the Bicep Femorous, Gastrocnemius, Soleus, Quadriceps and Tibialis Anterior muscles removed and placed directly into ice cold mitochondrial isolation buffer (250mM Sucrose, 20mM Tris, 40mM KCl, 2mM EGTA, 1mg/mL bovine serum albumin (BSA)). One Bicep Femorous from each mouse used during the study was saved in a NUNC™ CryoTube™ (Invitrogen) and frozen at -70°C to verify the absence of myostatin protein in the KO mice. The other muscles were used for mitochondrial isolation on that day.

As the animals used in this study were not subjected to any treatments, ethics approval was only required for the method of killing used (Protocol 650). This was approved by the University of Waikato's Animal Ethics Committee on 21 October 2005.

2.2.2 *Myostatin knockout verification*

2.2.2.1 *Protein extraction*

The Bicep Femorous muscle saved at -70°C was thawed in 1mL of PBS, stored at 4°C, and minced with dissecting scissors. This was transferred to a 15mL falcon tube cut off at the 10mL mark and homogenized, using a disperser (IKA® T10 basic ULTRA-TURRAX®), for 15 secs at 20,500 rpm. A 5G stainless steel dispersion tool was utilised, this attachment has a working range of 0.5 to 5mL.

The homogenate was left at 4°C for 1 hr for the cytosolic protein to solubilise and filtered through 75µm nylon net to remove connective tissue. This filtrate was aliquoted into 1.5mL microcentrifuge tubes and centrifuged at 16,000 rcf (Eppendorf 5415R) for 4 mins at 4°C to pellet unsolubilised material. The supernatant was removed to a new tube and frozen at -20°C until required.

2.2.2.2 *Protein estimation*

BCA Protein Assay Kit (Pierce) was used to estimate the protein concentration of sample solutions by comparison against a BSA standard curve. This kit contains BCA Reagent A, BCA Reagent B, 10 x 1mL ampules of BSA at 2,000µg/mL. To see the content of these reagents, please refer to table 2.1.

BSA standards in the range of 25 to 2,000µg/mL were made with PBS according to the manufacturer's directions. Samples were diluted 1/5 with PBS to ensure they registered on the standard curve. 10µL of standards, including a PBS blank, and

samples were pipetted into a 96- well microtitre plate. Standards and samples were assayed in duplicate. 200µL of BCA working reagent (50 parts BCA Reagent A to 1 part BCA Reagent B, which was mixed immediately before adding) was added to each well, the plate covered and incubated in a 37°C incubator (Contherm, Wellington, New Zealand) for 30 mins.

After cooling to room temperature, the absorbance of each well was measured at 570nm in a plate reader (Lab System Multiskan RC). DeltaSoft3™ software (BioMetallics, Princeton, NJ, USA) was used to control the plate reader and analyse the data. A linear standard curve was generated using the absorption values of the BSA standards. The concentration of the samples was then calculated using the formula of this line and the values for each sample.

2.2.2.3 *Sodium dodecyl sulphate – polyacrylamide gel electrophoresis*

The proteins were separated by discontinuous SDS-PAGE, using the method of Laemmli (1970). 0.75mm gels were cast/run using a Mini-Protean® 3 Cell gel apparatus (Bio-Rad)

The 12% polyacrylamide separating gel consisted of 3.35mL MilliQ water, 2.5mL 1.5M Tris-HCl pH 8.8, 100µL 10% (w/v) SDS, 4.0mL acrylamide-bis (30% acrylamide, 2.67% bis- acrylamide; Bio-Rad), 50µL of 10% (w/v) APS (Bio-Rad), prepared fresh daily, and 5µL of TEMED (Bio-Rad). A 4% stacking gel was laid on top of this and housed ten 5.08mm wells. This consisted of 3.05mL MilliQ water,

1.25mL 0.5M Tris-HCl pH 6.8, 50µL 10% (w/v) SDS, 650µL acrylamide-bis (30% acrylamide, 2.67% bis- acrylamide), 25µL of 10% (w/v) APS, prepared fresh daily, and 5µL of TEMED. Seen as there was no problem with inhibition of the acrylamide polymerization or air bubbles in the gel, neither of the gel monomer solutions were degassed.

Protein samples were prepared by dilution with sample loading buffer (Westermeier, 1993) according to the protein estimation, so that 20µg of protein could be loaded onto each lane within a volume of 10µL. 1 µL of Dithiothreitol (DTT) solution (250mg of DTT in 0.5mL of MilliQ water and stored at 4°C) was included in each sample to reduce disulphide bonds. This mixture was heated on a multi block heater (Lab-Line) at 95°C for 2 mins to break down the proteins' secondary, tertiary and quaternary structure.

The gels were assembled in the electrophoresis cell and 300mL of 1x electrode buffer (60mL of 5x electrode buffer and 240mL of MilliQ water) was added to the inner and lower buffer chambers. 10µL of each sample solution was loaded into a separate well using a Hamilton syringe. 4µL of Kaleidoscope pre-stained standard (Bio-Rad) was loaded onto the first lane of each gel to confirm transfer of the protein during the western blot and allow estimation of the molecular weight of the sample proteins. The gels were run at 200V (Power Pac 200, Bio-Rad) for 60 mins at room temperature. Duplicate gels were run at the same time, one for staining and the other for western blotting.

The gel to be stained was removed from the gel cassette and placed in coomassie blue stain (0.1% (w/v) brilliant blue R-250 in 40% (v/v) methanol/10% (v/v) acetic acid) for 45 mins. It was then de-stained with successive lots of fixative (40% (v/v) methanol/10% (v/v) acetic acid) until the colour was removed from the background of the gel. The gel image was acquired on a MiniBIS Pro (DNR Bio-Imaging Systems, Jerusalem, Israel) controlled by GelCapture software (DNR Bio-Imaging Systems).

2.2.2.4 *Western blot*

Proteins separated on polyacrylamide gels were transferred to 0.45µm polyvinylidene fluoride (PVDF) membranes (Millipore) using a semi-dry transfer cell (Trans-Blot® SD, Bio-Rad). The gel was removed from the gel cassette and the stacking gel discarded. The separating gel was equilibrated in Towbin transfer buffer (192mM glycine, 25mM Tris, 1.3mM SDS, 20% (v/v) Methanol) for 5 mins.

The PVDF membrane was activated by soaking in methanol for 10 mins and then equilibrated in Towbin transfer buffer, stored at 4°C, for 5 mins. Four pieces of extra thick blotting paper (Bio-Rad) were soaked in Towbin transfer buffer also. To perform the transfer, a sandwich was prepared as follows: two of the pieces of blotting paper were placed on the bottom platinum anode, the PVDF membrane was placed on top of these, followed by the equilibrated gel and the final two pieces of blotting paper. After each addition to the sandwich, air bubbles were removed by lightly rolling a 50mL falcon tube across the stack. The top stainless steel cathode

was placed on top of the sandwich and the proteins were transferred at 15V (Power Pac 200, Bio-Rad) for 60 mins at room temperature. The membrane was rinsed with MilliQ water, air dried at room temperature, and frozen at -20°C until required.

2.2.2.5 *Western analysis*

Non-specific binding sites on the membrane were blocked overnight at 4°C in a 5% (w/v) low-fat milk powder solution made up in TBST (150mM NaCl, 10mM Tris, 0.05% (w/v) Tween 20). The following day it was washed three times in TBST for 5 mins each. The membrane was incubated at room temperature for 90 mins in a 1:2,000 dilution of primary antibody, rabbit polyclonal to GDF8/Myostatin (Abcam) made up in TBST. The membrane was again washed three times in TBST for 5 mins each. It was then incubated in a 1:100,000 dilution of the secondary antibody, anti-rabbit IgG (whole molecule) conjugated to alkaline phosphatase grown in goat (Sigma) for 90 mins. The membrane was once again washed three times in TBST for 5 mins each and rinsed in MilliQ water. The membrane was developed in a 1/10 dilution of 1-STEP™ NBT/BCIP (Pierce), containing nitro blue tetrazolium made up in MilliQ water, for 60 secs and then immediately rinsed with MilliQ water to remove the substrate.

An image of the western was acquired on a MiniBIS Pro (DNR Bio-Imaging Systems, Jerusalem, Israel) controlled by GelCapture software (DNR Bio-Imaging Systems).

2.2.3 *Analysis of mitochondrial stress levels*

2.2.3.1 *Mitochondrial isolation*

A mitochondria enriched fraction was isolated from the Gastrocnemius muscle using the method of Rustin (1993) with slight modifications. The muscle was weighed in 5mL of fresh, ice cold mitochondrial isolation buffer. They were weighed in this manner to maintain the low temperature of the muscle and to avoid exposure to the air. The 5mL of solution was then supplemented with more mitochondrial isolation buffer so that there was 1mL per 100mg of tissue. All subsequent isolation procedures were performed at 4°C.

The tissue was finely diced using dissecting scissors, and homogenized in a 50mL falcon tube using a disperser (IKA® T10 basic ULTRA-TURRAX®) operating at 11,500 rpm for 15 secs. A 10G stainless steel dispersion tool was used to do this, which has a working range of 1 to 100mL. The homogenate was filtered through 100μm nylon net to remove the connective tissue.

1.5mL aliquots of the filtrate were placed in 1.5mL microcentrifuge tubes and centrifuged at 2,000 rcf for 8 mins (Eppendorf 5415R) to remove cell debris and nuclei. The supernatant was transferred to a new tube and spun at 10,000 rcf for 10 mins to pellet the mitochondria. This supernatant was discarded and the pellet resuspended in 0.75mL of mitochondrial isolation wash buffer (mitochondrial isolation buffer supplemented with 5% (v/v) Percoll (Sigma)) by flicking the base of the tube with fingertips. The resuspended pellet was spun at 10,000 rcf for 10 mins

and the supernatant once again discarded. Excess solution was removed from the sides of the tube using filter paper strips and the mitochondria enriched pellet was frozen at -70°C until required.

2.2.3.2 *Protein solubilisation*

Each tube was resuspended in 40µL of TENT buffer (50mM Tris pH 7.4, 150mM NaCl, 5mM EDTA, 0.5% (v/v) Triton X-100, supplemented fresh daily with 0.4mM phenylmethylsulfonyl fluoride) using a Teflon micropestle (Eppendorf). This suspension was left at 4°C for 1 hr and then centrifuged at 4°C for 4 mins at 16,000 rcf (Eppendorf 5415R). The resulting supernatants were removed to one 1.5mL microcentrifuge tube and stored at -20°C until required

2.2.3.3 *Protein separation and transfer*

Protein estimations were carried out on the samples as described earlier in section 2.2.2.2. The samples were prepared for SDS-PAGE as described in section 2.2.2.3, however they were diluted so that 15µg of protein could be loaded on the gel in 15µL. After the gel had run at 200V (Power Pac 200, Bio-Rad) for 60 mins, one gel was stained with coomassie blue stain as described in section 2.2.2.3, whilst the other was transferred to a PVDF membrane as detailed in section 2.2.2.4.

2.2.3.4 *Western analysis*

The membrane was probed for hsp60 and SOD2 protein in the same manner as that outlined in section 2.2.2.5. However the antibodies and dilutions utilised were altered.

The primary antibody was at a 1:5,000 dilution in TBST. This was a polyclonal antibody grown in rabbit, specific for either hsp60 or SOD2 (Stresgen). The secondary antibody was still anti-rabbit IgG (whole molecule) conjugated to alkaline phosphatase grown in goat, however, this was used at a 1:50,000 dilution. The membrane was incubated in each of these as before, and developed in the same manner with a 1/10 dilution of 1-STEP™ NBT/BCIP substrate made in MilliQ water.

An image of the western was acquired on a MiniBIS Pro (DNR Bio-Imaging Systems) and the band intensities measured using GelQuant (DNR Bio-Imaging Systems). The GelQuant software measures the pixel intensity of the bands on the western as a relative intensity compared to a reference band which is measuring background staining. So a value of 5 would mean that the band detected in the western is five times more intense than the background.

2.2.3.5 *Statistical analysis of western band intensities*

Statistical significance of any differences in the resulting western band intensity was performed using the student's t-test. It employs the following formula to determine if differences seen in western band intensities between the WT and KO samples are statistically valid.

$$t = \frac{\bar{x}_1 - \bar{x}_2}{\sqrt{\frac{s^2_1}{n_1} + \frac{s^2_2}{n_2}}}$$

Where: $\bar{x}_1$ = Mean of sample 1
$\bar{x}_2$ = Mean of sample 2
s^2_1 = Variance of sample 1
s^2_2 = Variance of sample 2
n_1 = Number of values in sample 1
n_2 = number of values in sample 2

If the calculated t-value obtained from the sample is greater than the tabulated t-value the difference between the two sample means is deemed to be statistically valid. The tabulated t-value depends upon the degrees of freedom for the sample, $df = n_1+n_2-2$, and the required level of significance.

2.2.4 *Proteomic analysis of knockout mitochondrial protein levels*

Only the Gastrocnemius muscles were used in this section of the study. It was chosen for this because it is an easily isolated muscle of a reasonable size, as in 150mg of tissue per muscle instead of 45mg of tissue from a Soleus muscle. It also has a mixed fibre composition, so it can display the effect of the changes that occur in the mitochondria after the fibre type switch mentioned in Chapter 1.2.1, as opposed to using a muscle which is primarily composed of fast twitch fibres.

2.2.4.1 *Mitochondrial isolation*

A mitochondria enriched fraction was isolated from the gastrocnemius muscle as described in section 2.2.3.1, except that the finely diced muscle was homogenised in a 15mL Potter-Elvehjem homogeniser (Wheaton Science, USA), by making 8 passes at a speed of 2,500 rpm. This was powered by a Baird and Tatlock motor with variable speed control.

2.2.4.2 *Protein solubilisation*

IPG rehydration/solubilisation solution was made fresh daily. It contained 8M urea, 2mM TBP (Sigma), 2% (w/v) CHAPS (Sigma) and 0.2% (w/v) 3-10 ampholytes (Bio-Rad). The 8.5M urea stock used to make this was treated with mixed bed ion

exchange resin (Sigma) for 10 mins to remove charged species. It was then vacuum filtered through #1 filter paper (Advantec) to remove the ion exchange beads and frozen at -20°C until required.

50µL of IPG rehydration/solubilisation solution was added directly to the mitochondrial pellet in each microcentrifuge tube. They were vortexed (Grant-Bio) twice for 5 secs each and left at 20°C for 1 hr so the protein could solubilise. The solution was centrifuged at 14,000 rcf in a miniSpin plus (Eppendorf) at room temperature for 4 mins to pellet unsolubilised material. The supernatant from each tube were transferred to a single tube which was kept at 20°C until required, this will subsequently be referred to as the IEF solution. TCA precipitation was not used in this study as the mitochondrial protein was in an already concentrated form after being pelleted during the mitochondrial isolation procedure described in section 2.2.4.1. Proteolysis action was not considered a major problem, as many of the proteolytic agents would have been removed in the mitochondrial isolation step, and because the IPG rehydration/solubilisation solution used is denaturing would rendered them inactive. Another precaution which was not observed was DNA removal from the sample, as the major contaminating DNA in proteomics samples is the nuclear DNA, which once again has been removed during the isolation procedure.

The pellets from each tube were resuspended in 25µL of TENT buffer with a Teflon micropestle (Eppendorf) and left at room temperature for 1 hr. The solutions were centrifuged at 14,000 rcf in a miniSpin plus (Eppendorf) at room temperature for 4

mins. The supernatant from each tube was transferred to a single tube and frozen at -20°C until required. This solution will be referred to as the IEF pellet solution.

2.2.4.3 *IEF protein estimation*

The IEF solution was subjected to the protein estimation assay described in Section 2.2.2.2 but with simple modifications. Because the IPG rehydration/solubilisation solution contains 8M urea, which interferes with the protein estimation assay, the standards and diluent used were altered to compensate for this. A 10,000µg/mL BSA solution was made up in IPG rehydration/solubilisation solution and frozen at -20°C in 100µL aliquots. This stock solution was diluted with 400µL of IPG rehydration/solubilisation solution to make a 2,000µg/mL solution and diluted further according to table 2.7 to make standards in the range of 125 to 2,000µg/mL. These standards replaced the standards in the previously described method.

Table 2.7 *Dilution scheme to make up standards to perform IEF protein estimation*

Final Concentration (µg/mL)	Volume and Concentration of BSA Solution	Volume of IPG Rehydration/ Solubilisation Solution
2,000	100µL of 2,000µg/mL	0µL
1,500	150µL of 2,000µg/mL	50µL
1,000	100µL of 2,000µg/mL	100µL
750	100µL of 1,500µg/mL	100µL
500	100µL of 1,000µg/mL	100µL
250	100µL of 500µg/mL	100µL
125	100µL of 250µg/mL	100µL
0	0µL	100µL

The rest of the protein estimation assay was the same as previously described, except that IPG rehydration/solubilisation solution was used as the blank and to dilute sample solutions.

2.2.4.4 *Isoelectric focusing*

IEF solutions were diluted with IPG rehydration/solubilisation solution so that the appropriate amount of protein could be loaded onto an IPG in 300 µL. WT and KO solutions were diluted to the same protein concentration so that the same amount of protein would be loaded onto each IPG. 0.2µL of 1% (w/v) Bromophenol blue solution was added to each millilitre of the diluted solution to track progress of the IEF. 300µL of sample was laid along the length of a 17cm IEF focusing tray (Bio-Rad) and a 17cm 3-10NL IPG (Bio-Rad) laid on top of this. This was left for 1 hr and then overlaid with 1.4mL of mineral oil (Bio-Rad). The focusing tray lid was replaced and the IPG left to passively rehydrate for another 16 hrs at 20°C in a Protean® IEF Cell (Bio-Rad).

Before running the IEF, the IPG was lifted at each end and an electrode wick (Bio-Rad) wet with 8µL of MilliQ water placed between the electrode and the gel. The focusing tray was replaced in the IEF Cell and ran at 20°C with a current limit of 50µA per gel. The focusing steps were as follows: the gels were held at 250V for 15 mins, and then subjected to a rapid ramp over 3 hrs to 10,000V, where the voltage was maintained at 10,000V for 60,000V/hrs. After completion of the IEF the gels were held at 500V until removed from the IEF cell, to limit diffusion of the proteins.

After removing excess mineral oil on filter paper, the IPG was placed gel side up in a rehydration/equilibration tray (Bio-Rad), wrapped in cling film and frozen at -70°C until the second dimension was run.

2.2.4.5 *Second dimension – SDS polyacrylamide gel electrophoresis*

The IPG was prepared for the second dimension by equilibrating it in 6mL of SDS-PAGE equilibration buffer I (6M Urea, 0.375 M Tris-HCl, pH 8.8, 2% (w/v) SDS, 20% (v/v) glycerol, 2% (w/v) DTT) for 15 mins to reduce disulphide bonds. This was decanted off and replaced with 6mL of SDS-PAGE equilibration buffer II (6M urea, 0.375 M Tris-HCl, pH 8.8, 2% (w/v) SDS, 20% (v/v) glycerol, 2.5% (w/v) iodoacetamide) for another 15 mins to acetylate the free thiol groups. The SDS-PAGE equilibration buffer was stored in 12mL aliquots at -20°C until required and then supplemented with DTT or iodoacetamide on the day it would be used.

After removing excess liquid, the IPG was laid on top of a 18.5cm by 20cm, 1.5mm thick, 12% SDS-PAGE gel consisting of 20.1mL MQ H_2O, 15mL 1.5M Tris-HCl pH 8.8, 600µL 10% SDS, 24mL acrylamide-bis (30% acrylamide, 2.67% bis-acrylamide), 300µL of 10% (w/v) APS prepared fresh daily, and 30µL of TEMED. A 1% (w/v) agarose LE (Roche) gel plug, made in 1x electrode buffer, containing 10 kDa protein markers (GibcoBRL®) was placed next to the acidic end of the IPG and both were covered in 2-D agar overlay, containing 0.003% (w/v) bromophenol blue to track progress of the electrophoresis.

The gel slab was loaded into a Protean II Xi gel apparatus with an IPG conversion kit (Bio-Rad). The gels were maintained at 15°C by circulating water, chilled by a refrigerated waterbath (RB-12A/TE-8D, Techne), through the cooling chamber and run at 35mA per gel (Power Supply 1000/500, Bio-Rad) for 5 hrs and 45 mins.

2.2.4.6 *Silver staining*

At completion of the electrophoresis, the gel was removed and stained using a silver stain plus kit (Bio-Rad). Silver stain plus is 60 times more sensitive than coomassie R-250 stains, but does not cross-link lysine residues like conventional silver stain, and therefore allows for downstream MS analysis. This kit contained fixative enhancer solution, silver complex solution, reduction moderator solution, image developer reagent, development accelerator reagent, and a 1L bottle to store the development accelerator solution. For composition of these reagents refer to table 2.2. The only preparation involved was to make up the development accelerator reagent to 1L with MilliQ water, which could then be stored at 4°C for up to three months.

All glassware and gel containers used for silver staining were washed in 2M nitric acid overnight and washed with MilliQ water. This is done to remove metallic silver residues which will act as nuclei for more silver deposition on the tray and cause inconsistent staining. Gels were fixed overnight in 400mL of 50% (v/v) methanol, 10% (v/v) acetic acid and 10% (v/v) fixative enhancer solution. The next day they were rinsed three times over two hrs in 3 x 800mL of MilliQ water. The silver stain was prepared just prior to staining the gel. This involved mixing 52.5mL of MilliQ

water, 7.5mL of silver complex solution, 7.5mL of reduction moderator solution, 7.5mL of image development solution, and 75mL of development accelerator solution at room temperature. The gel was agitated on a rocking platform (Bibby Sterlin Ltd), in this solution for 15 mins, then the staining solution was removed and the staining stopped with 400mL of 5% (v/v) acetic acid. After 15mins the acetic acid was removed and the gel left in MilliQ water.

2.2.4.7 *Quantitation of 2-DE spot intensities*

The gel image was captured on a luminescent image analyser (LAS-1000 plus, FujiFilm) controlled by Image Reader LAS-1000 Lite (FujiFilm). An exposure time of 1/60 secs was used. The resulting spot intensities were analysed using Image Gauge Version 4.0 (FujiFilm). The mouse was used to select an area that encompassed the spot of interest and also an area where no protein spots were present to be used as the background. Pixel intensities were expressed an arbitrary unit (AU) which were then divided by the size of the area selected in mm^2 to take account of the different spot sizes present. The background (BG), also divided by its spot size, was then subtracted from the AU/mm^2 to compensate for background staining.

2.2.4.8 *Statistical analysis of spot intensity differences between WT and KO gels*

Statistical significance of any differences in spot intensity between the WT and KO was determined as in section 2.2.3.5 using the student's t-test. In this case, intensities from each of the three replicate gels from the WT and KO sample were used to determine if there was a statistically valid difference between the mean spot intensity.

2.2.4.9 *In-gel tryptic digest*

Spots of interest were excised using 200µL pipette tips (Greiner Bio-one) cut off at the first mark, 12mm from the tip. They were deposited into 1.5mL microcentrifuge tubes and stored at -20°C until required. The gel plugs were destained in 300µL of 1% (v/v) hydrogen peroxide (H_2O_2), added directly to the tube which the plugs were stored in, and shaken (MS1 mini shaker, IKA) overnight at 600 rpm. The destain solution was removed and the plugs washed in 200µL of 25mM NH_4HCO_3 for 15 mins. After removing the wash solution, the plug was equilibrated in 100µL of 1:1 25mM NH_4HCO_3/Acetonitrile (ACN) for 1 hr before dehydrating it in 50µL of ACN. The ACN was removed after 15 mins and the gel plugs left to air dry in a hood for 2 hrs.

Reduction and alkylation of the protein contained in the gel plug could have been performed prior to tryptic digestion. However, this was done when the IPG was prepared for SDS-PAGE and it was deemed unnecessary to redo this as peptides which were known to contain cysteine residues still identified with an alkylation modification.

100µg of Trypsin Gold (Promega) was resuspended in 100µL of 50mM acetic acid to make a 1µg/µL solution which was stored in 2µL aliquots at -70°C. One of these was diluted in 398µL of 25mM NH_4HCO_3 to make a 0.005µg/µL trypsin solution. 15µL of this was added to each dehydrated gel plug and left at 4°C for 1 hr to rehydrate the gel. Excess trypsin solution was removed and the closed tubes were placed in a sealed

container with a wet paper towel to maintain humidity, which was incubated at 37°C for 6 hrs (Contherm Digital Series). The resulting peptides were extracted in 10µL of 20% (v/v) ACN/0.1% (v/v) TFA overnight at 4°C.

2.2.4.10 *MALDI-TOF mass spectrometry of tryptic digest products*

As mentioned in Chapter 1.4.2, proteins were identified during this study, by PMF and MALDI-TOF MS. Because trypsin cleaves specifically on the carboxylic side of lysine and arginine residues, unless followed by a proline, the peptides resulting from digests are specific for the protein digested. MALDI-TOF MS can be used to quickly analyse the mass of each of the peptides present in the resulting digest mixture, as it gives only a singly charged, protonated ion within this mass range.

Peptides samples were prepared for MALDI-TOF MS by applying 0.5µL of sample to a thinlayer of HCCA on a 600µm anchorchip (Bruker Daltonics). Once the sample had air dried in a hood, it was washed with 5µL of 0.1% (v/v) TFA in 10mM $NH_4H_2PO_4$ for around 5 secs before removing and allowing to air dry again.

The mass spectrometer used was an AutoFlex II™ (Bruker Daltonics) operated using FlexControl™ (Bruker Daltonics). The instrument was calibrated against a peptide calibration standard (Bruker Daltonics) which was loaded in the same manner as the samples, onto calibanchors, located at the centre of every four sample anchors. Sample spectra were acquired over a 500 to 4,000m/z range by summing 500 shots, with an acceleration voltage of 19kV and a reflector voltage of 20kV. Pulsed ion

extraction of 80ns was used to build up the concentration of ions in the ion source and ions below 500m/z were suppressed to avoid detector saturation from matrix ions. Spectra were automatically annotated by FlexAnalysis™ (Bruker Daltonics) to peak the mono-isotopic peaks within 800 and 4,000m/z, and Mascot™ database searches were performed via BioTools™ 3.0 (Bruker Daltonics), searching the NCBI database for sequences from either mammalia (mammals) or mus musculus (house mouse).

2.2.4.11 *SDS-PAGE of IEF pellet proteins*

The IEF pellet solution was subjected to the protein estimation assay described in section 2.2.2.2. The samples were diluted in sample loading buffer (Westermeier, 1993) so that 1µg of protein could be loaded onto the polyacrylamide gel in a 15µL volume. The gel was run as previously described in section 2.2.2.3, however 10 kDa protein markers (GibcoBRL®) were run next to the samples.

The gel was silver stained as described in section 2.2.4.6 with silver stain plus (Bio-Rad). The only differences in the staining were the volumes used, 200mL of fixative and 50mL of stain (17.5mL of MilliQ water, 2.5mL of silver complex solution, 2.5mL of reduction moderator solution, 2.5mL of image development solution, and 25mL of development accelerator solution) was used. The gel was stained for 15mins, stopped with 200mL of acetic acid and rinsed in MilliQ water. The gel image was captured on a LAS-1000 plus (FujiFilm) controlled by Image Reader LAS-1000 Lite (FujiFilm), with an exposure time of 1/60 secs.

CHAPTER THREE

Myostatin Knockout Verification

3.1 Introduction

Muscle tissues used during this study were acquired from the Growth and Development Group at AgResearch, Ruakura, Hamilton. The myostatin knockout mouse model was generated by genetic deletion of the third exon of the myostatin gene, which codes for the functional portion of the myostatin protein (McPherron *et al.*, 1997). This results in a truncated myostatin protein which is unable to inhibit muscle growth leading to the myostatin knockout phenotype described in Chapter 1.2.1.

Even though this model has been well characterised and shown to not contain mature myostatin, at both mRNA and protein levels. Western blot analysis using anti-myostatin antibodies raised against the mature portion of myostatin was carried out to verify that the knockout mice did not express the myostatin protein.

3.2 Materials and methods

3.2.1 *Sample preparation*

Bicep Femorous muscle were dissected from wild type (approximately 130mg) and myostatin knockout mice (approximately 190mg) as described in Chapter 2.2.1. This was stored in a NUNC™ CryoTube™ (Invitrogen) and frozen at -70°C until required. The muscle was diced in 1mL of PBS and homogenized as described in Chapter 2.2.2.1. The homogenate was left at 4 °C for 1 hr for the cytoplasmic protein to solubilise, filtered through 75µm nylon net and centrifuged at 16,000 rcf to pellet the unsolubilised material.

3.2.2 *Western analysis*

An estimate of the total protein concentration was found using the BCA Protein Assay Kit (Pierce) as described in Chapter 2.2.2.2 to ensure equal protein loadings when protein was loaded onto SDS-PAGE gels. Cytoplasmic protein (20µg) was separated on 12% SDS-PAGE gels as outlined in Chapter 2.2.2.3. The protein was transferred to a 0.45µm PVDF membrane (Millipore) as in Chapter 2.2.2.4 by semi-dry electroblotting. Western analysis was performed as described in Chapter 2.2.2.5. The membrane was blocked in TBST/5% milk powder at 4 °C overnight, washed in TBST and incubated in anti-myostatin antibody for 90 mins. The membrane was washed again and incubated in anti-rabbit IgG antibody coupled to alkaline phosphatase for 90 mins. The membrane was developed in a 1/10 dilution of 1-STEP™ NBT/BCIP (Pierce).

3.3 Results

3.3.1 *Western analysis optimisation*

The antibody used in this study to detect myostatin, Rabbit polyclonal to GDF8 / Myostatin (Abcam), had not previously been used in our lab. This meant that the antibody dilutions used needed to be optimised, to obtain specific staining of the protein of interest whilst reducing background staining. The starting point for the primary antibody was taken at the manufacturers lowest advised concentration (1:5,000 dilution). A reasonably high concentration of secondary antibody was used (1:15,000 dilution) to ensure detection of the primary antibody. As can be seen in Figure 3.1 *A*, a faint band, marked with an arrow, is detected in the wild type sample at approximately 36kDa which is not detected in the knockout sample. But the antibodies are cross-reacting with the high abundance proteins in both the wild type and knockout samples. To try and reduce the background staining and increase the signal of the detected band, the primary antibody concentration was then increased to a dilution of 1:2,000 and the secondary antibody's concentration decreased to 1:50,000. Figure 3.1 *B* shows an increase in detection of the band and a reduction in the staining intensity of the other protein bands. The secondary antibody concentration was decreased further to 1:100,000, whilst maintaining the primary antibody's concentration at 1:2,000. This is shown in Figure 3.1 *C*, with the background staining becoming fainter again.

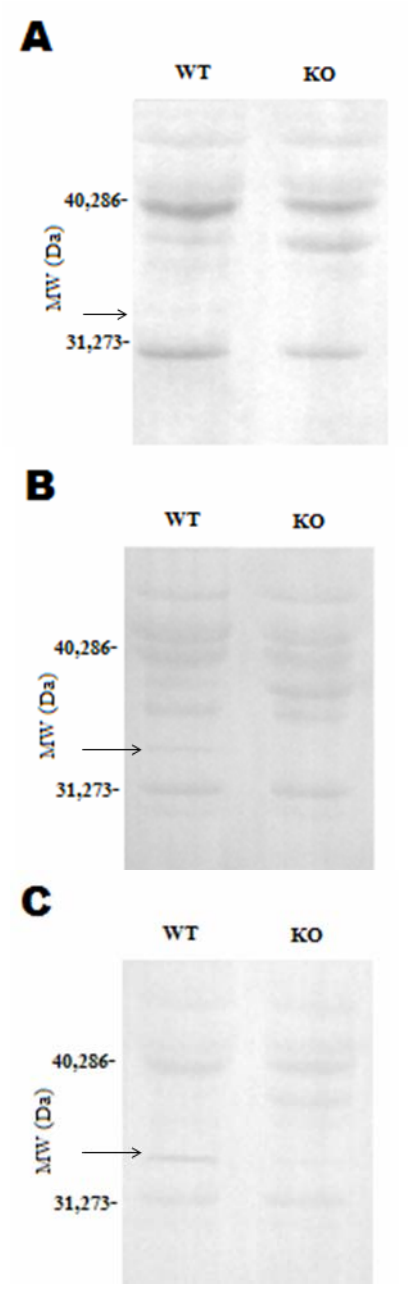

Figure 3.1 *Optimisation of anti-myostatin antibody staining in western blot analysis of wild type and knockout cytoplasmic skeletal muscle protein.* **(A)** Western using a 1:5,000 dilution of primary antibody and 1:15,000 dilution of secondary antibody. **(B)** Western using a 1:2,000 dilution of primary antibody and 1:50,000 dilution of secondary antibody. **(C)** Western using a 1:2,000 dilution of primary antibody and 1:100,000 dilution of secondary antibody.

3.3.2 *Myostatin knockout verification*

As mentioned in section 3.3.1, background staining was reduced but not eliminated in this experiment. However an intense band is seen in the wild type sample at approximately 36kDa, which is barely detectable in the knockout, marked with an arrow in Figure 3.2 *A*. The background staining which is observed in the western can be attributed to the most abundant proteins in each sample, by comparing the staining pattern in the western, Figure 3.2 *A*, with that of the coomassie stained 12% SDS-PAGE gel, Figure 3.2 *B*. Figure 3.2 *C* is an intensity profile of each lane of the western and the gel laid side by side. It shows a similar profile between the western and the gel, for the wild type and the knockout lane, except for one location, marked with an arrow. This band detected on the wild type western is not present in the intensity profile for the corresponding gel lane, so cannot be attributed to a high abundance protein in the sample, nor is it detected in the knockout western. Interestingly, the molecular weight of this band does not correlate with the 52kDa full length myostatin protein, this will be discussed further in section 3.4.

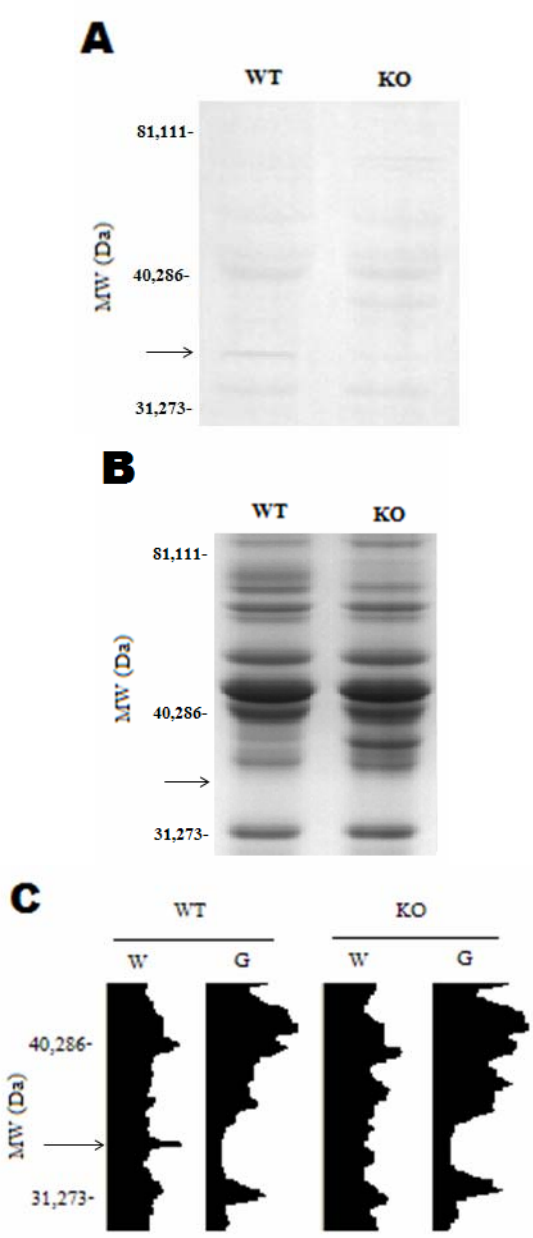

Figure 3.2 *Western blot and SDS-PAGE analysis of anti-myostatin staining pattern seen in wild type and knockout cytoplasmic skeletal muscle.* **(A)** Western analysis showing an intense band at approximately 36kDa in the WT muscle which is barely present in the KO muscle. **(B)** Coomassie stained 12% SDS-PAGE gel replicating the separated proteins in the western. **(C)** Intensity profile of the WT and KO lanes from the western and the gel showing various matching peaks between the western and the gel for each lane, 'W' = western and 'G' = gel.

3.4 Discussion

The intense band detected at 36kDa in the wild type sample and not in the knockout sample, could not be attributed to any of the highly abundant proteins in the samples. This molecular weight, however, does not correlate with that of full length myostatin (52kDa) or mature myostatin (12kDa). Interestingly, other researchers using antibodies raised against the mature portion of myostatin have observed a band between 36 and 40kDa which they attribute to the LAP, the cleavage product of full length myostatin shown in Figure 1.1 (McCroskery *et al.*, 2003; Berry *et al.*, 2002; Hill *et al.*, 2002; Lee and McPherron, 2001; Thomas *et al.*, 2000).

If it is the LAP being detected, a further question to be asked is why it is not also being detected in the knockout samples. The genetic deletion of myostatin used in this mouse model only deletes the mature portion of myostatin (McPherron *et al.*, 1997), so the LAP should still be present. Whether the genetic deletion of the mature portion of myostatin in the knockout samples would cause the LAP to not be detected by anti-myostatin antibodies is unknown. The results of this study suggest that it does in some way reduce the binding of the anti-myostatin antibodies, as the LAP was barely detectable in the knockout mice.

In the future, a myostatin antigen could be run at the same time as samples, this would allow one to check the specificity of the anti-myostatin antibodies.

CHAPTER FOUR

Analysis of Mitochondrial Stress Levels

4.1 Introduction

As mentioned in Chapter 1.2.1, double-muscled cattle (due to non-functional myostatin being produced) have been shown to be more susceptible to environmental stressors including heat stress (Menissier, 1982). Heat stress is known to impair mitochondrial functions in skeletal muscle (Mujahid *et al.*, 2006; Hsu *et al.*, 1995), and is also known to induce mitochondrial stress proteins, such as hsp60 (Martinus *et al.*, 1996). To determine if muscle tissue from myostatin knockout mice were being subjected to increased levels of mitochondrial stress, expression levels of heat shock protein 60 (hsp60) and superoxide dismutase 2 (SOD2) protein were assessed by western blot analysis.

4.2 Materials and methods

4.2.1 *Sample preparation*

A mitochondria enriched fraction was isolated from the Gastrocnemius muscle as described in Chapter 2.2.3.1. The muscle was homogenised, filtered, and the cell debris removed by centrifuging at 2,000 rcf. Mitochondria were pelleted at 10,000 rcf, these were washed and then pelleted again. The protein from this mitochondria enriched fraction was solubilised in TENT buffer as in Chapter 2.2.3.2.

4.2.2 *Western analysis*

An estimate of the total protein concentration was determined using the BCA Protein Assay Kit (Pierce) as described in Chapter 2.2.2.2 to ensure equal protein loadings when samples were loaded onto SDS-PAGE gels. Mitochondrial protein (15µg) was separated on 12% SDS-PAGE gels as outlined in Chapter 2.2.2.3. The protein was transferred to a 0.45µm PVDF membrane (Millipore) as in Chapter 2.2.2.4 by semi-dry electroblotting. Western analysis was performed as described in Chapter 2.2.3.4. The membrane was blocked in TBST/5% milk powder at 4 °C overnight, washed in TBST and incubated in a 1:5,000 dilution of primary antibody (anti-hsp60 or anti-SOD2 (Stressgen)) for 90 mins. The membrane was washed again and incubated in a 1:50,000 dilution of anti-rabbit IgG antibody coupled to alkaline phosphatase (Sigma) for 90 mins. The membrane was developed in a 1/10 dilution of 1-STEP™ NBT/BCIP (Pierce).

4.3 Results

4.3.1 *Mitochondrial stress levels*

Western analysis was performed on wild type and knockout mitochondria to determine the amount of hsp60 and SOD2 protein present in each. The coomassie blue stained 12% SDS-PAGE gel in Figure 4.1 *A*, was used to show consistent sample loadings during the separation of mitochondrial proteins by SDS-PAGE. The bands show little variation in protein levels between the wild type and knockout samples, except for the band just below 70,000Da. This is BSA from the mitochondrial isolation procedure, its level depends on how well excess solution was removed from the mitochondria enriched fraction. The western blots visually show no differences in band intensity for both hsp60, Figure 4.1 *B*, and SOD2, Figure 4.1 *C*. The graphs in Figures 4.2 *A* and *B*, which show the western band intensities measured on GelQuant (DNR Bio-Imaging Systems), further support this. They display very little difference in the intensity levels, of both stress proteins, between the wild type and knockout mitochondria. Student's t-test was used to determine that there was no statistically significant difference between the two samples ($p<0.05$).

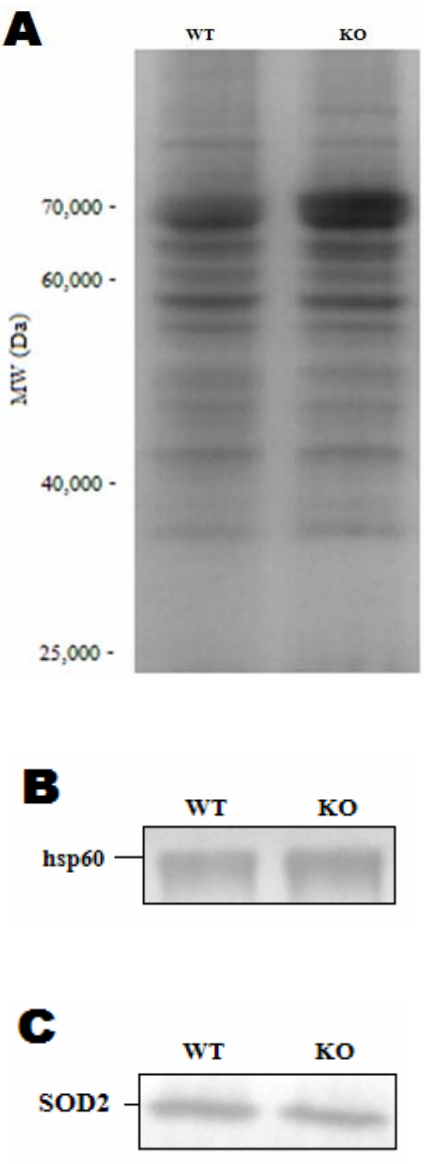

Figure 4.1 *Expression of hsp60 and SOD2 in wild type and knockout skeletal muscle mitochondria.* **(A)** Coomassie stained 12% SDS-PAGE gel replicate of western loadings, showing consistent sample loadings between WT and KO samples. **(B)** Western blot showing the protein levels of hsp60. **(C)** Western blot showing the protein levels of SOD2.

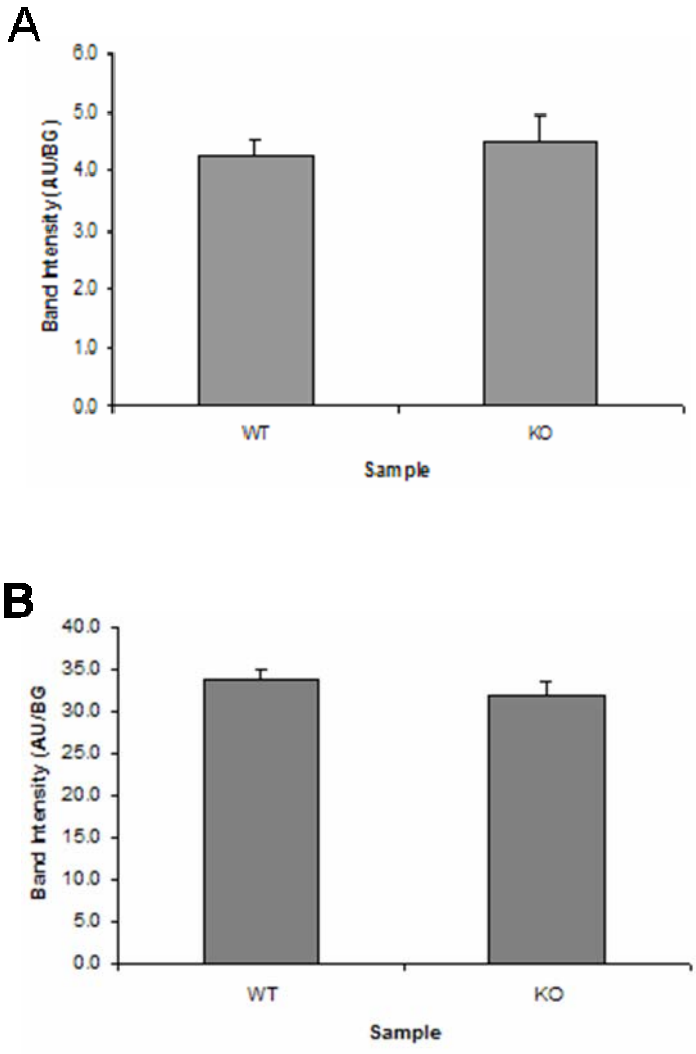

Figure 4.2 *Quantitation of hsp60 and SOD2 protein levels in wild type and knockout skeletal muscle mitochondria.* **(A)** Graph showing the level of hsp60 protein present in wild type and knockout mitochondria. The bars represent the average of four replicates, ± one standard deviation. No significant difference was seen by t-test. **(B)** Graph showing the level of SOD2 protein present in wild type and knockout mitochondria. The bars represent the average of three replicates, ± one standard deviation. No significant difference was seen by student's t-test.

4.4 Discussion

Similar levels of hsp60 and SOD2 were found in the wild type and myostatin knockout skeletal muscle mitochondria. Mitochondria which are not functioning properly produce more reactive oxygen species and express higher levels of stress proteins (reviewed in Reddy and Beal, 2005). These results indicate that the mitochondria from myostatin knockout skeletal muscle tissue are not being subjected to any increase in basal stress levels due to the knockout phenotype.

To further investigate whether the knockout phenotype has any effect on the mitochondria's ability to respond to stressors, mice could have been placed in a stress inducing environment (such as restraint, or raised temperature) prior to sample collection, or cultured myoblast cells from wild type and knockout skeletal muscle could have been subjected to in-vitro stressors.

CHAPTER FIVE

Proteomic Analysis of Knockout Mitochondrial Protein Levels

5.1 Introduction

A comparative proteomics approach was used to detect if there were any differences in expression of proteins from myostatin knockout skeletal muscle mitochondria compared to those from wild type mice. This was performed on a 2-DE gel format, where proteins are separated first by their net charge and then by their molecular weight, allowing for the separation of hundreds of proteins (Encarnacion *et al.*, 2005).

Comparative proteomics involves separating out individual proteins, quantitating their expression, looking for differences and then identifying the proteins which are modulated. In this study, proteins were separated by 2-DE. After optimisation of the level of protein loaded onto the 2-DE gel and reproducible profiles were obtained between replicate gels, expression levels were quantitated by silver staining. The resulting spot intensities were analysed for differences and proteins identified by in-gel tryptic digestion and MALDI-TOF MS.

5.2 Materials and methods

5.2.1 *Sample preparation*

A mitochondria enriched fraction was isolated from the Gastrocnemius muscle as described in Chapter 2.2.4.1. The muscle was homogenised, filtered, and the cell debris removed by centrifuging at 2,000 rcf. Mitochondria were pelleted at 10,000 rcf, these were washed and then pelleted again. The protein from this mitochondria enriched fraction was solubilised in IPG rehydration/solubilisation solution as in Chapter 2.2.4.2. An estimate of the total protein concentration was determined using the BCA Protein Assay Kit (Pierce) as described in Chapter 2.2.4.3 to ensure equal protein loadings onto IPGs. The IEF pellet protein was solubilised in TENT buffer as in Chapter 2.2.4.2 and protein estimation carried out as detailed in Chapter 2.2.2.2.

5.2.2 *Two-dimensional gel electrophoresis*

17cm 3-10NL IPGs (Bio-Rad) rehydrated in the IEF solution doped with 0.0002% bromophenol blue, as detailed in Chapter 2.2.4.4, for 17 hrs at 20°C. The rehydrated IPGs were focused at 10,000V for 60,000V/hrs. The focused IPG was prepared for the second dimension by equilibrating in SDS-PAGE equilibration buffer with DTT and then with IAA, as outlined in Chapter 2.2.4.5. The IPG was laid on a SDS-PAGE gel and electrophoresed at 15°C for 5 hrs and 45 mins. The gel was stained with silver stain plus (Bio-Rad), MS compatible silver stain, as in Chapter 2.2.4.6, the subsequent spot intensities measured using Image Gauge Version 4.0 (FujiFilm), as described in Chapter 2.2.4.7.

5.2.3 *Protein identification*

Spots of interest were excised and digested with trypsin, as detailed in Chapter 2.2.4.9, for PMF identification. Gel plugs were destained in 1% H_2O_2, washed with 25mM NH_4HCO_3, equilibrated in 1:1 25mM NH_4HCO_3/ACN, and dehydrated in ACN. The plug was air dried and rehydrated in a 0.005μg/μL trypsin solution at 4°C for 1 hr. Excess trypsin was removed and the plug incubated at 37°C for 6 hrs. The resulting peptides were extracted overnight at 4°C in 20% ACN/0.1% TFA. Peptide masses were determined using MALDI-TOF MS, as described in Chapter 2.2.4.10. Identifications were made by Mascot™ database searches which were performed via BioTools™ 3.0 (Bruker Daltonics).

5.2.4 *SDS-PAGE of IEF pellet proteins*

Protein estimation was performed using the BCA Protein Assay Kit (Pierce) as described in Chapter 2.2.2.2 to ensure equal amounts of protein were loaded onto SDS-PAGE gels. IEF pellet protein (1μg) was separated on a 12% SDS-PAGE gel as outlined in Chapter 2.2.4.11, which was silver stained and imaged.

5.3 Results

5.3.1 *Two-dimensional electrophoresis gel protein loadings*

As a starting point, it was unknown how much protein to load onto the 2-DE gels, so the first study to be undertaken was to load known amounts of protein, to determine how much sample protein to load. 100, 200 and 300μg of protein was loaded onto 17 cm 3-10NL IPGs, and the 2-DE gels were run and visualised as usual. As more protein is loaded on the gel, more proteins can be seen, but some resolution is lost as closely migrating proteins begin to obscure each other. Figure 5.1 *A* shows a loading of 100μg, at this loading approximately 80 spots are visible. Figure 5.1 *B* is a loading of 200μg, with this amount of protein loaded, approximately 120 spots are present. Figure 5.1 *C* is loaded with 300μg of protein, this gel shows 180 spots, but it is starting to look overloaded with vertical and horizontal streaks appearing.

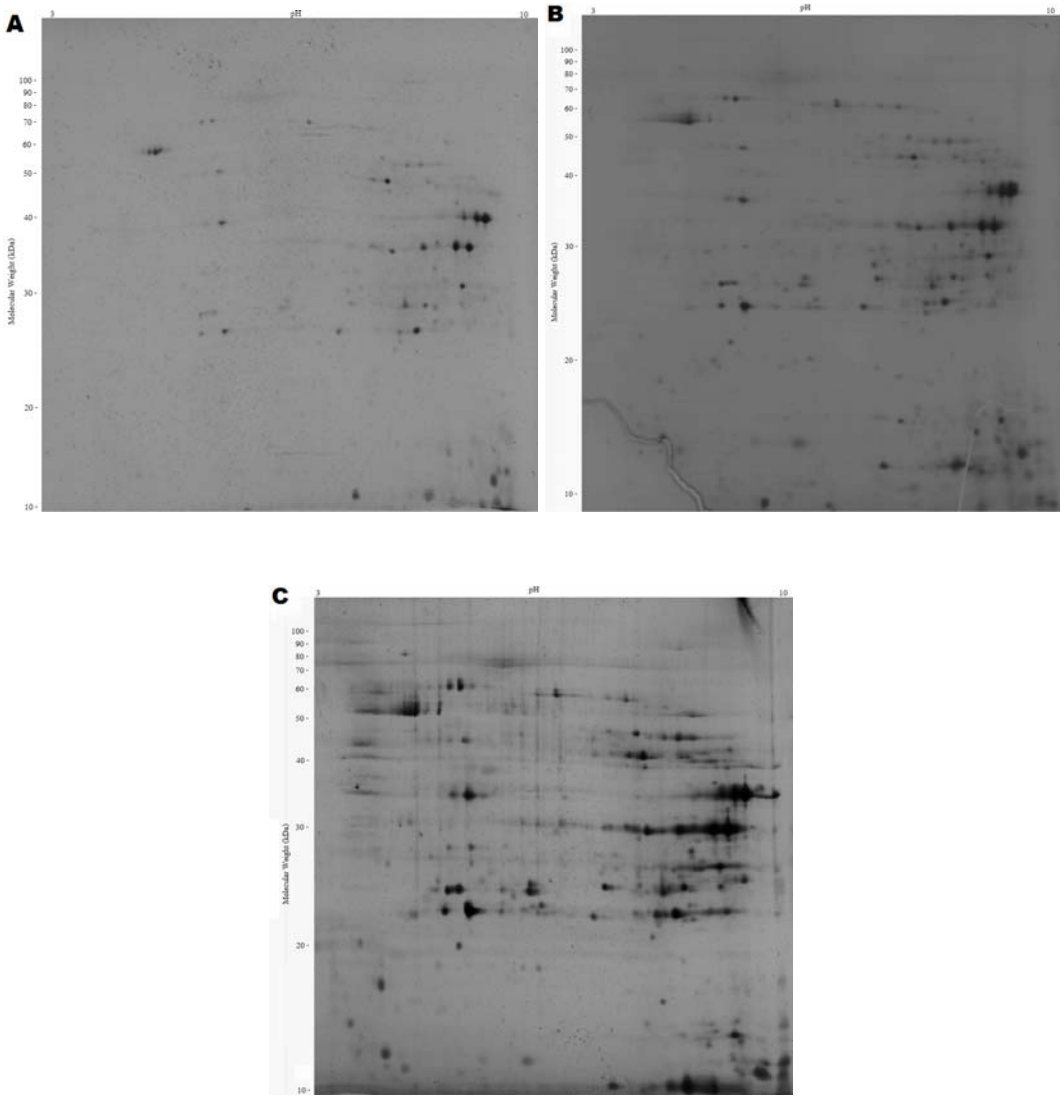

Figure 5.1 *Visualisation of mitochondrial proteins separated by 2-DE as a function IPG protein loadings.* 17cm 3-10NL IPG loaded with different of mitochondrial protein, second dimension run on a 12% SDS-PAGE gel, stained with silver stain plus MS compatible silver stain **(A)** 100µg of protein loaded. **(B)** 200µg of protein loaded. **(C)** 300µg of protein loaded. (See Appendices A to C for full page versions)

The horizontal streaking is due to the IEF not being run long enough for the amount of protein present to focus. The IEF method could have been adjusted by increasing the amount of V/hrs the IPG had to be maintained at 10,000V, so that the protein could focus properly. The vertical streaking is from protein not equilibrating properly before SDS-PAGE and could have been alleviated by equilibrating the IPGs for longer prior to running the second dimension, possibly agitating them to aid diffusion of the solution into the IPG. Because an outside source was relied upon for the samples used during this study, the amount of sample was limited, and a lower protein loading was opted for. A loading amount between 200 and 300µg (220µg) was chosen to use with the experimental samples. This amount allows for approximately 160 spots to be visualised, whilst still maintaining resolution and keeping within sample availability.

5.3.2 *Reproducibility of two-dimensional electrophoresis gels*

One of the major issues with 2-DE has always been the low level of reproducibility. Reproducibility of the isoelectric focusing step has been improved since the introduction of commercially available IPGs (Gorg *et al.*, 1988). However, the greatest reproducibility issue faced during this study was maintaining a consistent protein loading from gel to gel. There are a number of issues confronted when rehydrating an IPG with the sample solution. The volume of sample must be the same if the amount of protein loaded is to be consistent and all of this solution must be absorbed by the gel. If the sample solution splashes onto the IPG's plastic backing, or if it is beaded by the mineral oil used to overlay the IPG, it will not enter the gel. Lastly, the higher molecular weight proteins cannot enter the IPG until the gel has rehydrated enough so that the protein can fit through the gel's pores. But the IPG cannot be left to rehydrate too long or it will dry out and chemicals in the IEF solution will begin to break down.

Figure 5.2 shows a set of four 2-DE gels which were run using the same IEF sample solution. Figures 5.2 *A* and *C* show low protein loadings for gels which were supposedly loaded with 220µg of protein. By looking back at Figure 5.1, these two gels look to have an intermediate amount between 100µg (Figure 5.1 *A*) and 200µg (Figure 5.1 *B*). Figure 5.2 *B* contrasts the previous two gels mentioned, having a very large protein loading, possibly even more than that seen with 300µg (Figure 5.1 *C*) of protein loaded. Figure 5.2 *D* has a loading closer to what would be expected for 220µg of protein.

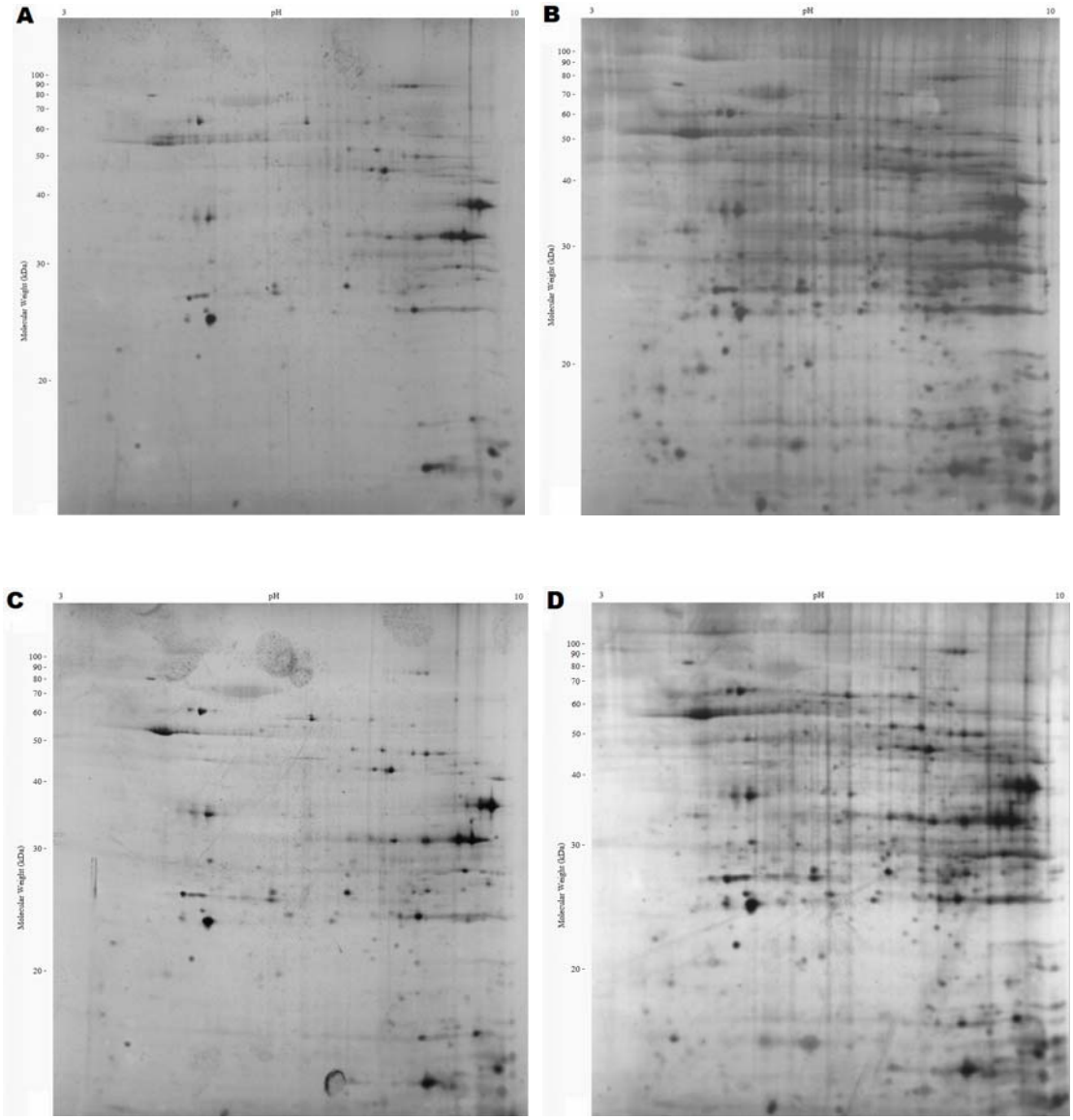

Figure 5.2 *Reproducibility of 2-DE gel protein loadings.* 17cm 3-10NL IPG loaded with 220µg of mitochondrial protein, second dimension run on a 12% SDS-PAGE gel, stained with silver stain plus MS compatible silver stain **(A)** Replicate number one. **(B)** Replicate number two. **(C)** Replicate number three. **(D)** Replicate number four. (See Appendices D to G for full page versions)

5.3.3 *SDS-PAGE analysis of the insoluble fraction of the IEF solution*

As mentioned in Chapter 1.4.1, 2-DE is generally not capable of resolving hydrophobic proteins, unless measures are taken to increase the solubilising power of the solution used. In an attempt to gauge the level of protein which was being lost in the solubilisation step, the pellet left after the mitochondrial protein was solubilised in IPG rehydration/solubilisation solution was re-solubilised in TENT buffer, see Chapter 2.2.4.2 for details. The amount of protein retrieved from these pellets accounted for only 3% of the total amount of protein retrieved, showing that either the TENT buffer was ineffective in solubilising the remaining protein or most of the protein had been solubilised in the IEF solution. These pellet proteins were run on a 12% SDS-PAGE gel and as is seen in Figure 5.3 relatively few proteins were detected by silver stain. This, and the low amount of protein detected by BCA protein estimation (detailed in Chapter 2.2.2.2), suggests that many of the hydrophobic proteins may have been solubilised and were not resolved in the 2-DE gels as they were lost on the IPG matrix or precipitated out of solution during focusing, as described by Adessi *et al.* (1997).

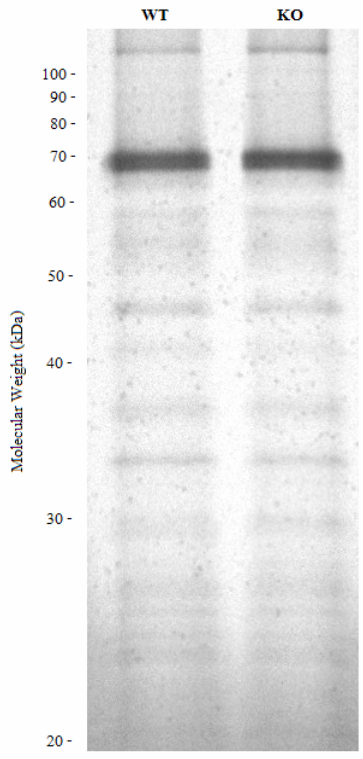

Figure 5.3 *Separation of proteins remaining after solubilisation in IPG rehydration/equilibration solution.* WT and KO IEF pellet protein (1µg) separated on a 12% SDS-PAGE gel and stained with silver stain plus MS compatible silver stain.

5.3.4 *Mitochondrial 2-DE protein map of WT and KO gastrocnemius muscle*

A reproducible gel set was achieved by taking immense care during the IPG loading stage. This consisted of three wild type gels and three knockout gels, each showing mitochondrial proteins from the gastrocnemius muscle separated by their isoelectric point and then by their molecular weight. Figure 5.4 *A* is a representative gel from the wild type sample, and Figure 5.4 *B* is a representative from the knockout sample. The full set of 2-DE gels can be found in Appendices H to M.

Each of these replicates showed a consistent loading pattern and approximately 160 individual protein spots were detected by silver staining. There is a concentration of proteins in the alkaline region of the gel, and in the higher molecular weight acidic region. Few proteins were resolved in the neutral pH region. Proteins of a low molecular weight were not resolved well, showing large amounts diffusion and no proteins over a molecular weight of 90kDa were ever seen.

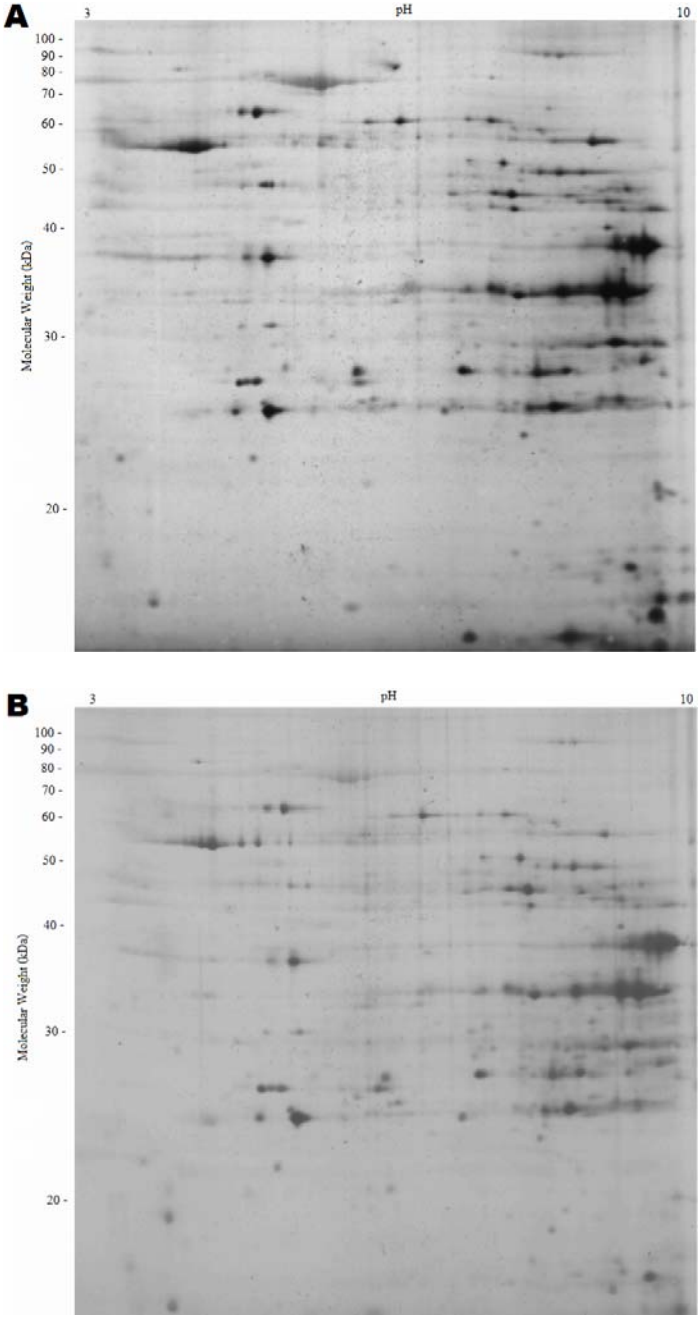

Figure 5.4 *2-DE gels of wild type and knockout mitochondrial protein.* 17cm 3-10NL IPG loaded with 220µg of mitochondrial protein, second dimension run on a 12% SDS-PAGE gel, stained with silver stain plus MS compatible silver stain. **(A)** Wild type sample. **(B)** Knockout sample. (See Appendix H to M for full page versions of entire gel set)

5.3.5 *Modulation of mitochondrial proteins seen in knockout skeletal muscle*

70 of the 160 spots detected in the 2-DE gels had their spot intensity analysed using Image Gauge (FujiFilm). These were chosen on the basis of spots which had already had proteins identified and others which showed visible differences. The assigned spot numbers are displayed on a 2-DE map in Figure 5.5.

As shown in Table 5.1, the majority of the spots quantitated showed no difference in expression between the wild type and knockout mitochondria. However some proteins did show significant changes in their levels of expression. Spot numbers 49 and 68 were up-regulated in the knockout sample and numbers 63 and 67 was down-regulated, but were only significant at $p<0.1$. Spot number 59 was expressed 1.2 times less in the knockout mitochondria ($p<0.05$) and number 46 was expressed 2.4 times higher ($p<0.005$). However, all these modulated proteins were expressed at levels too low to be identified during this study.

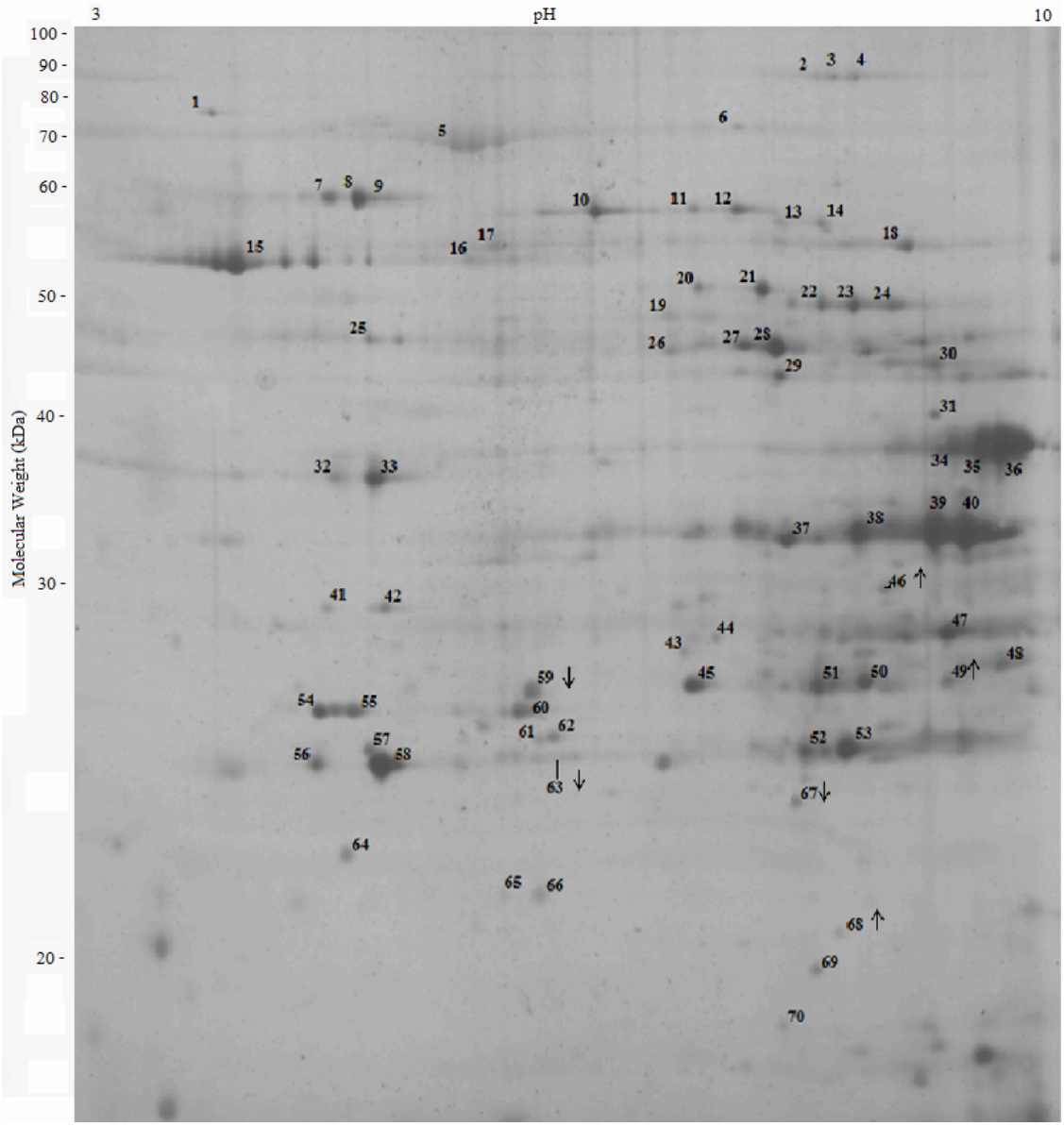

Figure 5.5 *2-DE gel showing assigned spot numbers.* These spot numbers were assigned to spots which already had proteins identified and others which showed visible differences in intensity. The pixel intensity of only these spots was measured. Arrows to the right hand side of a spot number indicates an up-regulation (↑) or down-regulation (↓) in the KO sample, which was at a level of significance of at least $p<0.1$.

Table 5.1 *Modulation of knockout proteins shown by changes in 2-DE spot intensities.* Table listing the change in spot intensity, significance level of that change and protein which that spot corresponds to (if that protein has been identified).

Spot	Change	Sig.	Protein
1	↑ 1.4		Glucose Regulated Protein 75
2	↓ 1.5		Aconitase 2
3	↓ 1.2		Aconitase 2
4	↓ 1.1		Aconitase 2
5	↑ 1.2		BSA
6	N/C		Inner Membrane Protein
7	↓ 1.1		Heat Shock Protein 60
8	N/C		Heat Shock Protein 60
9	↓ 1.1		Heat Shock Protein 60
10	N/C		Dihydrolipoamide Dehydrogenase
11	↓ 1.2		Dihydrolipoamide Dehydrogenase
12	N/C		Dihydrolipoamide Dehydrogenase
13	↓ 1.2		Aldehyde Dehydrogenase 6a1
14	↓ 1.1		Not Identified by PMF
15	N/C		ATP Synthase, H+ transporting, F_1 complex, beta subunit
16	↓ 1.2		Not Identified by PMF
17	↓ 1.1		Not Identified by PMF
18	N/C		ATP Synthase, H+ transporting, F_1 complex, alpha subunit
19	↑ 1.1		Not Identified by PMF
20	↑ 1.2		Not Identified by PMF
21	↑ 1.1		Enolase 3
22	N/C		Fumarate Hydratase 1
23	↑ 1.1		Fumarate Hydratase 1
24	↑ 1.1		Fumarate Hydratase 1
25	↓ 1.2		Succinate-CoA ligase, beta subunit
26	↓ 1.1		IsoValeryl CoA Dehydrogenase
27	N/C		Creatine Kinase
28	N/C		Creatine Kinase
29	N/C		Isocitrate Dehydrogenase 3, beta subunit
30	N/C		Aldolase A
31	↓ 1.1		Not Identified by PMF
32	↓ 1.2		Pyruvate Dehydrogenase, beta subunit
33	N/C		Pyruvate Dehydrogenase, beta subunit
34	N/C		Malate Dehydrogenase 2
35	N/C		Malate Dehydrogenase 2
36	N/C		Malate Dehydrogenase 2
37	N/C		Electron Transferring Flavoprotein, beta subunit
38	N/C		Voltage Dependent Anion Channel 1
39	N/C		Voltage Dependent Anion Channel 1
40	N/C		Voltage Dependent Anion Channel 1

41	↓ 1.2		Prohibitin
42	N/C		Prohibitin
43	↓ 1.1		Not Identified by PMF
44	↑ 1.2		Not Identified by PMF
45	N/C		Not Identified by PMF
46	↑ 2.4	$p<0.005$	Not Identified by PMF
47	N/C		Electron Transferring Flavoprotein, alpha subunit
48	N/C		Hydroxyacyl-Coenzyme A Dehydrogenase 2
49	↑ 1.3	$p<0.1$	Not Identified by PMF
50	N/C		ES1
51	N/C		Not Identified by PMF
52	N/C		Super Oxide Dismutase 2
53	N/C		Super Oxide Dismutase 2
54	N/C		Apolipoprotein A-1
55	N/C		NADH Dehydrogenase (Ubiquinone) Flavoprotein 2
56	↓ 1.1		ATP Synthase, H+ transporting, F_0 complex, subunit d
57	↑ 1.1		Adenylate Kinase 1
58	N/C		ATP Synthase, H+ transporting, F_0 complex, subunit d
59	↓ 1.2	$p<0.05$	Not Identified by PMF
60	↑ 1.1		Peroxiredoxin 3
61	↓ 1.4		Not Identified by PMF
62	↑ 1.1		Not Identified by PMF
63	↓ 2.1	$p<0.1$	Not Identified by PMF
64	↑ 1.1		Not Identified by PMF
65	↓ 1.1		Not Identified by PMF
66	N/C		Not Identified by PMF
67	↓ 1.3	$p<0.1$	Not Identified by PMF
68	↑ 1.4	$p<0.1$	Not Identified by PMF
69	↑ 1.3		Nucleoside-Diphosphate Kinase 2
70	↓ 1.3		Not Identified by PMF

Spot numbers correspond to those shown in Figure 5.5. Change in protein expression is expressed as a fold increase or decrease in the knockout spot intensity compared to wild type spot intensity. ↑ signifies an up-regulation of protein in the knockout mitochondria and ↓ signifies a down-regulation, N/C signifies no change in protein expression. Levels of significance were determined by student's t-test. A full list of information on identified proteins is available in Appendix N.

An attempt was made to identify the proteins in spots 46 and 59, by combining gel plugs from each of the 2-DE gels and performing a tryptic digest as per usual. Gel plugs for spot 46 came from the knockout gels, and plugs for spot 59 came from the wild type gels, as this was the sample each was expressed at higher amounts in. But this still yielded only low spectra, Figure 5.6 *B* shows the spectrum acquired from spot 46. Compared to the spectrum in Figure 5.6 *A*, which was used to identify spot 4 as Aconitase 2, sample 46's peak intensities are low and the spectrum has a rising baseline in the low mass region as the laser power had to be increased to ionise the sample. The peak at m/z = 842.5 is a cleavage product of trypsin acting upon itself.

Many of the proteins which were identified did not show statistically significant changes in expression levels between the wild type and knockout mitochondria, but are important metabolic enzymes or critical to the proper functioning of the mitochondria. These proteins will be discussed further in section 5.4.

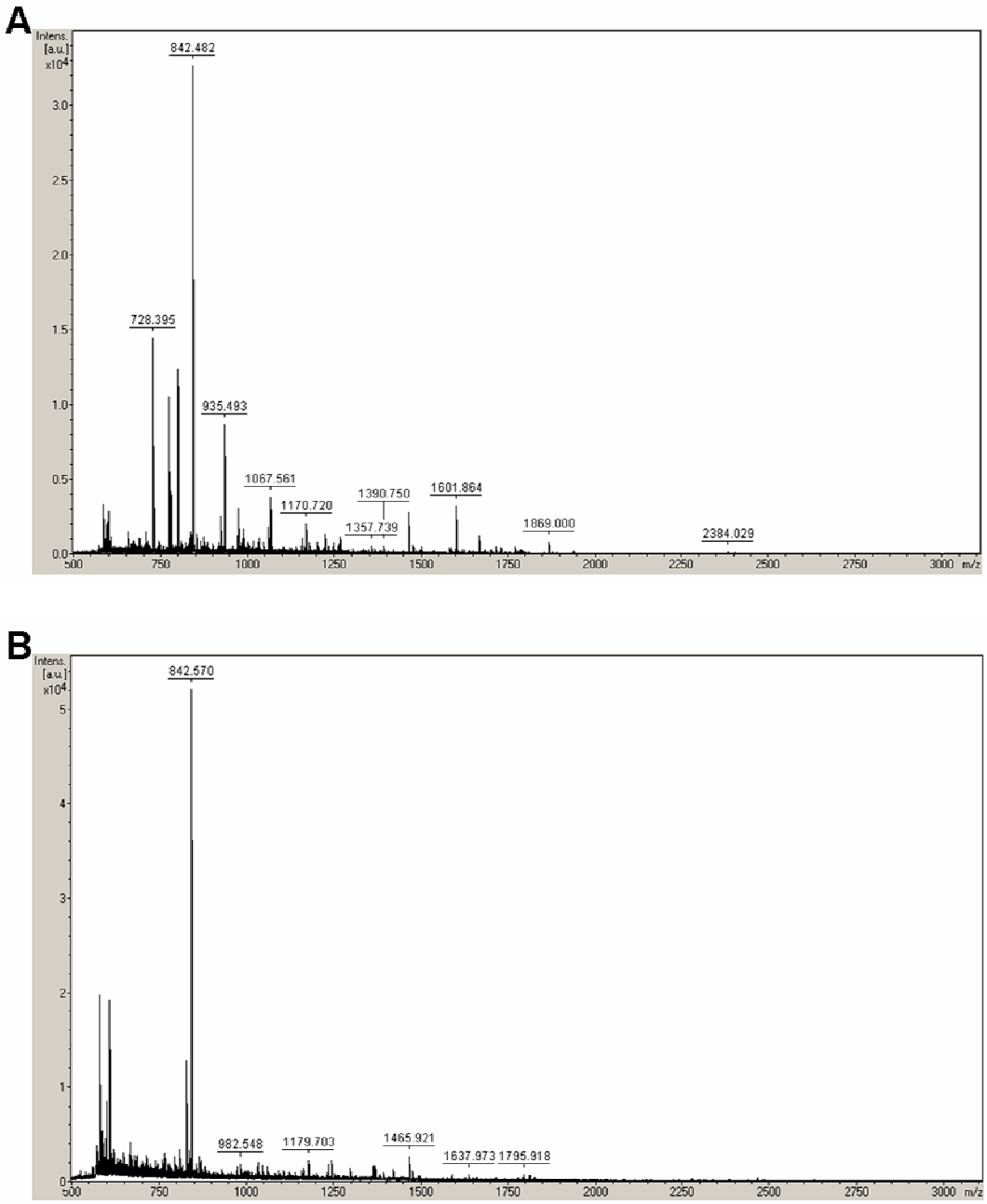

Figure 5.6 *MALDI-TOF spectra of tryptic digests.* **(A)** Spectrum of the tryptic digest of spot number 4, which was identified as aconitase 2. **(B)** Spectrum of the tryptic digest of spot number 46, which could not be identified by PMF.

5.4 Discussion

5.4.1 *Loading of two-dimensional electrophoresis gels*

This study identified two parameters that needed to be addressed prior to achieving reproducible 2-DE gels.

a) The amount of protein loaded had to be optimised, if too little was loaded not many spots were detected, if too much was loaded vertical and horizontal streaking appeared.

b) And the IPGs had to be rehydrated very carefully, to avoid protein being lost on its backing or in the mineral oil overlay. This was found to be the most important parameter to obtain a consistent loading between gels, as gels laid from the same solution, with the same volume which were left to rehydrate for the same amount of time showed vast differences in their protein loading.

Attempts to normalise the spot intensities obtained from each gel against a protein maintained at a consistent level in mitochondria, such as actin, were unsuccessful as the protein was present in quantities below the detection limits of this study.

5.4.2 *Protein detection and identification from 2-DE gels*

Estimates of the total number of proteins present in the mitochondria vary between 1,000 to 2,000 proteins, these numbers are gauged from genomic analysis with only

685 of these being identified at a protein level (Gibson, 2005). In the final 2-DE gel set, around 160 spots were visualised using silver stain plus (Bio-Rad). This corresponds to around one tenth of the proteins present in the mitochondrial proteome. Granting that many of the proteins present in the mitochondria are hydrophobic proteins and are difficult to resolve by 2-DE, there are still many more hydrophilic proteins present in the mitochondria which cannot be seen in this gel set.

Two strategies could have been undertaken to detect more of this portion of the mitochondrial proteome. The amount of protein loaded onto the gel could have been increased, but as explained in section 5.3.1, this leads to a reduction in resolution and sample availability did not allow for this. A more sensitive detection method could have been used, fluorescent staining would have given a two fold increase in detection. This was not undertaken because increasing the staining sensitivity would still not allow for the newly detected proteins to be identified as the level of protein present would still be below that required to obtain a spectrum capable of positive identification by PMF.

Of the 160 protein spots detected in the 2-DE gels, only 29 of these were identified as a known protein. The general consensus for identification of a 2-DE protein spot is a coomassie blue stained spot (10ng of protein), seen as silver stain (1ng of protein) was used during this study, many of the spots seen were not able to be identified. To identify more of the proteins seen in the 2-DE gels, one would have to load more protein onto the gel. Preparative gels could have been run as described in Chapter

1.4.2, but was not applied during this study due to sample restrictions and economic constraints.

5.4.3 *Relevant protein identifications from 2-DE gels*

Once a reproducible 2-DE gel set was obtained, modulation and identification of the proteins detected in the knockout skeletal muscle mitochondria was undertaken. Four of these proteins showed changes at the $p<0.1$ level, and two proteins showed changes at a level of significance greater than $p<0.05$. Unfortunitely, none of these proteins were able to be identified during this study by PMF.

Hsp60 and SOD2 proteins were identified during the 2-DE analysis. Similar levels of expression were observed between wild type and knockout mitochondria in this study, which is in agreement with the western blot analysis detailed in Chapter 4.

Nearly all of the proteins identified in the 2-DE gels were high abundance mitochondrial proteins. None of these showed any significant change in expression but are important mitochondrial proteins.

Aconitase 2 (Spots 2, 3 and 4), fumarate hydratase 1 (Spots 23, 24 and 27), succinate-CoA ligase (Spot 25), isocitrate dehydrogenase 3 (Spot 29), malate dehydrogenase 2 (Spots 34, 35 and 36) and nucleoside-diphosphate kinase 2 (Spot 69) are all enzymes present in the TCA cycle involved in the oxidation of acetyl-CoA and the subsequent generation of NADH used to produce ATP via oxidative phosphorylation (Garrett

and Grisham, 1999). Aconitase has been implicated in aging, as its activity declines more dramatically than the other TCA enzymes (Yarian *et al.*, 2006), this is theorised to be because of oxidative modifications to the protein (Hunzinger *et al.*, 2006). The $NADP^+$ dependent isoform of isocitrate dehydrogenase generates NADPH which is used to regenerate reduced glutathione an essential part the NADPH-dependent thioredoxin system for detoxifying ROS produced by aerobic metabolism (Kim *et al.*, 2005; Kil *et al.*, 2004). Impaired fumarate hydratase has been linked with cancer, as a build up of fumarate in the TCA cycle, due to inactive fumarate hydratase, inhibits prolyl hydroxylase enzymes in the cell, producing an apoptosis-resistant phenotype (King *et al.*, 2006).

Pyruvate dehydrogenase beta (Spots 32 and 33) and dihydrolipoamide dehydrogenase (Spots 10, 11 and 12) are two of the components which make up the pyruvate dehydrogenase complex, which is the link between glycolysis and the TCA cycle. Dihydrolipoamide is a regulatory subunit of the complex, being allosterically inhibited by either of its products, acetyl-CoA and NADH (Garrett and Grisham, 1999). Defects in pyruvate dehydrogenase results in impaired aerobic metabolism and has been shown to cause congenital lactic acidosis (Saijo *et al.*, 1997) as well as being linked with several neurodegenerative diseases (Klivenyi *et al.*, 2004). Other enzymes important in metabolic pathways outside of the TCA cycle are isovaleryl-CoA dehydrogenase (Spot 26), hydroxyacyl-CoA dehydrogenase (Spot 48) and aldehyde dehydrogenase (Spot 13), each is involved in oxidation of: the amino acid

leucine (Mohsen and Vockley, 1995), lipids (Bajpai *et al.*, 1998) and aldehydes (Quintanilla *et al.*, 2005), respectively.

Oxidative phosphorylation components identified were various ATP synthase subunits (Spots 15, 18, 56 and 58), NADH dehydrogenase (Ubiquinone) flavoprotein 2 (Spot 55) and both subunits of the electron transferring flavoprotein (Spots 37 and 47). ATP synthase is the final stage of oxidative phosphorylation, and uses the proton gradient generated by the ETS to produce ATP (Garrett and Grisham, 1999). NADH dehydrogenase flavoprotein and the electron transferring flavoprotein transfer electrons to the ETS in order to generate the proton gradient mentioned above (Garrett and Grisham, 1999). The electron transferring flavoprotein is particularly important as it oxidises at least eleven matrix dehydrogenases, making it important link between fatty acid and amino acid oxidation and the ETS. So much so that defective copies of the protein results in metabolic disorders (Schiff *et al.*, 2006).

Creatine kinase (Spots 27 and 28) is used in ATP homeostatis, as it transfers a phosphate group from phosphocreatine stores. This is of particular importance in muscle mitochondria as it is used as a way of maintaining ATP levels in times of high energy consumption, such as muscle contraction (Bruton *et al.*, 2003; Dahlstedt *et al.*, 2000).

Proteins important in the maintenance of the mitochondria include: Glucose regulated protein 75 (GRP75) (Spot 1), hsp60 (Spots 7, 8 and 9), prohibitin (Spots 41 and 42),

SOD2 (Spots 52 and 53) and peroxiredoxin 3 (Spot 60). GRP75, hsp60 and prohibitin are all involved in facilitating the folding and assembly of proteins imported into the mitochondria (Nijtmans *et al.*, 2000; Martinus *et* al, 1995; Mizzen *et al.*, 1991). SOD2 and peroxiredoxin both detoxify ROS produced by the mitochondrial ETS. SOD2 reduces superoxide to hydrogen peroxide (Reddy and Beal, 2005) and peroxiredoxin reduces hydrogen peroxide to water (Chang *et al.*, 2004).

The presence of aldolase and enolase, considered to be cytoplasmic proteins, suggests a low level of cytoplasmic contamination of the mitochondrial preparation. However, these proteins have recently been shown to be present in or to interact with the mitochondria (Brandina *et al.*, 2006; Giege *et al.*, 2003). Apolipoprotein A-1 has been shown to interact with the beta subunit of ATP synthase (Martinez *et al.*, 2003), and prohibitin is a protein which acts as a chaperone to stabilise newly synthesised proteins in the mitochondria (Nijtmans *et al.*, 2000) and required in the mitochondria as most of the proteins are encoded by nuclear DNA (Paschen and Neupert, 2001).

CHAPTER SIX

Final Discussion and Future Directions

6.1 Final discussion

This study used a global shot-gun approach to try and detect differences in the mitochondria from wild type and myostatin knockout muscle. A large muscle group with a mixed fibre type was used, so that there would be adequate sample and so that the changes to the fibre type switch, outlined in Chapter 1.2.1, would be apparent. Comparative proteomics was used, as it allows you to look at changes in protein expression levels without knowing what protein you are looking for. And a broad pH range was used in the IEF step so that a wide spectrum of mitochondrial proteins could be analysed.

This resulted in six proteins being shown to be modulated in the knockout mitochondria. These proteins were unable to be identified by PMF due to the amount of protein present being too little to obtain an adequate spectrum. The majority of the proteins identified were high abundance mitochondrial proteins and showed no significant changes between the wild type and knockout mitochondria.

Interestingly, two of the mitochondrial enzymes identified in this study have been reported to have decreased activity in glycolytic muscle mitochondria compared to mitochondria from oxidative fibres. Mogenson and Sahlin (2005) reported a two-fold

decrease in 3-hydroxyacyl-CoA dehydrogenase activity in EDL mitochondria compared to soleus mitochondria and Jackman and Willis (1996) have reported malate dehydrogenase to have a decreased activity in glycolytic fibre mitochondria. As the myostatin knockout mice serve as a model for glycolytic muscle metabolism due to their increased proportion of type IIB fibres (Girgengrath *et al.*, 2005; Wegner *et al.*, 2000). This suggests that the increased enzymatic activity observed by other researchers could be due to either enzyme activation in the oxidative fibre mitochondria or inhibition in the glycolytic fibre mitochondria, since the present study showed no significant change in the expression levels of these enzymes between wild type and myostatin knockout mitochondria.

Proteomics studies analysing whole skeletal muscle samples from oxidative and glycolytic fibres have reported modulation of mitochondrial metabolic proteins between the fibre types. Aconitase, ATP synthase subunits, malate dehydrogenase, mitochondrial creatine kinase and NADH dehydrogenase were reported to be down-regulated in the glycolytic fibres (Sayd *et al.*, 2006; Donoghue *et al.*, 2005; Okumura *et al.*, 2005). Our study, using only mitochondrial samples isolated from the muscle, shows no significant change in expression of these proteins, suggesting the observations made by these researchers could be due to a decrease in mitochondrial density in these fibre types. This re-iterates observations made by other investigators that there is a decrease in the number of mitochondria present in glycolytic muscle fibres (Schmidt and Herpin, 1997; Jackman and Willis, 1996).

6.2 Future directions

Having shown that spots 46, 49, 59, 63, 67 and 68 are being modulated at a level of significance greater than $p<0.1$, an effort should be made to try and identify these proteins. This would require loading more protein onto the 2-DE gel to bring the level of protein separated in the gel spot within the detection limits of MS based methods of identification (around 10ng of protein). This study has utilised MADLI-TOF MS and PMF to assign identity to protein spots, this however requires that the protein being identified already exist in a database. Analysing the samples by LC-MS/MS would give additional information and would be particularly useful if the proteins were unknown. Because the peptides are separated by LC, greater resolution of the peptides is achieved, and information is obtained on the lower mass peptides (below 700Da) which are obscured by matrix peaks in MALDI-TOF MS. As described in Chapter 1.4.2, identification of unknown proteins can be facilitated by peptide sequencing performed using tandem MS.

Having only detected 160 proteins in the 2-DE gels a more complete mitochondrial proteome could also be built up. To facilitate this, the resolution of the IEF step could be increased by using a narrower pH gradient, either focusing on one portion of the proteome or using a series of overlapping IPGs to build up a complete picture of the more hydrophilic proteins present. The protein loading could then be increased so that the lower intensity proteins can be detected with an appropriate protein stain. The increased resolution will allow for the proteins to resolve without overloading the gels. In order to resolve more high and low molecular weight proteins, gradient SDS-

PAGE gels could be utilised for the second dimension. The increasing acrylamide concentration would limit the diffusion of lower mass proteins, and allow higher mass proteins to migrate further into the gel, than the continuous 12% SDS-PAGE gels which were used in this study.

Two of the proteins which were identified during the study, 3-hydroxyacyl-CoA dehydrogenase and malate dehydrogenase, have been reported to have a decreased activity in mitochondria from glycolytic muscle, but were shown to be expressed at the same level during this study. This finding should first be confirmed by western blot analysis, using antibodies specific for these two enzymes. If no change in expression is occurring, the change in activity documented by Mogenson and Sahlin (2005) and Jackman and Willis (1996) could be because of a different isoform of the enzyme being expressed in mitochondria from the different fibre types, or some type of PTM of the enzyme.

Protein isoforms are produced via differential mRNA splicing, and the proteins produced will quite often have different specificities or activities (Michael *et al.*, 1997). PTM of an enzyme can alter its activity, specificity, localisation and stability (Peck, 2005). Over 300 types of PTMs are known, the most common two being phosphorylation and glycosylation (Jenson, 2004). Different forms of various proteins were seen in this 2-DE experiment, including malate dehydrogenase, but no significant change in expression of these was detected. The different forms of proteins seen in 2-DE gels result from a change in net charge or molecular weight, this can be due to either differential mRNA splicing or PTM.

To determine how if the change in activity of the enzymes identified in this study were due to isoforms or PTM, the resolution of the IPG used would need to be increased to detect the different forms of the proteins being expressed in mitochondria from oxidative and glycolytic fibres. Specific PTMs, such as phosphorylation of a tyrosine residue, can be identified by western blot analysis. More specific information on where the PTM is located on the protein can be detected by MS, looking for differences in the mass of peptides generated by proteolytic digestion of the protein, and even the residue it is located on from peptide fragmentation information.

Research comparing mitochondria from oxidative and glycolytic muscle fibres has pointed out two targets for further research into differences between the two subspecies of mitochondria, COX and the ANT. COX has consistently been shown to have decreased activity in mitochondria from glycolytic muscle fibres (Gueguen *et al.*, 2005A; Gueguen *et al.*, 2005B; Willis and Jackman, 1995), the reason for which is unknown. And glycolytic fibre mitochondria have been shown to have a higher affinity for ADP than oxidative fibre mitochondria, which is theorised to be because of differences in the ANT (Gueguen *et al.*, 2005A; Gueguen *et al.*, 2005B; Willis and Jackman, 1995).

These targets are both membrane bound complexes and are thus highly hydrophobic and cannot be resolved by conventional 2-DE. Other methods for isolating membrane bound complexes of the mitochondria have been developed which separate out intact complexes, which are then subjected to further analysis by methods such as SDS-

PAGE. Immuno-affinity techniques use antibodies specific for the complex of interest are conjugated to agarose beads, and are able to 'fish out' the complex from a mixture of mitochondrial proteins (Keeney *et al.*, 2006; Schilling *et al.*, 2005). Sucrose density gradient fractionation has been optimised to separate out the oxidative phosphorylation complexes from the mitochondrial membrane according to their mass (Hanson *et al.*, 2001). Blue native gel electrophoresis separates out complexes under non-reducing conditions so the complexes remain intact. If this gel is rotated 90° and laid on a SDS-PAGE gel, it creates a 2-D map of the membrane bound components of the mitochondria (Brookes *et al.*, 2002; Schagger and von Jagow 1991). Differences in the components of these complexes, detected by the analysis carried out after isolation could indicate functional differences in the complexes of mitochondria from glycolytic and oxidative fibres.

References

Adessi, C., Miege, C., Albrieux, C. and Rabilloud, T. (1997) Two-dimensional electrophoresis of membrane proteins: a current challenge for immoblized pH gradients. *Electrophoresis*, **18**, 127-135.

Ahmed, N. and Rice, G.E. (2005) Strategies for revealing lower abundance proteins in two-dimensional protein maps. *Journal of Chromatography B*, **815**, 39-50.

Amthor, H., Huang, R., McKinnell, I., Christ, B., Kambadur, R., Sharma, M. and Patel, K. (2002) The regulation and action of myostatin as a negative regulator of muscle development during avian embryogenesis. *Developmental Biology*, **251**, 241-257.

Bailey, S.M., Landar, A. and Darley-Usmar, V. (2005) Mitochondrial proteomics in free radical research. *Free Radical Biology and Medicine*, **38**, 175-188.

Bajpai, M., Gupata, G., Jain, S.K. and Setty, B.S. (1998) Lipid metabolizing enzymes in isolated rat testicular germ cells and changes associated with meiosis. *Andrologia*, **30**, 311-315.

Bass, J., Oldham, J., Sharma, M. and Kambadur, R. (1999) Growth factors controlling muscle development. *Domestic Animal Endocrinology*, **17**, 191-197.

Bellinge, R.H.S., Liberles, D.A., Laschi, S.P.A., O'Brien, P.A. and Tay, G.K. (2005) *Myostatin* and its implications on animal breeding: a review. *Animal Genetics*, **36**, 1-6.

Berry, C, Thomas, M., Langley, B., Sharma, M. and Kambadur, R. (2002) Single cysteine to tyrosine transition inactivates the growth inhibitory function of Piedmontese myostatin. *American Journal of Physiology*, **283**, C135-141.

Boccard, R. (1981) Facts and reflections on muscular hypertrophy in cattle: double muscling or culard. In Lawrie, R. (ed.), *Developments in meat science*. Applied Science Publishers, London, Vol. 2, pp. 1-28.

Bouley, J., Meunier, B., Chambon, C., De Smet, S., Hocquette, J.F. and Picard, B. (2005) Proteomic analysis of bovine skeletal muscle hypertrophy. *Proteomics*, **5**, 490-500.

Brandina, I., Graham, J., Lemaitre-Guillier, C., Entelis, N., Krasheninnikov, I., Sweetlove, L., Tarassov, I. and Martin, R.P. (2006) Enolase takes part in a macromolecular complex associated to mitochondria in yeast. *Biochimica et Biophysica Acta*, **1757**, 1217-1228.

Brookes, P.S., Pinner, A., Ramachandran, A., Coward, L., Barnes, S., Kim, H. and Darley-Usmer, V.M. (2002) High throughput two-dimensional blue-native electrophoresis: a tool for functional proteomics of mitochondria and signaling complexes. *Proteomics*, **2**, 969-977.

Bruton, J.D., Dahlstedt, A.J., Abbate, F. and Westerblad, H. (2003) Mitochondrial function in intact skeletal muscle fibres of creatine kinase deficient mice. *Journal of Physiology*, **552**, 393-402.

Bullough, W. (1962) The control of mitotic activity in adult mammalian tissues. *Biological Reviews*, **37**, 307-342.

Carlson, C.J., Booth, F.W. and Gordon, S.E. (1999) Skeletal muscle myostatin mRNA expression is fiber-type specific and increases during hindlimb unloading. *American Journal of Physiology*, **277**, R601-606.

Chang, T.S., Cho, C.S., Park, S., Yu, S., Kang, S.W. and Rhee, S.G. (2004) Peroxiredoxin III, a mitochondrion-specific peroxidase, regulates apoptotic signaling by mitochondria. *The Journal of Biological Chemistry*, **279**, 41975-41984.

Cortright, R.N., Muoio, D.M. and Dohm, G.L. (1997) Skeletal muscle lipid metabolism: a frontier for new insights into fuel homeostasis. *Nutritional Biochemistry*, **8**, 228-245.

Culley, G. (1807) *Observations in Livestock*. G. Woodwall, London.

Dahlstedt, A.J., Katz, A., Wieringa, B. and Westerblad, H. (2000) Is creatine kinase responsible for fatigue? Studies of isolated skeletal muscle deficient in creatine kinase. *The FASEB Journal*, **14**, 982-990.

Dennler, S., Itoh, S., Vivien, D., ten Dijke, P., Huet, S. and Gauthier, J.M. (1998) Direct binding of Smad3 and Smad4 to critical TGF beta-inducible elements in the promoter of human plasminogen activator inhibitor-type 1 gene. *Embo J*, **17**, 3091-3100.

Derynck, R., Zhang, Y. and Feng, X.H. (1998) Smads: transcriptional activators of TGF-beta responses. *Cell*, **95**, 737-740.

Donoghue, P., Doran, P., Dowling, P. and Ohlendieck, K. (2005) Differential expression of the fast skeletal muscle proteome following chronic low-frequency stimulation. *Biochemica et Biophysica Acta*, **1752**, 166-176.

Douette, P., Gerkins, P., Navet, R., Leprince, P., Pauw, E.D. and Sluse, F.E. (2006) Uncoupling protein 1 affects the yeast mitoproteome and oxygen free radical production. *Free Radical Biology and Medicine*, **40**, 303-315.

Encarnacion, S., Herandez, M., Martinez-Batalla, G., Contreras, S., Vargas, M.D.C. and Mora, J. (2005) Comparative proteomics using 2-D gel electrophoresis and mass spectrometry as tools to dissect stimulons and regulons in bacteria with sequenced or partially sequenced genomes. *Biol. Proced. Online*, **7**, 117-135.

Forner, F., Foster, L.J., Companaro, S., Valle, G. and Mann, M. (2006) Quantitative proteomic comparison of rat mitochondria from muscle, heart, and liver. *Molecular and Cellular Proteomics*, **5**, 608-619.

Fountoulakis, M., Soumaka, E., Rapti, K., Mavroidis, M., Tsangaris, G., Maris, a., Weisleder, N. and Capetanaki, Y. (2005) Alterations in the heart mitochondrial proteome in a desmin null heart failure model. *Journal of Molecular and Cellular Cardiology*, **38**, 461-474.

Garrett, R.H. and Grisham, C.M. (1999) *Biochemistry*. Saunders College Publishing, USA.

Gibson, B.W. (2005) The human mitochondrial proteome: oxidative stress, protein modifications and oxidative phosphorylation. *The International Journal of Biochemistry and Cell Biology*, **37**, 927-934.

Giege, P., Heazlewood, J.L., Roessner-Tunali, U., Millar, A.H., Fernie, A.R., Leaver, C.J. and Sweetlove, L.J. (2003) Enzymes of glycolysis are functionally associated with the mitochondrion in Arabidopsis cells. *Plant Cell*, **15**, 2140-2151.

Girgenrath, S., Song, K. and Whittemore, L.A. (2005) Loss of myostatin expression alters fiber-type distribution and expression of myosin heavy chain isoforms in slow- and fast-type skeletal muscle. *Muscle and Nerve*, **31**, 34-40.

Gorg, A., Weiss, W. and Dunn, M.J. (2004) Current two-dimensional elextrophoresis technology for proteomics. *Proteomics*, **4**, 3665-3685.

Gorg, A., Obermaier, C. Boguth, G., Harder, A., Scheibe, B., Wildgruber, R. and Weiss, W. (2000) The current state of two-dimensional electrophoresis with immobilized pH gradients. *Electrophoresis*, **21**, 1037-1053.

Gorg, A., Postel, W. and Gunther, S. (1988) The current state of two-dimensional electrophoresis with immobilized pH gradients. *Electrophoresis*, **9**, 531-546.

Grobet, L., Pirottin, D., Farnir, F., Poncelet, D., Royo, L.J., Brouwers, B., Christians, E., Desmecht, D., Coignoul, F., Kahn, R. and Georges, M. (2003) Modulating skeletal muscle mass by postnatal, muscle-specific inactivation of the myostatin gene. *Genesis*, **35**, 227-238.

Grobert, L., Martin, L.J.R., Poncelet, D., Pirottin, D., Brouwers, B., Riauet, J., Schoeberlein, A., Dunner, S., Menissier, F., Massabanda, J., Fries, R., Hanset, R. and Georges, M. (1997) A deletion in the bovine myostatin gene causes the double-muscled phenotype in cattle. *Nature Genetics*, **17**, 71-74.

Gueguen, N., Lefaucheur, L., Fillaut, M. and Herpin, P. (2005A) Muscle fiber contractile type influences the regulation of mitochondrial function. *Molecular and Cellular Biochemistry*, **276**, 15-20.

Gueguen, N., Lefaucheur, L., Fillaut, M., Vincent, A. and Herpin, P. (2005B) Control of skeletal muscle mitochondria respiration by adenine nucleotides:

differential effect of ADP and ATP according to muscle contractile type in pigs. *Comparative Biochemistry and Physiology*, **140B**, 287-297.

Hallauer, P.L. and Hastings, K.E. (2002) Coregulation of fast contractile protein transgene and glycolytic enzyme expression in mouse skeletal muscle. *American Journal of Physiology*, **282**, C113-C124.

Hanson, B.J., Schulenberg, B., Patton, W.F. and Capaldi, R.A. (2001) A novel subfractionation approach for mitochondrial proteins: a three-dimensional mitochondrial proteome map. *Electrophoresis*, **22**, 950-959.

Herbert, B.R., Molloy, M.P., Gooley, A.A., Walsh, B.J., Bryson, W.G. and Williams, K.L. (1998) Improved protein solubility in two-dimensional electrophoresis using tributyl phosphine as reducing agent. *Electrophoresis*, **19**, 845-851.

Hill, J.J., Davies, M.V., Pearson, A.A, Wang, J.H., Hewick, R.M., Wolfman, N.M. and Qiu, Y. (2002) The myostatin propeptide and the follistatin-related gene are inhibitory binding proteins of myostatin in normal serum. *Journal of Biological Chemistry*, **277**, 40735-40741.

Hunzinger, C., Wozny, W., Schwall, G.P., Poznanovic, S., Stegmann, W., Zengerling, H., Schoepf, R., Groebe, K., Cahill, M.A., Osiewacz, H.D., Jagemann, N., Bloch, M., Dencher, N.A., Krause, F. and Schrattenholz, A. (2006) Comparative profiling of the mammalian mitochondrial proteome: multiple aconitase-2 isoforms including n-formylkynurenine modifications as part of a protein biomarker signature for reactive oxygen species. *Journal of Proteome Research*, **5**, 625-633.

Hsu, Y.D., Chen, S.S., Lee, W.H., Lee, S.Z., Kao, M.C. and Tsao, W.L. (1995) Mitochondrial alterations of skeletal muscle in a heat stress rat model.

Proceedings of the National Science Council of the Republic of China B, **19**, 233-239.

Jackman, M.R. and Willis, W.T. (1996) Characteristics of mitochondria isolated from type I and type IIb skeletal muscle. *Cell Physiology*, **270**, C673-C678.

Jeanplong, F., Sharma, M., Somers, W.G., Bass, J.J. and Kambadur, R. (2001) Genomic organization and neonatal expression of the bovine myostatin gene. *Molecular and Cellular Biochemistry*, **220**, 31-37.

Jenson, O.N. (2004) Modification-specific proteomics: characterization of post-translational modifications by mass spectrometry. *Current Opinion in Chemical Biology*, **8**, 33-41.

Ji, S., Losinski, R.L., Cornelius, S.G., Frank, G.R., Willis, G.M., Gerrard, D.E., Depreux, F.F. and Spurlock, M.E. (1998) Myostatin expression in porcine tissues: tissue specificity and developmental and postnatal regulation. *American Journal of Physiology*, **275**, R1265-1273.

Joulia, D., Bernardi, H., Garandel, V., Rabenoelina, F., Vernus, B. and Cabello, G. (2003) Mechanisms involved in the inhibition of myoblast. *Experimental CellResearch*, **286**, 263-275.

Kambadur, R., Sharma, M., Smith, T.P.L and Bass, J.J. (1997) Mutations in *myostatin* (GDF8) in double-muscled belgian blue and piedmontese cattle. *Genome Research*, **7**, 910-915.

Keeney, P.M., Xie, J., Capaldi, R.A. and Bennett Jr., J.P. (2006) Parkinson's disease brain mitochondrial complex I has oxidatively damaged subunits and is functionally impaired and misassembled. *Neurobiology of Disease*, **26**, 5256-5264.

Kil, I.S., Lee, Y.S., Bae, Y.S., Huh, T.L. and Park, J.W. (2004) Modulation of $NADP^+$-dependent isocitrate dehydrogenase in aging. *Redox Report*, **9**, 271-277.

Kim, H.J., Kang, B.S. and Park, J.W. (2005) Cellular defense against heat shock-induced oxidative damage by mitochondrial $NADP^+$-dependent isocitrate dehydrogenase. *Free Radical Research*, **39**, 441-448.

Kim, N.K., Joh, J.H., Park, H.R., Kim, O.H., Park, B.Y. and Lee, C.H. (2004) Differential expression profiling of the proteomes and their mRNA in porcine white and red skeletal muscles. *Proteomics*, **4**, 3422-3428.

King, A., Selak, M.A. and Gottlieb, E. (2006) Succinate dehydrogenase and fumarate hydratase: linking mitochondrial dysfunction and cancer. *Oncogene*, **25**, 4675-4682.

Klivenyi, P., Starkov, A.A., Calingasan, N.Y., Gardian, G., Browne, S.E., Yang, L., Bubber, P., Gibson, G.E., Patel, M.S. and Beal, M.F. (2004) Mice deficient in dihydrolipoamide dehydrogenase show increased vulnerability to MPTP, malonate and 3-nitropropionic acid neurotoxicity. *Journal of Neurochemistry*, **88**, 1352-1360.

Kocamis, H., Kirkpatrick-Keller, D.C., Richter, J. and Killefer, J. (1999) The ontogeny of myostatin, follistatin and activin-B mRNA expression during chicken embryonic development. *Growth, Development and Aging*, **63**, 143-150.

Laemmli, U.K. (1970) Cleavage of structural proteins during the assembly of the head bacteriophage T4. *Nature*, **227**, 680-685.

Langely, B., Thomas, M., Bishop, A., Sharma, M., Gilmour, S. and Kambadur, R. (2002) Myostatin inhibits myoblast differentiation by down-regulating MyoD expression. *The Journal of Biological Chemistry*, **277**, 49831-49840.

Lee, S.J. and McPherron, A.C. (2001) Regulation of Myostatin activity and muscle growth. *Proceedings of the National Academy of Sciences USA*, **98**, 9306-9311.

Liu, D., Black, B.L. and Derynck, R. (2001) TGF-β inhibits muscle differentiation through functional repression of myogenic transcription factors by Smad3. *Genes and Development*, **15**, 2950-2966.

Martinez, L.O., Jacquet, S., Esteve, J.P., Rolland, C., Cabezon, E., Champagne, E., Pineau, T., Georgeaud, V., Walker, J.E., Terce, F., Collet, X., Perret, B. and Barbaras, R. (2003) Ectopic beta-chain of ATP synthase is an apolipoprotein A-1 receptor in hepatic HDL endocytosis. *Nature*, **421**, 75-79.

Martinus, R.D., Garth, G.P., Webster, T.L., Cartwright, P., Naylor, D.J., Hoj, P.B. and Hoogenraad, N.J. (1996) Selective induction of mitochondrial chaperones in response to loss of the mitochondrial genome. *European Journal of Biochemistry*, **240**, 98-103.

Martinus, R.D., Ryan, M.T., Naylor, D.J., Herd, S.M., Hoogenraad, N.J. and Hoj, P.B. (1995) The role of chaperones in the biogenesis and maintenance of the mitochondrion. *The FASEB Journal*, **9**, 371-378.

McCroskery, S., Thomas, M., Maxwell, L., Sharma, M. and Kambadur, R. (2003) Myostatin negatively regulates satellite cell activation and self-renewal. *The Journal of Cell Biology*, **162**, 1135-1147.

McPherron, A.C. and Lee, S.J. (2002) Supression of body fat accumulation in myostatin-deficient mice. *The Journal of Clinical Investigation*, **109**, 595-601.

McPherron, A.C., Lawler, A.M. and Lee, S.J. (1997) Regulation of skeletal muscle mass in mice by a new TGF-β superfamily member. *Nature*, **387**, 83-90.

McPherron, A.C. and Lee, S.J. (1997) Double muscling in cattle due to mutations in the myostatin gene. *Proceedings of the National Academy of Science USA*, **94**, 12457-12461.

Menissier, F. (1982) General survey of the effect of double muscling on cattle performance. In King, J.W.B and Menissier, F. (eds.), *Muscle Hypertrophy of Genetic Origin and its use to Improve Beef Production*. Martinus Nijhoff Publishers, The Hague, Vol. 16, pp 23-53.

Michael, A.E., Evagelatou, M., Norgate, D.P., Clarke, R.J., Antoniw, J.W., Stedman, B.A., Brennan, A., Wilsby, R., Bujalska, I., Stewart, P.M. and Cooke, B.A. (1997) Isoforms of 11β-hydroxysteroid dehydrogenase in human granulose-lutein cells. *Molecular and Cellular Endocrinolgy*, **132**, 43-52.

Mizzen, L.A., Kabiling, A.N. and Welch, W.J. (1991) The two mammalian mitochondrial stress proteins, grp 75 and hsp 58, transiently interact with newly synthesized mitochondrial proteins. *Cell Regulation*, **2**, 165-179.

Mogensen, M. and Sahlin, K. (2005) Mitochondrial efficiency in rat skeletal muscle: influence of respiration rate, substrate and muscle type. *Acta Physiol. Scan.*, **185**, 229-236.

Mohsen, A.W.A and Vockley, J. (1995) Identification of the active site catalytic residue in human isovaleryl-CoA dehydrogenase. *Biochemistry*, **34**, 10146-10152.

Molloy, M.P., Herbert, B.R., Walsh, B.J., Tyler, M.I., Traini, M., Sanchez, J.C., Hochstrasser, D.F., Williams, K.L. and Gooley, A.A. (1998) Extraction of membrane proteins by differential solubization for separation using two-dimensional gel electrophoresis. *Electrophoresis*, **19**, 837-844.

Mujahid, A., Sato, K., Akiba, Y. and Toyomizu, M. (2006) Acute heat stress stimulates mitochondrial superoxide production in broiler skeletal muscle, possibly via downregulation of uncoupling protein content. *Poult Sci*, **85**, 1259-1265.

Nijtmans, L.G., de Jong, L., Artal Sanz, M., Coates, P.J., Berden, J.A., Back, J.W., Muijsers, A.O., van der Spek, H. and Grivell, L.A. (2000) Prohibitins act as a membrane-bound chaperone for the stabilization of mitochondrial proteins. *EMBO Journal*, **19**, 2444-2451.

Nishi, M., Yasue, A., Nishimatu, S., Nohno, T., Yamaoka, T., Itakura, M., Moriyama, K., Ohuchi, H. and Noji, S. (2002) A missense mutant myostatin causes hyperplasia without hypertrophy in the mouse muscle. *Biochemical and Biophysical Research Communications*, **293**, 247-251.

Okumura, N., Hashida-Okumura, A., Kita, K., Matsube, M., Matsubara, T., Takao, T. and Nagai, K. (2005) Proteomic analysis of slow- and fast-twitch skeletal muscles. *Proteomics*, **5**, 2896-2906.

Oldham, J.M., Martyn, J.A., Sharma, M., Jeanplong, F., Kambadur, R. and Bass, J.J. (2001) Molecular expression of myostatin and MyoD is greater in double-muscled than normal-muscled cattle fetuses. *American Journal of Physiology*, **280**, R1488-1493.

Paschen, S.A. and Neupert, W. (2001) Protein import into mitochondria. *IUBMB Life*, **52**, 101-112.

Peck, S.C. (2005) Update on proteomics in Arabidopsis. Where do we go from here? *Plant Physiology*, **138**, 591-599.

Potts, J.K, Echternkamp, S.E., Smith, T.P.L. and Reecy, J.M. (2003) Characterization of gene expression in double-muscled and normal-muscled bovine embryos. *Animal Genetics*, **34**, 438-444.

Quintilla, M.E., Tampier, L., Sapag, A. and Israel, Y. (2005) Polymorphisms in the mitochondrial aldehyde dehydrogenase gene (Aldh2) determine peak blood acetaldehyde levels and voluntary ethanol consumption in rats. *Pharmacoqeuet Genomics*, **15**, 427-431.

Reddy, P.H. and Beal, M.F (2005) Are mitochondria critical in the pathogenesis of Alzheimer's disease? *Brain Research Reviews*, **49**, 618-632.

Rios, R., Carneiro, I., Arce, V.M. and Devesa, J. (2001) Myostatin regulates cell survival during C2C12 myogenesis. *Biochemical and Biophysical Research Communications*, **280**, 561-566.

Rivero, J.L., Talmadge, R. and Edgerton, V.R. (1998) Fibre size and metabolic properties of myosin heavy chain-based fibre types in rat skeletal muscle. *Journal of Muscle Research and Cell Motility*, **19**, 733-742.

Ruiz-Romero, C., Lopez-Armada, M.J. and Blanco, F.J. (2006) Mitochondrial proteomic characterization of human normal articular chrondrocgytes. *Osteoarthritis and Cartilage*, **14**, 507-518.

Rustin, P., Chretien, D., Bourgeron, T., Gerard, B., Rotig, A., Sandubray, J.M. and Munnich, A. (1993) Biochemical and molecular investigations in respiratory chain deficiencies. *Clinica Chimica Acta*, **228**, 35-51.

Saijo, H., Tanaka, H., Ito, J., Tasaki, T., Cho, K., Tokumitsu, A., Takahashi, S., Miyamoto, A. and Oki, J. (1997) Pyruvate dehydrogenase complex deficiency with multiple minor anomalies. *ACTA Paediatrica Japonica*, **39**, 230-232.

Sayd, T., Morzel, M., Chambon, C., Franck, M., Figwer, P., Larzul, C., Le Roy, P., Monin, G., Cherel, P. and La Ville, E. (2006) Proteome analysis of the sarcoplasmic fraction of pig *Semimembranosus* muscle: implications on meat color development. *Journal of Agricultural and Food Chemistry*, **54**, 2732-2737.

Schagger, H. and von Jagow, G. (1991) Blue native electrophoresis for isolation of membrane protein complexes in enzymatically active form. *Analytical Biochemistry*, **199**, 223-231.

Scheffler, N.K., Miller, S.W., Carroll, A.K., Anderson, C., Davis, R.E., Ghosh, A.C. and Gibson, B.W. (2001) Two-dimensional electrophoresis and mass spectrometric identification of mitochondrial proteins from an SH-SY5Y neuroblastoma cell line. *Mitochondrion*, **1**, 161-179.

Schiff, M., Froissart, R., Olsen, R.K.J., Acquaviva, C. and Vianey-Saban, C. (2006) Electron transfer flavoprotein deficiency: functional and molecular aspects. *Molecular Genetics and Metabolism*, **88**, 153-158.

Schilling, B., Bharath, S., Row, R.H., Murray, J., Cusack, M.P., Capaldi, R.A., Freed, C.R., Prasad, K.N., Anderson, J.K. and Gibson, B.W. (2005) Rapid purification and mass spectrometric characterization of mitochondrial NADH

dehydrogenase (complex I) from rodent brain and a dopaminergic neuronal cell line. *Molecular and Cellular Proteomics*, **4**, 84-96.

Schmidt, I. and Herpin, P. (1997) Postnatal changes in mitochondrial protein mass and respiration in skeletal muscle from the newborn pig. *Comparative Biochemistry and Physiology*, **118B**, 639-647.

Scott, I.C., Blitz, I.L., Pappano, W.N., Imamura, Y., Clark, T.G., Steiglitz, B.M., Thomas, C.L., Maas, S.A., Takahara, K., Cho, K.W.Y. and Greenspan, D.S. (1999) Mammalian BMP-1/tolloid-related metalloproteinases, including novel family member mammalian tolloid-like 2, have differential enzymatic activities and distributions of expression relevant to patterning and skeletogenesis. *Developmental Biology*, **213**, 283-300.

Sharma, M., Kambadur, R., Matthews, K.G., Somers, W.G, Devlin, G.P., Conaglen, J.V., Fowke, P.J. and Bass, J.J. (1999) Myostatin, a transforming growth factor-β superfamily member, is expressed in heart muscle and is upregulated in cardiomyocytes after infarct. *Journal of Cellular Physiology*, **180**, 1-9.

Shi, Y. and Massague, J. (2003) Mechanisms of TGF-beta signaling from cell membrane to the nucleus. *Cell*, **113**, 685-700.

Thomas, M., Langley, B., Berry, C., Sharma, M., Kirk, S., Bass J. and Kambadur, R. (2000) Myostatin, a negative regulator of muscle growth, functions by inhibiting myoblast proliferation. *The Journal of Biological Chemistry*, **275**, 40235-40243.

Wegner, J., Albrecht, E., Fiedler, I., Tescher, F., Papstein, H.J. and Ender, K. (2000) Growth- and breed-related changes of muscle fiber characteristics in cattle. *Journal of Animal Science*, **78**, 1485-1496.

Westermeier, R. (1993) *Electrophoresis in Practice*. Verlagsgesellschaft, Weinham, Germany.

Whittemore, L.A., Song, K., Li, X., Aghajanian, J., Davies, M., Girgenrath, S., Hill, J.J., Jalenak, M., Kelley, P., Knight, A., Maylor, R., O'Hara, D., Pearson, A., Quazi, A. Ryerson, S., Tan, X.T., Tomkinson, K.N., Veldman, G.M., Widom, A., Wright, J.F., Wudyka, S., Zhao, L. and Wolfman, N.M. (2003) Inhibition of myostatin in adult mice increases skeletal muscle mass and strength. *Biochemical and Biophysical Research Communications*. **300**, 965-971.

Willis, W.T. and Jackman, M.R. (1995) Respiratory control in mitochondria isolated from types I and IIb skeletal muscle. *Medicine and Science in Sports and Exercise*, **27**, S33.

Wolfman, N.M., McPherron, A.C., Papano, W.N., Davies, M.V., Song, K., Tomkinson, K.N., Wright, J.F., Zhao, L., Sebald, S.M., Greenspan, D.S. and Lee, S.J. (2003) Activation of latent myostatin by the BMP-/tolloid family of metalloproteinases. *Proceeding of the National Academy of Sciences USA*, **100**, 15842-15846.

Yarian, C.S., Toroser, D. and Sohal, R.S. (2006) Aconitase is the main functional target of again in the citric acid cycle of kidney mitochondria from mice. *Mechanisms of Aging and Development*, **127**, 79-84.

Zawel, L., Dai, J.L., Buckhaults, P., Zhou, S., Kinzler, K.W., Vogelstein, B. and Kern, S.E. (1998) Human Smad3 and Smad4 are sequence-specific transcription activators. *Molecular Cell*, **1**, 611-617.

Zhang, S., Fu, J. and Zhou, Z. (2005) Changes in the brain mitochondrial proteome of male Sprague-Dawley rats treated with manganese chloride. *Toxicology and Applied Pharmacology*, **202**, 13-17.

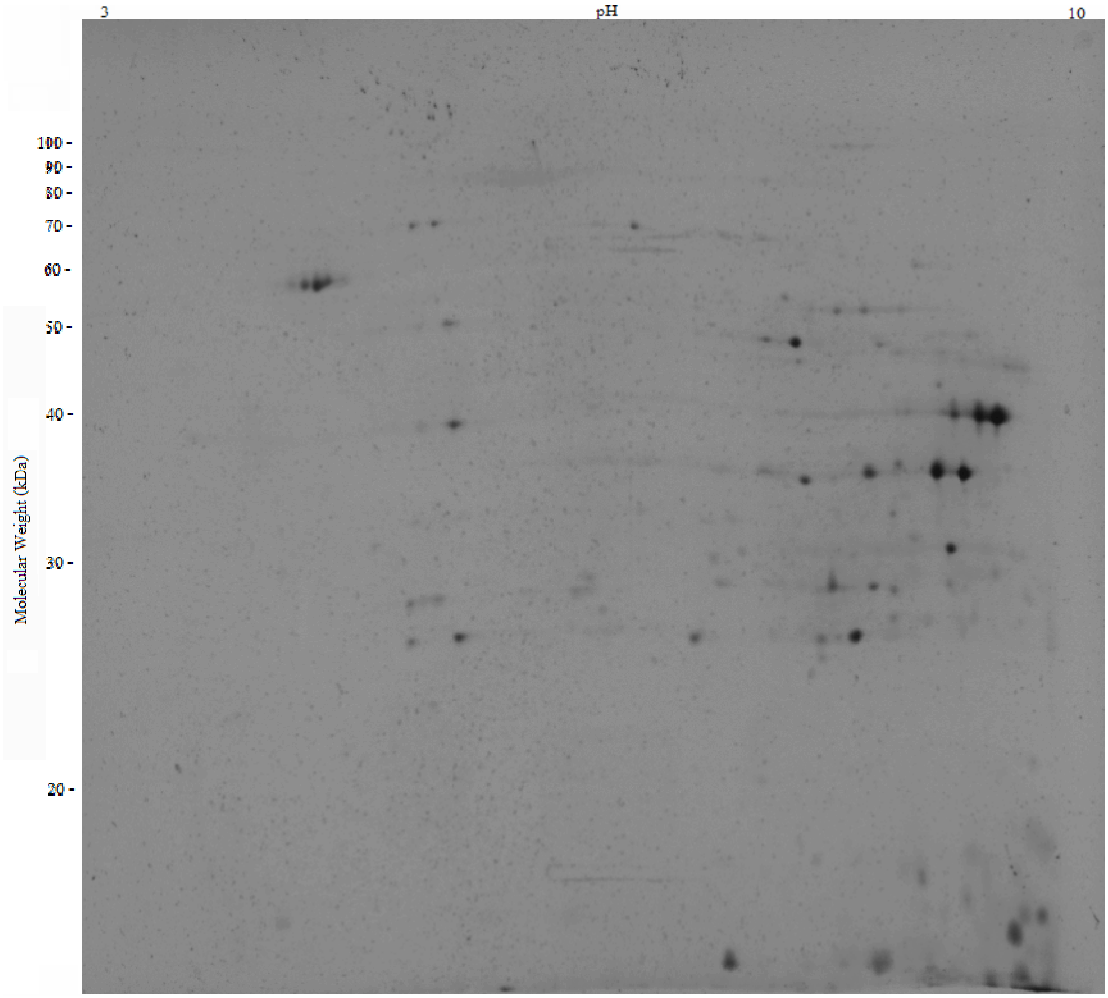

Appendix A *100µg of mitochondrial protein loaded onto 2-DE gel.* 17cm 3-10NL IPG loaded with 100µg of mitochondrial protein from the knockout sample, second dimension run on a 12% SDS-PAGE gel, stained with silver stain plus MS compatible silver stain.

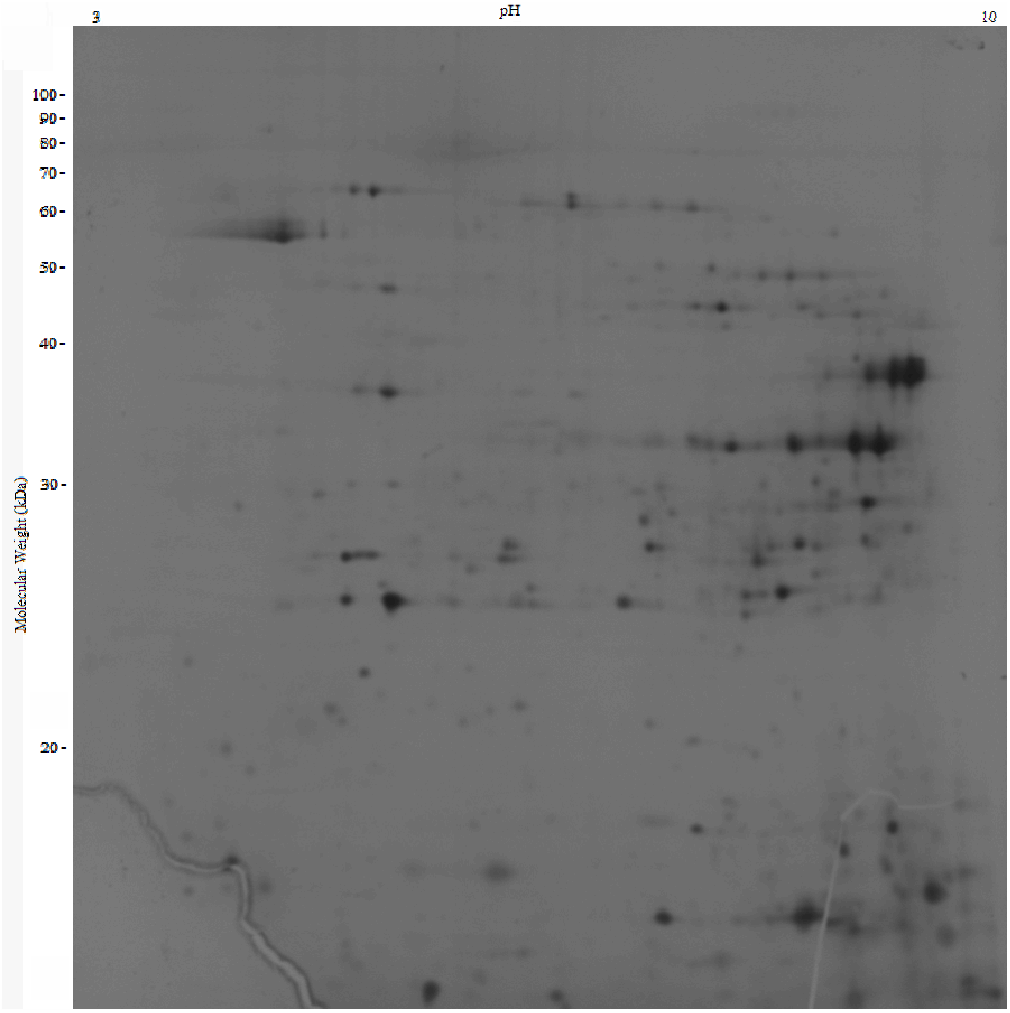

Appendix B *200µg of mitochondrial protein loaded onto 2-DE gel.* 17cm 3-10NL IPG loaded with 200µg of mitochondrial protein from the knockout sample, second dimension run on a 12% SDS-PAGE gel, stained with silver stain plus MS compatible silver stain.

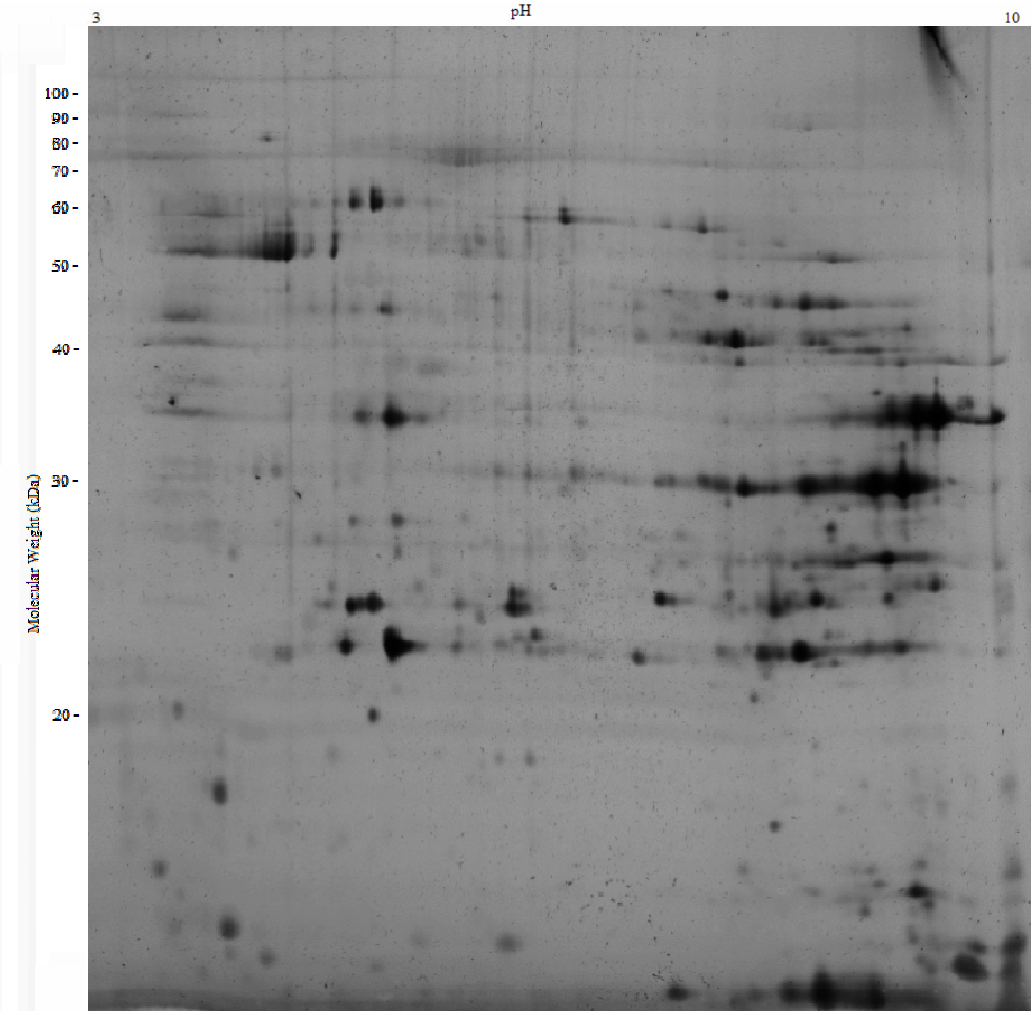

Appendix C *300µg of mitochondrial protein loaded onto 2-DE gel.* 17cm 3-10NL IPG loaded with 300µg of mitochondrial protein from the knockout sample, second dimension run on a 12% SDS-PAGE gel, stained with silver stain plus MS compatible silver stain.

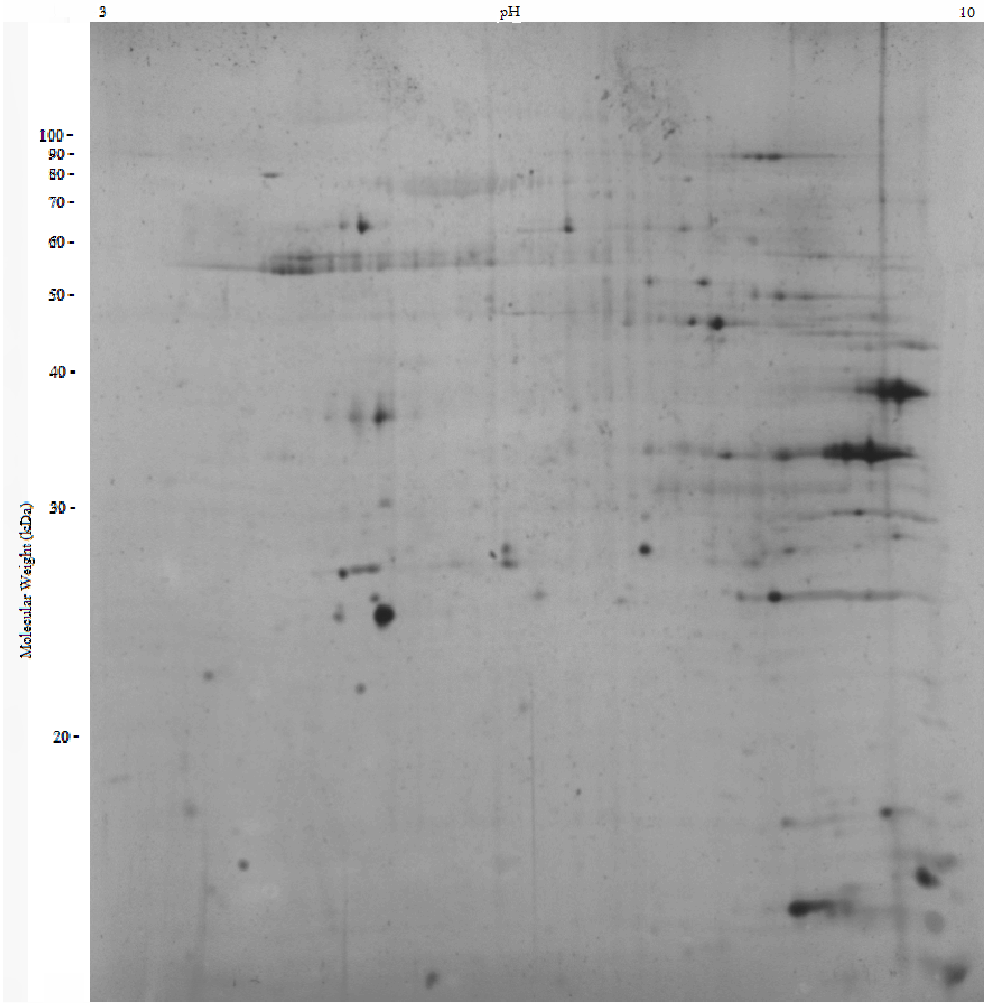

Appendix D *Reproducibility of 2-DE gel protein loadings replicate number one.* 17cm 3-10NL IPG loaded with 220µg of mitochondrial protein from the knockout sample, second dimension run on a 12% SDS-PAGE gel, stained with silver stain plus MS compatible silver stain.

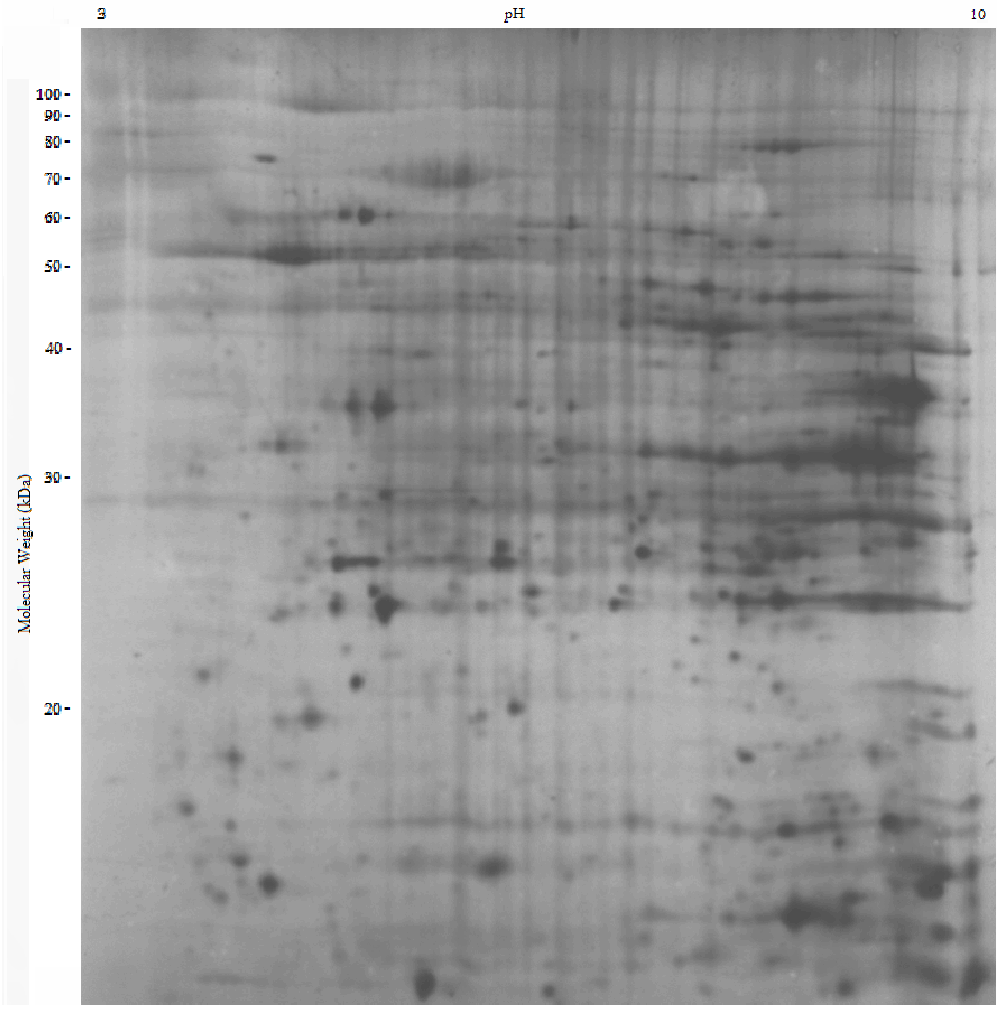

Appendix E *Reproducibility of 2-DE gel protein loadings replicate number two.* 17cm 3-10NL IPG loaded with 220µg of mitochondrial protein from the knockout sample, second dimension run on a 12% SDS-PAGE gel, stained with silver stain plus MS compatible silver stain.

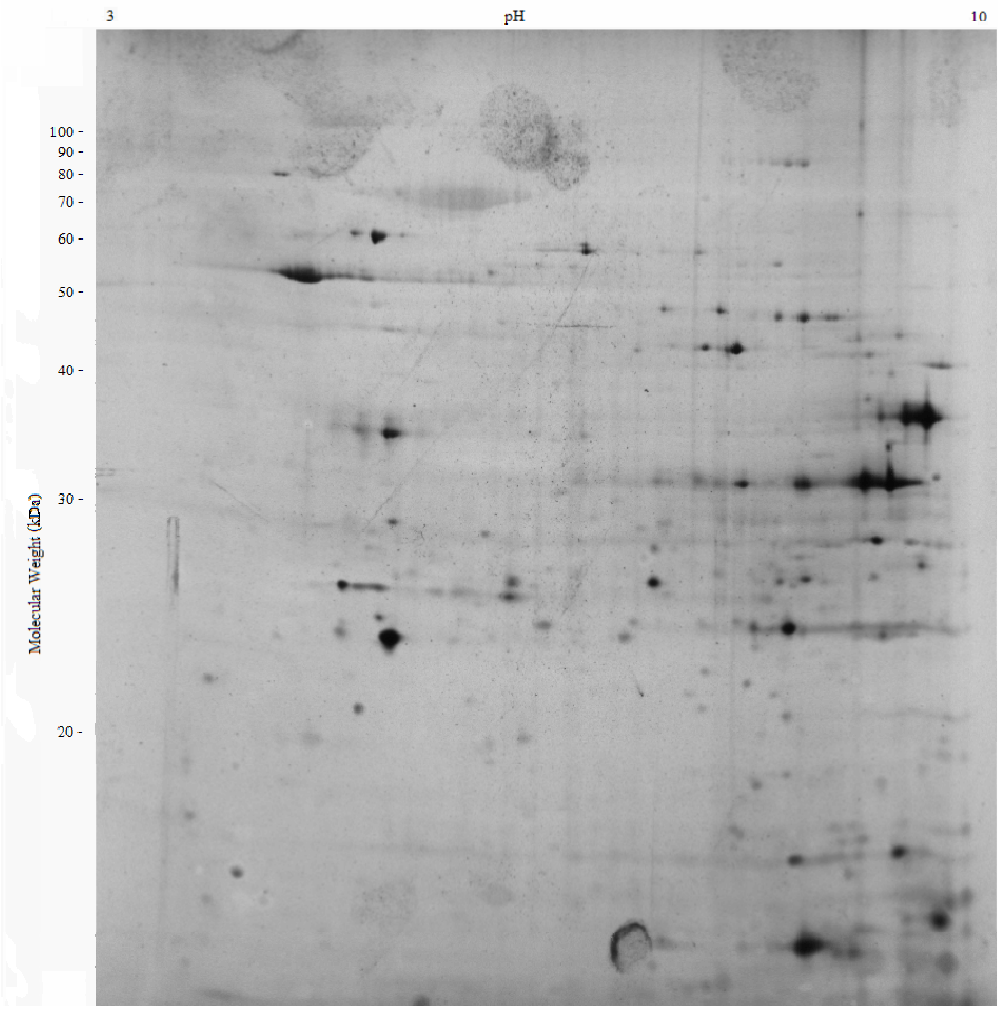

Appendix F *Reproducibility of 2-DE gel protein loadings replicate number three.* 17cm 3-10NL IPG loaded with 220µg of mitochondrial protein from the knockout sample, second dimension run on a 12% SDS-PAGE gel, stained with silver stain plus MS compatible silver stain.

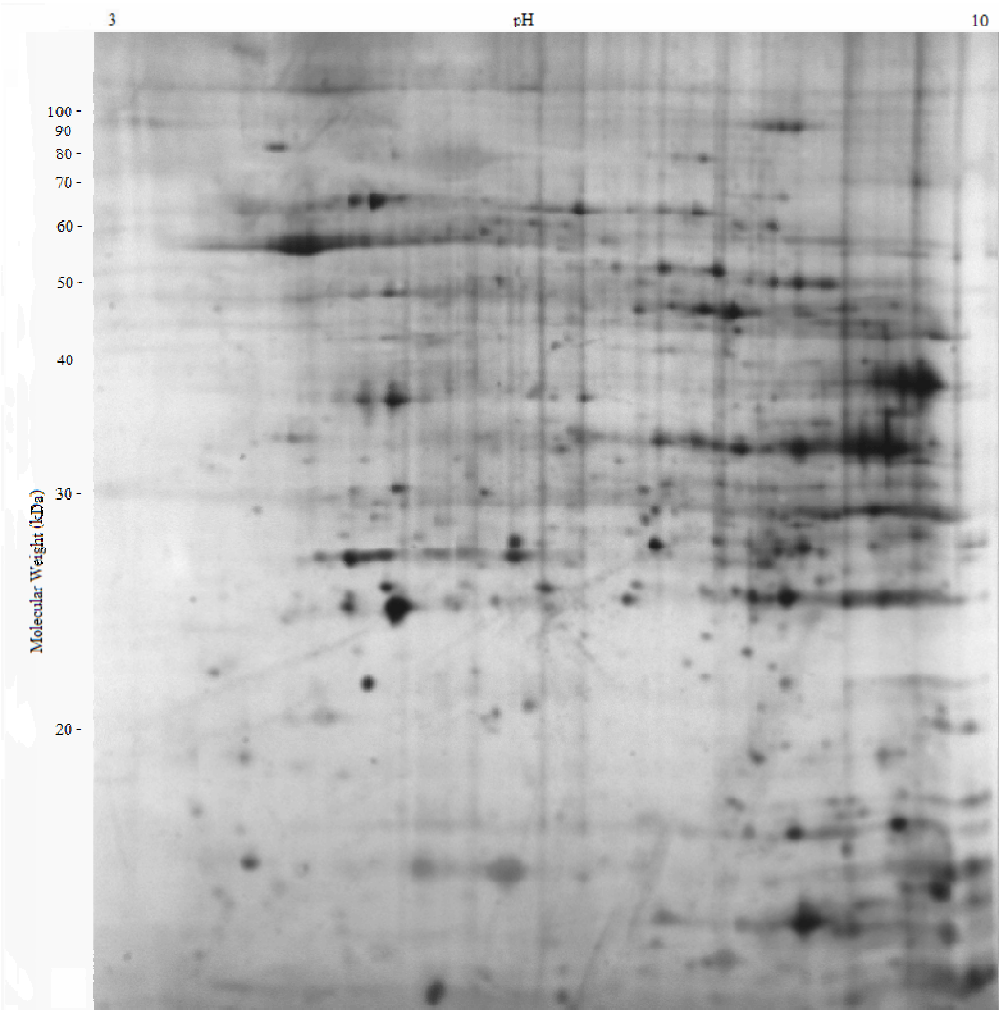

Appendix G *Reproducibility of 2-DE gel protein loadings replicate number four.* 17cm 3-10NL IPG loaded with 220µg of mitochondrial protein from the knockout sample, second dimension run on a 12% SDS-PAGE gel, stained with silver stain plus MS compatible silver stain.

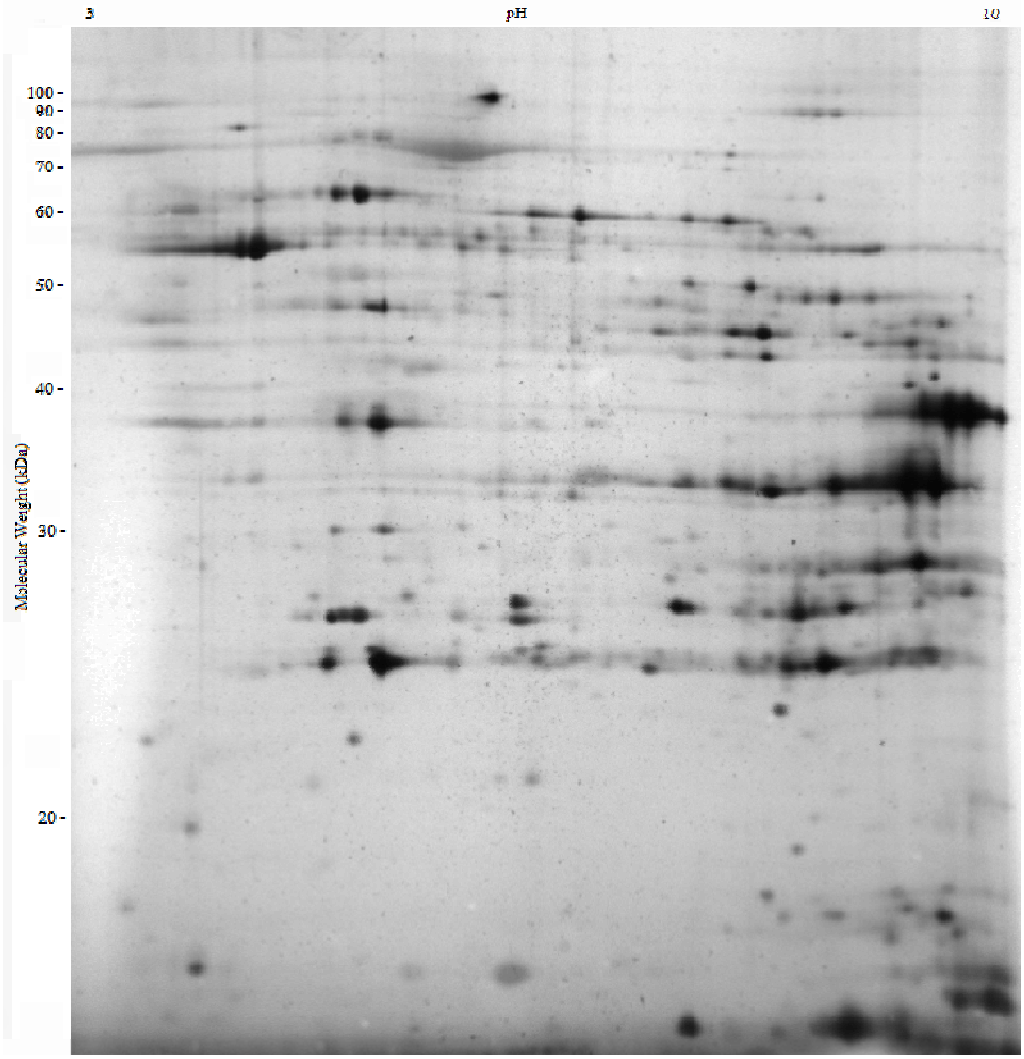

Appendix H *Wild type replicate number one.* 17cm 3-10NL IPG loaded with 220µg of mitochondrial protein from the wild type sample, second dimension run on a 12% SDS-PAGE gel, stained with silver stain plus MS compatible silver stain.

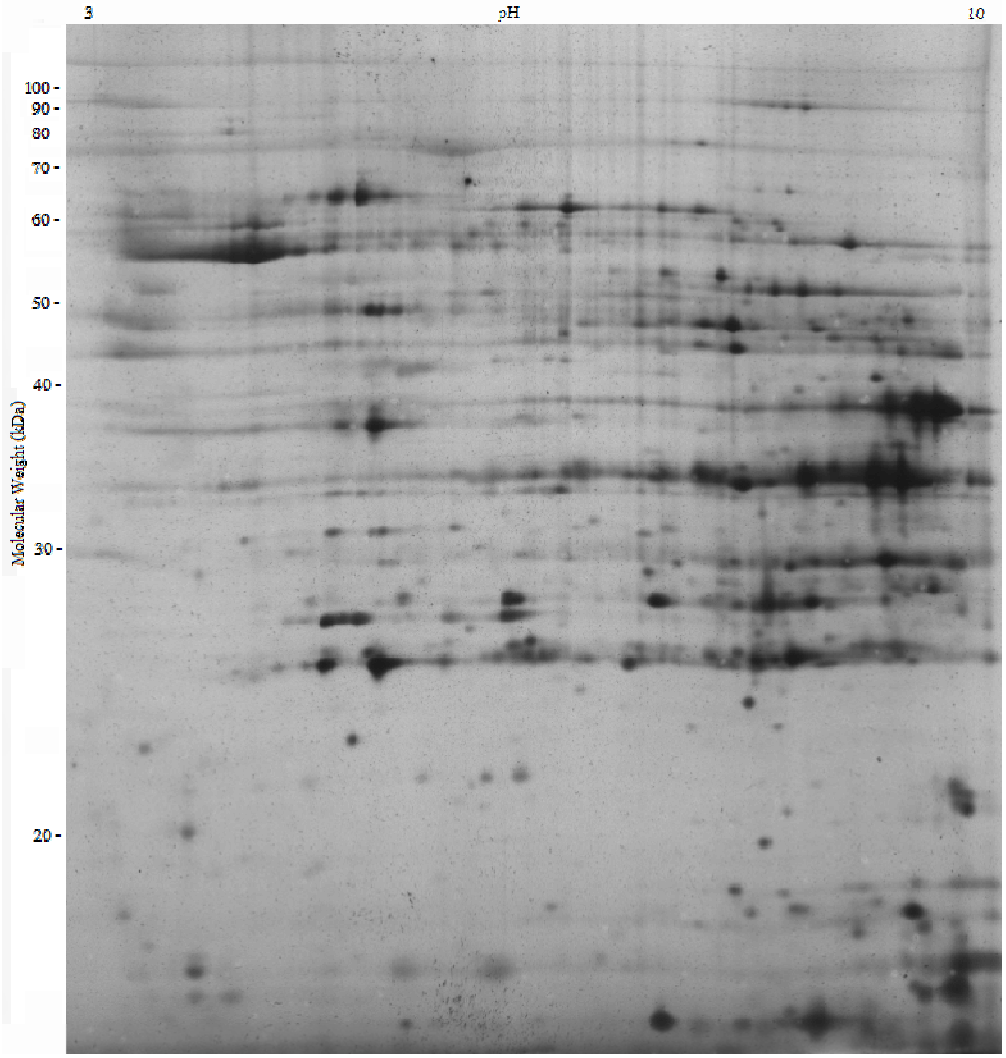

Appendix I *Wild type replicate number two.* 17cm 3-10NL IPG loaded with 220µg of mitochondrial protein from the wild type sample, second dimension run on a 12% SDS-PAGE gel, stained with silver stain plus MS compatible silver stain.

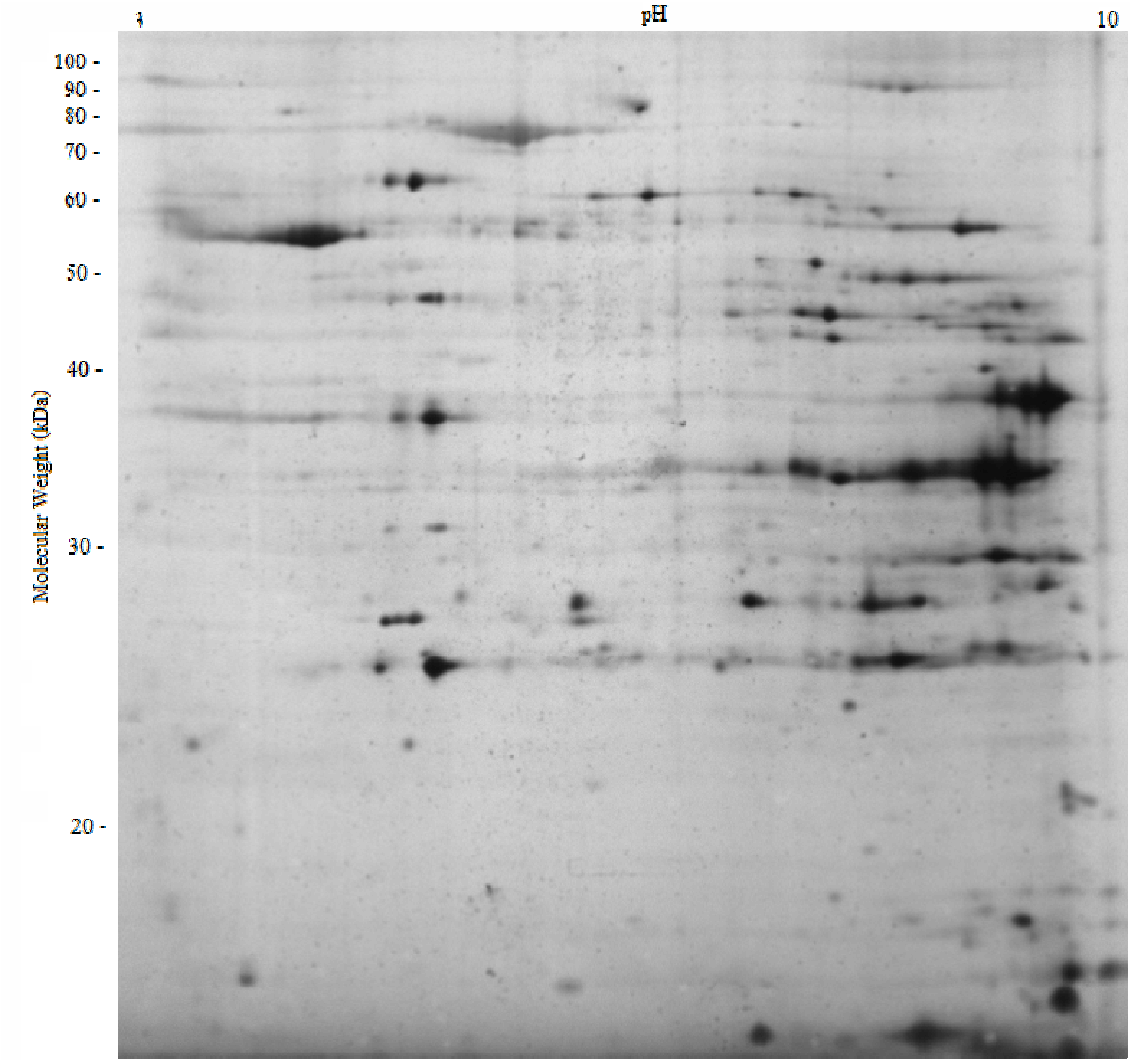

Appendix J *Wild type replicate number three.* 17cm 3-10NL IPG loaded with 220µg of mitochondrial protein from the wild type sample, second dimension run on a 12% SDS-PAGE gel, stained with silver stain plus MS compatible silver stain.

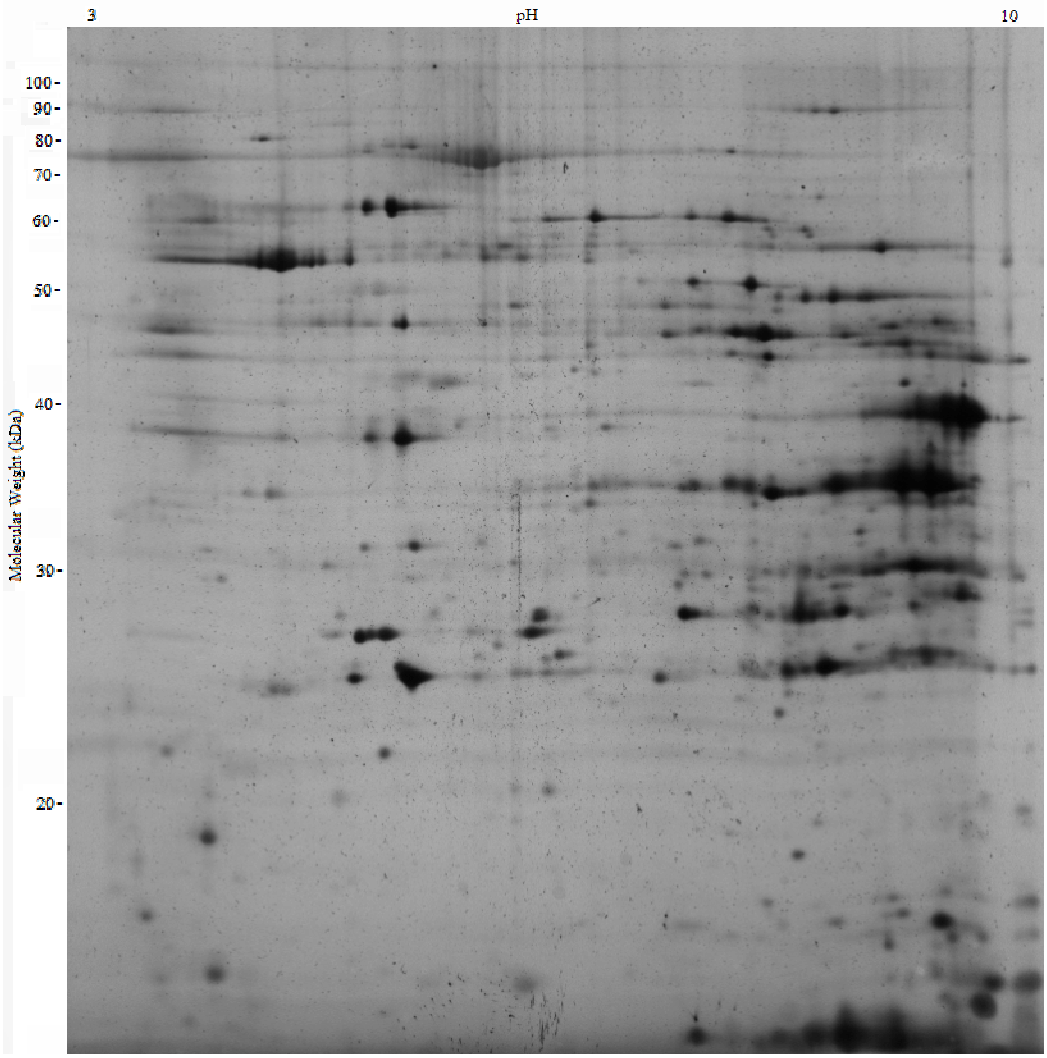

Appendix K *Knockout replicate number one.* 17cm 3-10NL IPG loaded with 220µg of mitochondrial protein from the knockout sample, second dimension run on a 12% SDS-PAGE gel, stained with silver stain plus MS compatible silver stain.

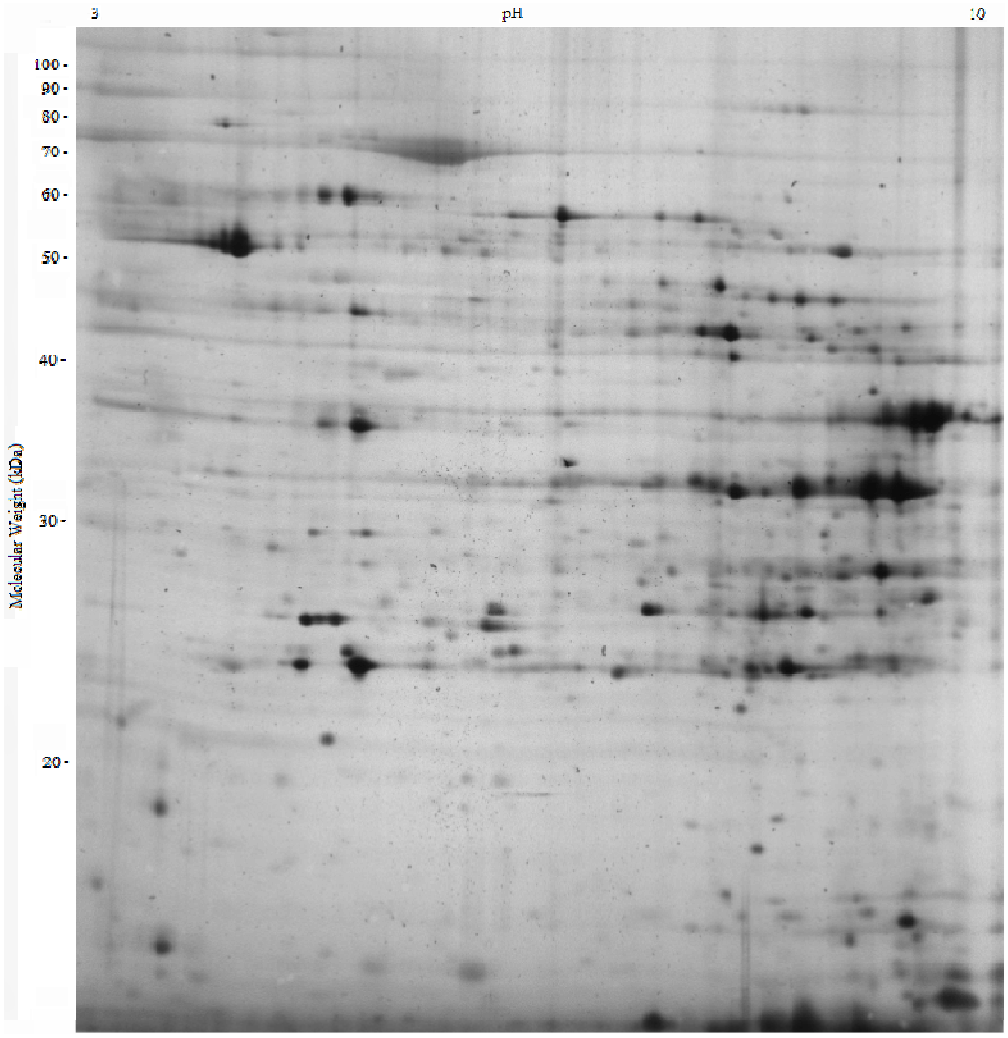

Appendix L *Knockout replicate number two.* 17cm 3-10NL IPG loaded with 220µg of mitochondrial protein from the knockout sample, second dimension run on a 12% SDS-PAGE gel, stained with silver stain plus MS compatible silver stain.

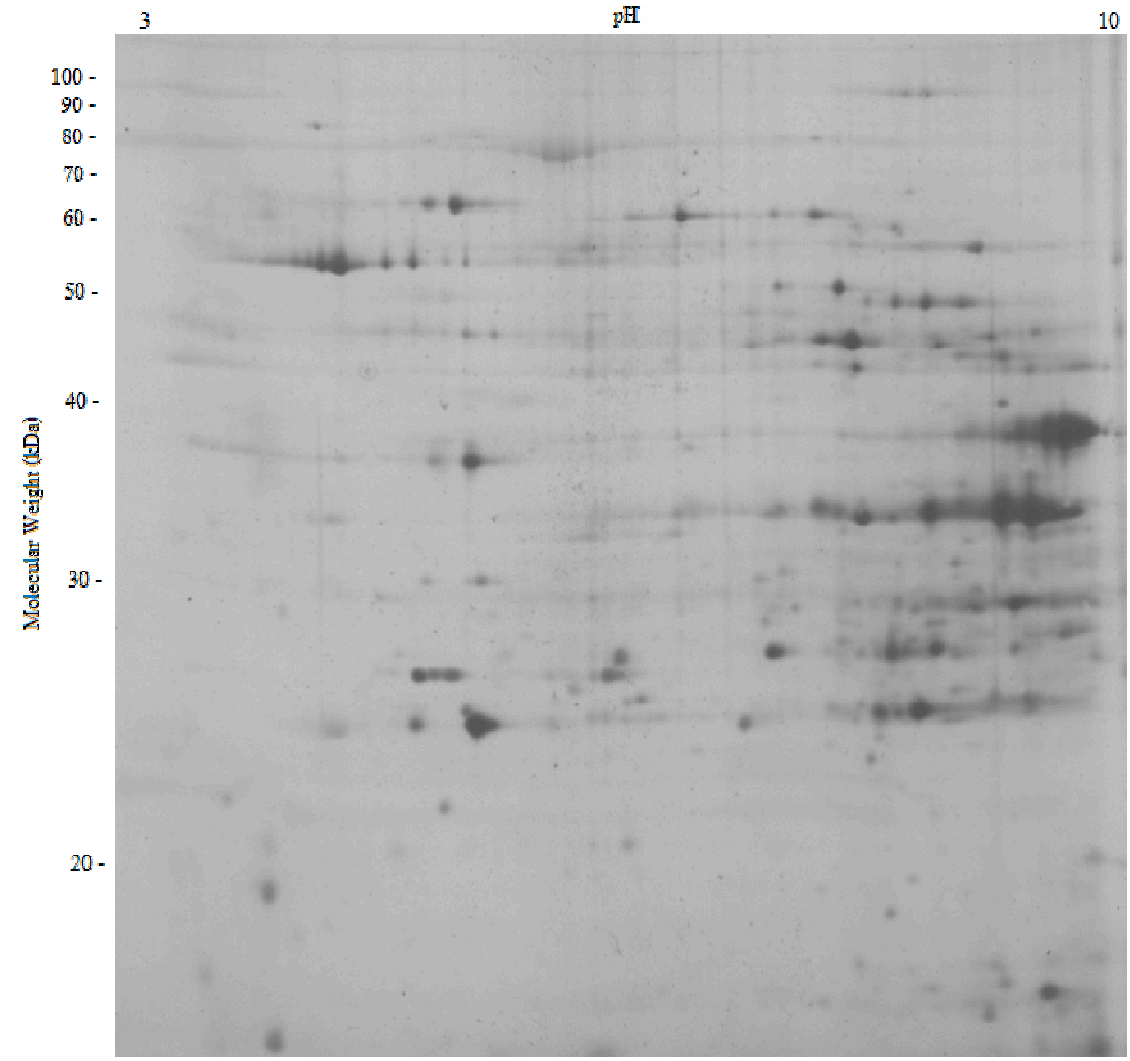

Appendix M *Knockout replicate number three.* 17cm 3-10NL IPG loaded with 220µg of mitochondrial protein from the knockout sample, second dimension run on a 12% SDS-PAGE gel, stained with silver stain plus MS compatible silver stain.

Appendix N *Information on proteins identified from 2-DE gel spots.*

Protein	Species	MW	pI	Mascot Score	Accession #	Spot #s
Aconitase 2	Mus musculus	86,185	8.9	153.0	gi| 63101587	2,3,4
Adenylate Kinase 1	Not Specified	21,640	5.6	98.0	gi| 13959400	57
Aldehyde Dehydrogenase 6a1	Mus musculus	50,018	7.7	91.7	gi| 21410418	13
Aldolase A	Mus musculus	39,925	9.2	129.0	gi| 7548322	30
Apolipoprotein A-1	Bos taurus	30,258	5.5	129.0	gi| 74268269	54
ATP Synthase, F0 complex, subunit d	Mus musculus	18,795	5.4	106.0	gi| 21313679	56,58
ATP Synthase, F1 complex, alpha subunit	Mus musculus	59,829	9.7	218.0	gi| 6680748	18
ATP Synthase, F1 complex, beta subunit	Homo sapiens	56,525	4.8	121.1	gi| 16741373	15
Bovine Serum Albumin	Bos taurus	71,274	5.8	77.4	gi| 30794280	5
Creatine Kinase	Mus musculus	43,246	6.6	152.0	gi| 6671762	27,28
Dihydrolipoamide Dehydrogenase	Mus musculus	54,748	9.0	90.1	gi| 2078522	10,11,12
Electron Transferring Flavoprotein, alpha subunit	Mus musculus	35,360	9.5	89.5	gi| 13097375	47
Electron Transferring Flavoprotein, beta subunit	Mus musculus	27,834	9.3	72.3	gi| 38142460	37
Enolase 3, beta subunit	Mus musculus	47,310	6.9	71.8	gi| 71059715	21
ES1	Mus musculus	28,415	9.9	89.0	gi| 20070402	50
Fumarate Hydratase 1	Mus musculus	54,564	9.7	78.6	gi| 33859554	23,24,27
Glucose Regulated Protein 75	Homo sapiens	72,402	4.9	87.6	gi| 16507237	1
Heat Shock Protein 60	Mus musculus	61,111	6.4	147.0	gi| 1247242	7,8,9
Hydroxyacyl-CoA Dehydrogenase 2	Mus musculus	27,371	9.6	92.8	gi| 61888838	48
Inner Membrane Protein	Mus musculus	84,247	6.2	84.6	gi| 70608131	6

Protein	Species	MW (Da)	pI	Mascot Score	Accession #	Spot #s
Isocitrate Dehydrogenase 3, beta subunit	Mus musculus	42,453	9.4	71.7	gi| 18700024	29
IsoValeryl CoA Dehydrogenase	Mus musculus	46,695	9.3	68.9	gi| 20073124	26
Malate Dehydrogenase 2	Mus musculus	32,113	9.8	104.0	gi| 89574115	34,35,36
NADH Dehydrogenase (Ubiquinone) flavoprotein 2	Mus musculus	27,610	7.8	70.9	gi| 110625954	55
Nucleoside-Diphosphate Kinase 2	Mus musculus	17,466	7.8	92.6	gi| 6679078	69
Peroxiredoxin 3	Mus musculus	28,337	8.0	90.7	gi| 6680690	60
Prohibitin	Mus musculus	29,859	5.5	213.0	gi| 6679299	41,42
Pyruvate Dehydrogenase, beta subunit	Mus musculus	35,156	5.6	74.1	gi| 12805431	32,33
Superoxide Dismutase 2	Not Specified	24,848	9.5	96.2	gi| 832851	52,53
Succinate-CoA ligase, beta subunit	Mus musculus	50,424	6.7	72.0	gi| 46849708	25
Voltage Dependent Anion Channel 1	Rattus norvegicus	30,851	9.2	94.6	gi| 13786200	38,39,40

MW = molecular weight, pI = isoelectric point, a mascot score greater than 69 is a significant match, unless the species is Mus musculus in which case it is greater than 62, the accession number supplied is for the Ncbi database, spot numbers correlate with those shown in Figure 5.5 and listed in Table 5.1.